U.S. DEPARTMENT OF COMMERCE
National Technical Information Service

Procured through
M/S. ALLIED PUBLISHERS PVT LTD
NTIS DEPARTMENT
751 MOUNT ROAD
MADRAS 600 002
INDIA

PB-267 210

Research on the Application of Solar Energy to the Food Drying Industry

California Polytechnic State Univ, San Luis Obispo

Prepared for

National Science Foundation, Washington, D C Research Applied to National Needs

31 Dec 75

TR/539

CSTRI LIBRARY
TR/534
Date 31/3/83
MYSORE-2A.

NSF-RA-N 75 294

PB 267 210

Research on the Application of SOLAR ENERGY to the Food Drying Industry

NSF Grant ERT 7419063

Prepared with the Support of the
National Science Foundation
Research Applied to National Needs
Initiated in April 1974

By Thomas Lukes, Principal Investigator

California Polytechnic State University
San Luis Obispo
93407

December 31, 1975

Final Report

Report: NSF/RANN/SE/ERT 7419063/FR/75/4

REPRODUCED BY
NATIONAL TECHNICAL
INFORMATION SERVICE
U.S. DEPARTMENT OF COMMERCE
SPRINGFIELD, VA. 22161

RANN DOCUMENT CENTER
NATIONAL SCIENCE FOUNDATION

Prepared with the Support of the
National Science Foundation
Research Applied to National Needs
Initiated in April 1974

NSF Grant ERT 7419063

Research on the Application of Solar Energy to the Food Drying Industry

by
Thomas Lukes, Principal Investigator

California Polytechnic State University
San Luis Obispo
93407

Final Report
December 1975

Report: NSF/RANN/SE/ERT 7419063/F/75/4

Any opinions, findings, conclusions or recommendations expressed in this publication are those of the author(s) and do not necessarily reflect the views of the National Science Foundation.

TABLE OF CONTENTS

	Page
NTIS	i
Table of Contents	ii
Summary	iii
Introduction	1
Materials and Equipment	4
Experimental Procedure and Results	12
Determination of the Size of Collector Required to Operate a Dehydrator	39
Discussion and Conclusions	45
Acknowledgment	47
Appendix A	49
Appendix B	58
Appendix C (TRW Report)	77
Other Reports Generated	
Distribution List	

BIBLIOGRAPHIC DATA SHEET	1. Report No. NSF-RA-N-75-294	2.	3. Recipient's Accession No.
4. Title and Subtitle: Research on the Application of Solar Energy to the Food Drying Industry (Final Report)			5. Report Date: December 31, 1975 6.
7. Author(s): T. Lukes			8. Performing Organization Rept. No.
9. Performing Organization Name and Address: California Polytechnic State University San Luis Obispo, CA 93407			10. Project/Task/Work Unit No. 11. Contract/Grant No. ERT7419063
12. Sponsoring Organization Name and Address: Research Applied to National Needs (RANN) National Science Foundation Washington, D.C. 20550			13. Type of Report & Period Covered: Final Report 14.

15. Supplementary Notes

16. Abstracts

Several solar collector configurations were investigated as to their suitability for drying food crops. Various fruits and vegetables were dried using a mixture of solar energy and steam heat or solar energy alone. Cost estimates (based on initial construction material costs only) indicate that when the price of oil delivered to this country reaches $17 per barrel, then solar energy becomes competitive. An earlier report included in this document consists of results on related tasks including: literature review of dehydrated food industry; current and projected energy demands; projected cost studies for dehydrating carrots and prunes in the years 1975, 1985 and 2000; socio-legal implications; and economic and technical feasibility of solar energy to the food drying industry.

17. Key Words and Document Analysis. 17a. Descriptors

Solar energy
Solar heating
Dried foods
Crop dryers
Food
Drying
Food processing
Dehydrators

17b. Identifiers/Open-Ended Terms

Solar energy systems
Roof top solar heat collectors
Energy conservation by solar collectors
Auxiliary heat from solar energy
Food drying
Food dehydration

17c. COSATI Field Group

18. Availability Statement: NTIS	19. Security Class (This Report): UNCLASSIFIED	21. No. of Pages: 112
	20. Security Class (This Page): UNCLASSIFIED	22. Price: PC A06-A01

ERRATA:

p. 9, l. 24 for "Matric" read "Matrix"

p. 14, ll 10-12 should read "The relationship between efficiency (defined as collector output divided by solar input times one hundred) and ΔT/Insolation is shown on Figs. 4, 7, 10, 13, and 16."

p. 35, l. 17 should read "The percent of energy supplied by the collector to the system goes up as the volume of air through the collector goes down."

p. 42, l. 12 for "20% replacement" read "26% replacement"

Figure 15: Legend should read "Relationship between Heat out and Air Flow thru the 140' collector with one glazing."

Table 1: delete "Hr" in headings for columns entitled "Total Available."

Appendix A: Figure 2, G should have units of lb/hr - ft^2, and abscissa should have word "insolation" rather than "isolation"; Figure 5, the (-.8) exponent in the equation should be (-.2); p. 11, the exponent (-.8) in equation (6) should be (-.2).

SUMMARY

Test results are reported for the operation of unglazed and single glazed solar collectors used to heat air for the dehydration of food crops. The collectors, constructed of black painted metal ducting, were attached to a laboratory scale dehydrating cabinet. Detailed measurements showed collector performance was substantially predictable. Various fruits and vegetables were dried using solar energy and steam heat. The dried product was equivalent to that dried by steam heat alone.

Although not competitive with natural gas at its current cost, the studies show that solar collection systems (including heat storage for 24 hour operation) could viably replace natural gas if it becomes unavailable. Initial capital costs for a collector and storage system (ignoring financing, taxes, maintenance, operating costs) when amortized over a ten year period would compare favorably with oil (the most likely fossil fuel replacement for natural gas) when the price of oil reaches $17 a barrel.

INTRODUCTION

The fact that the United States faces a severe energy shortage needs no elaboration. The pinch is felt strongest in the supply of natural gas which peaked in 1972 and the supply is expected to decline at an ever increasing rate in the future.

The fruits and vegetables dehydration industry is mainly centered in the western states, with California the main producer. Most dehydrators use natural gas, and the California dehydrators alone yearly use a quantity of gas equivalent to that used by a city of nine million people. In 1974, the gas allotment to dehydration firms was cut back, and in 1975 there was a further reduction in the quantity supplied to the dehydrators.

Solar energy represents an attractive alternate source of energy for dehydration. The direct exposure of fruits to the sun for drying goes back to prebiblical times. The Andes Mountain Indians dried potatoes in the sun; grains and nuts dry on the plant itself; and in California, certain fruits are still mainly sun-dried. However, in modern processing, all vegetables are now dried in hot-air dehydrators, and of the fruits, prunes are also mainly dehydrated. The advantage of hot-air dehydration over sun-drying is mainly sanitation and less vulnerability to the weather.

Previous experiments in using solar collectors for dehydration have tried a combination of exposure of the product to direct sun with added heat from a collector (1, 3, 4, 5). Others have separated the solar collector from the dryer so that no direct sunlight falls upon the product (8, 6, 2). Corn is being dried in bins heated by solar collectors (9) and timber drying has been studied (7). Löf (10) has reviewed the investigations in solar drying. Most of these food drying investigations were relatively small scale experiments, using dryers not typical of those used

in the modern dehydration industry. Because of the need to investigate the possibility of interfacing a solar collector to the present-day dehydration equipment, NSF awarded this grant.

Extensive background studies (Third Quarter Progress Report: NSF/RANN/SE/GI 42944/P2/74/3 and TRW's previous report: NSF/RANN/SE/GI142944/TR/74/4) were performed prior to arriving at the collector design and test results that are the main subject of this report. The basic unglazed and single glazed collector configurations chosen were selected on the basis of expected performance predictability, availability of air channel metal decking, and system economic studies of alternate systems. The system optimization studies indicated that, for heat transfer reasons, particularly long collectors (for the 3" depth of standard air channel available) resulted in minimum system life cycle cost. Fortuitously, the long length proved to be useful for large scale application, and the long narrow experimental collectors tested represent typical modules of such near optimum length collectors.

The main body of this report covers the general system design specifications, raw data from the collector, and solar dehydration experiments. The data acquisition system is discussed in detail in Appendix A.

In order to aid future needs for collector performance optimization, the experiment was designed so that convective heat transfer rates and pressure losses could be varied independent of collector operating temperature. The detailed results of this study are contained in Appendix B, along with a comparison of the experimental collector performance, (including pressure drop data) and predicted theoretical results.

Appendix C, prepared by TRW, contain some additional details of the system design and performance, and a critique of the potential economics of the system if applied on a large scale dehydration system.

THE INSTITUTION AND THE GRANT

California Polytechnic State University is part of the California State University and Colleges System located in San Luis Obispo, midway between Los Angeles and San Francisco. It has the second largest undergraduate enrollment in Agriculture of any university in the United States. It is noted for a practical approach to education which stresses the technical side and close ties with Industry.

In April, 1974, the National Science Foundation awarded a grant to the University for the study of the "Application of Solar Energy to the Food Drying Industry." The goal was to determine if it was feasible to use solar energy to replace or supplement fossil fuels in the Food Dehydration Industry. The T.R.W. Corporation was made a subcontractor. Its task was to design the collector and assist in the evaluation of the results. The University was to construct the collector, test it, and evaluate the data. The collector was to be used to provide air to a cabinet food dryer.

MATERIALS AND EQUIPMENT

THE CABINET DEHYDRATOR

The design of the laboratory food dryer was developed by workers at the Western Regional Research Laboratory, of the U.S. Department of Agriculture (WRRL), Berkeley, California. It was this type of dryer which was used in the extensive work done in the Fourties on food drying at that Laboratory.

WRRL provided the project with the blueprints (Drawings C-112 and C-113, 1943), and the shell was constructed from these plans at a local cabinet shop. The fan, steam heating coils, controls, etc., were installed by Agricultural Engineering Graduates associated with this grant. This dehydrator had a centrifugal fan capable of delivering 9000 CFM @ 1½" water pressure and was driven by a five horse power electric motor. An adjustable plug was placed in the inlet of the fan to throttle the amount of air that could be blown. Steam coils provided auxiliary heat so that the unit could be operated by solar energy alone, steam heat, or a combination of the two. An automatic controller adjusted the steam flow to maintain a constant temperature, and it also controlled the humidity in the dryer by injecting steam into the air stream if needed. The food product was dried on stainless steel eight mesh screens.

THE COLLECTOR

The T.R.W. Corporation of Redondo Beach, California, investigated the economic and enginecring feasibility of many types of collcctors and finally settled on a flat-plate type collector which used air as the heat transfer medium. The rational of the decision was given in a Technical Report (NSF/RANN/SE/GI 42944/TR/74/4 Kaminskas, R.A.). A drawing, prepared by T.R.W., of the collector on the roof of a metal building is shown in Fig. 1. Inside the building is the cabinet dehydrator, and the data collection system. The heat collectors consisted of Ryerson galvanized steel decking, two feet wide and seventy feet long. The seventy feet was actually made up of two thirty-five feet sections joined. A cross section of the decking is shown in Fig. 2. This type of decking is a standard item widely used for roofing and floor construction in buildings.

The rational behind this choice of material was that the cost of a collector is a major factor in using solar energy. If the collector could actually be a structural part of the roof itself, then part of the cost could be written off as roofing. All one would have to add is ducting at the ends, insulation, and some sheet metal to close off the open channels.

The collector surface sheet was 0.059" thick and the fins were 0.039". The top surface was coated with Nextel Black Velvet Paint (3M Corp.). which was sprayed on and air-dried. The interiors of two of the collectors were coated with Dull Black Rust-Olium which was applied by inclining the collectors at a 20° angle and pouring the paint down the ducts. Thermocouple wire was installed to measure both surface

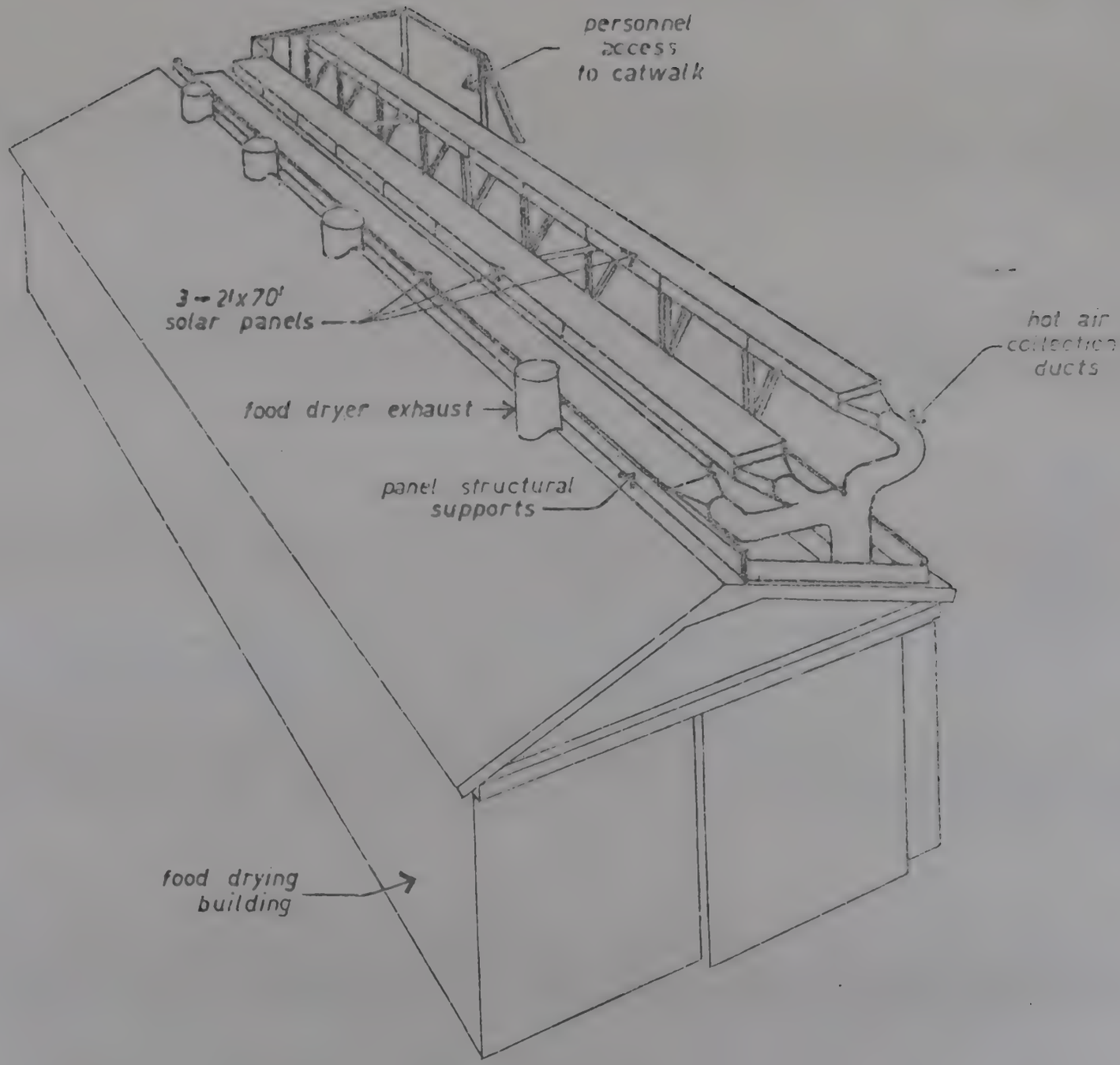

Fig. 1

Perspective Solar Panel Installation

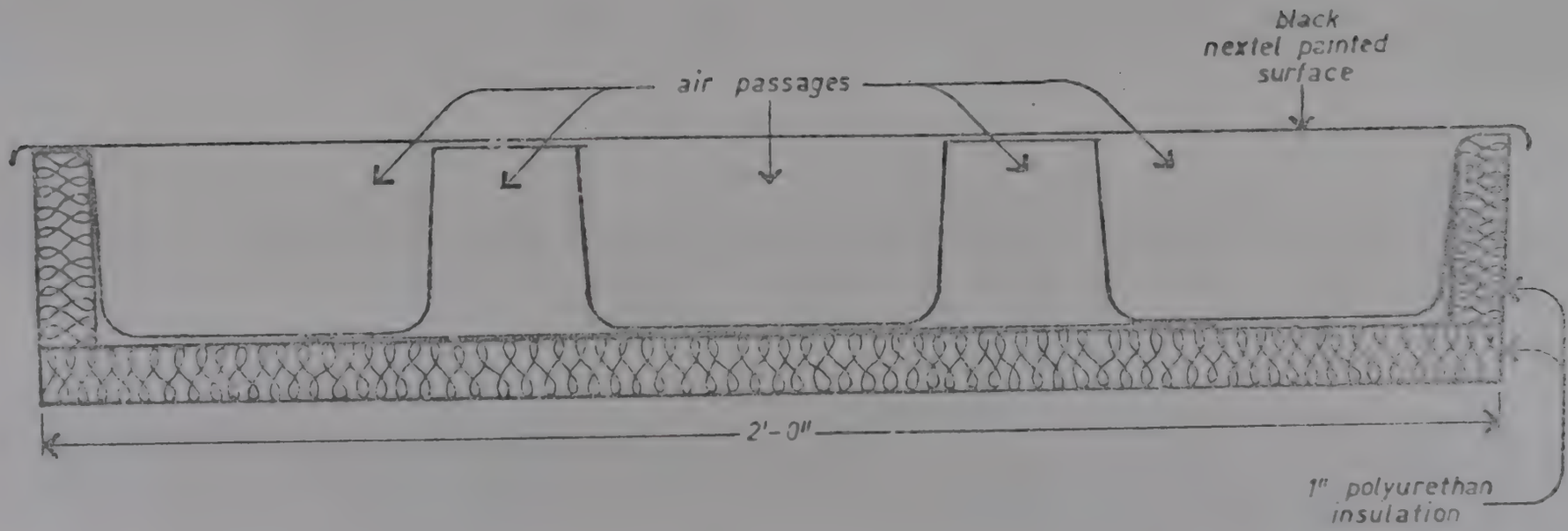

FIG. 2

CROSSECTION OF SOLAR COLLECTOR PANEL

temperature and air temperature at many places in the collector. The thermocouple arrangement will be described in more detail under instrumentation.

One inch thick sheets of polyurethene foam insulation was applied to the sides and the bottom of the units with contact cement. The ducting which lead from the end of the collectors to the dehydrators was insulated with 1" of fiber glass battin, and covered with waterproof cloth wrapping.

The collectors were horizontal instead of being inclined. There were structural advantages in this installation in using horizontal collectors. The increased energy that would be collected by tilting the collectors to the proper angle can be easily calculated.

These units were tested both with and without glazing. Two types of glazing materials were used: Tedlar and Sunlite Premium Plastic Sheet. The former was .004" thick and the latter was .04" thick. Sunlite is made by the Kalwall Corporation and the company reported that it transmits 85% of the light. Tedlar is made by Dupont. The glazing needed support in the center and also needed a slope to drain off moisture. A steel rod, .26" in diameter, was run the length of the center line of each collector and supported by short rods of the same material to accomplish this. There was a 2" space between the glazing and the collector surface.

THE DATA COLLECTION SYSTEM

Temperatures were measured by means of copper-constantine thermocouple wire. The junctions were attached to the metal surface with epoxy cement to provide close contact and electrical insulation. Air temperature measurements inside the air channels of the collector were initially measured by means of shielded junctions as shown in Fig. 3. The purpose of enclosing the junction in an aluminum tube was to protect it from radiation from the hot surface. These units were placed in each channel of the collectors. In practice, it was found that you could not get the temperature of the air even in a small duct by measuring one point in the center. It was fairly representative at high air flows but not at low air flows, even though still turbulent, stratification took place. The air next to the hot metal was much hotter than at the bottom of the duct. One would think that with turbulent flow it would average out, but it did not. As a consequence, the temperature of the air was measured by means of thermocouples placed in the duct which collected the air for delivery to the dehydrator. Sixteen thermocouple junctions were connected in parallel and were so placed that they each measured the same cross-section of the duct. The air temperature measured was an average of the sixteen thermocouples.

The wind direction and velocity were determined by a model No. W121-2 Windicator produced by the Weather Measure Corporation. This was mounted to take measurements near the center of the collectors and about two feet above their surface.

The solar insolation was determined by means of a "Sol-A-Meter", model MK 1-b, made by the Matric Corporation. An Eppley Solar Meter was used also as a cross check. It was found that both units were in close agreement.

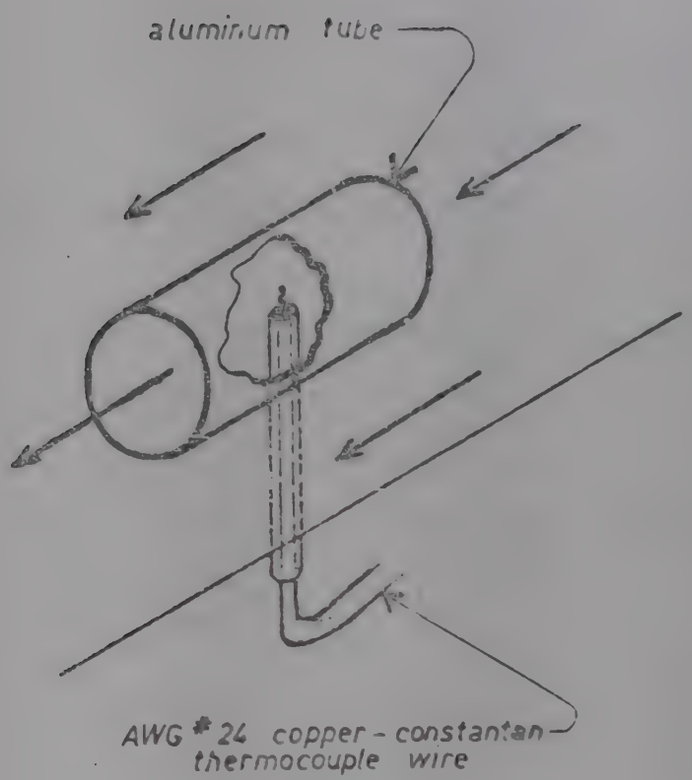

FIG. 3
AIR TEMPERATURE MEASUREMENT SET UP INSIDE THE COLLECTOR

Air velocities were measured by means of an orifice plate placed in a long straight section of the duct leading to the dehydrator. There was an egg-crate air straightenor placed up stream eight diameters from the orifice plate and the pipe continued straight ten pipe diameters past the orifice. The accuracy of the orifice readings were checked by a pitot tube traverse of the pipe in which it was placed. The air speed at low air velocities was checked by means of a hot wire anemometer. The pressure differential across the orifice plate was measured and reported as inches of water.

All the electrical signals from the thermocouples, the wind velocity, the wind speed, and the solar insolation, were measured with a data collection system, and the results printed on tape for a permanent record. The data collection system and the programs used in the calculations will be described in Appendix A of this report.

EXPERIMENTAL PROCEDURE AND RESULTS

A. Tests of the solar collectors.

There were five configurations used for testing the collectors.

1. A 70' x 2' length unglazed.
2. A 140' x 2' length unglazed.
3. A 70' x 2' length glazed with Sunlite Plastic.
4. A 140' x 2' length glazed with Sunlite Plastic.
5. A 70' length glazed but operated double pass. In this configuration all the air was first moved from one end to the other between the black-absorber plate and the glazing. Then it flowed counter current back to the starting end under the black-absorber plate and then was discharged.

In all configurations, the air was sucked through the collector by means of the fan in the dehydrator.

The initial experiments were performed by starting the fan in the morning and a constant rate of flow was maintained until 10 AM. A series of temperature and other measurements were taken for 30 minutes. Then the air flow through the collector was changed and after 30 minutes another series of measurements were made. It was felt that the unit would come to equilibrium in thirty minutes. This process was repeated several times, until 1600 hours. Preliminary analysis of the data indicated that this procedure was quite unsatisfactory. It took much more than 30 minutes for the unit to come to equilibrium. Especially when the air was changed from a high rate of flow to a low rate of flow, this occurred. Furthermore, results from experiments done in the morning were significantly different

from those of the afternoon, even though the solar insolation, ambient air temperature, air flow, and wind speed were the same. This was due to the mass of the collector which was absorbing energy as the sun rose and releasing it as the sun went past solar noon. (Solar noon is at 1300 daylight saving time at this longitude.) The tests were then repeated and only the data between one hour before and after solar noon were used. No change in air flow through the collectors was made during this time, nor was any other change made. This procedure, although very time consuming, did provide data which allowed comparison between collectors to be made accurately.

Data was collected on:

1. Ambient air temperature (which was the temperature of the air entering the collector).
2. Wet bulb of the ambient air.
3. Air flow in cubic feet of air per minute through the collector.
4. Air temperature leaving the collector.
5. Solar insolation. ($Btu/ft^2/Hr$).
6. Wind direction.
7. Wind speed.

The ambient air temperature between 1200 and 1400 hours varied between $68^{o}F$ and $87^{o}F$. The wet bulb varied but to a small degree during the test period. The absolute humidity ran between .009 and .013 pounds of water per pound of dry air.

In a similar manner, the effect of wind speed and direction upon the results was small, although one could detect a drop in temperature of the collector discharge air if a sudden breeze came up. This factor was so erratic that no valid conclusion could be reached as to the effect of wind on the unit.

The solar insolation varied slightly during the 1200 to 1400 time period and usually was between 260 and 301 Btu/ft^2/Hr. No data were used unless the sky was free of clouds and haze during the entire test period.

The factor which influenced efficiency, ΔT, and Btu/ft^2/Hr out of the collector, the most was CFM through the unit. It by far overshadowed any other input for a given collector configuration. The relationship between ΔT and CFM/ft^2 is shown in Figs. 5, 8, 11, 14, and 17. The formula for the regression line is also given. The relationship between Btu/ft^2/Hr output and CFM/ft^2 is shown in Figs. 6, 9, 12, 15, and 18.

The relationship between efficiency (defined as solar input divided by collector output times one hundred) and ΔT/Insolation is shown on Figs. 4, 7, 10, 13, and 16. Again, the most important factor which affected the efficiency of the collectors was the CFM/ft^2 of collector surface. As the amount of air through was reduced, the efficiency went down, the ΔT went up, and the Btu/ft^2/Hr went down.

Examination of the efficiency graphs revealed that, as one would expect, the glazed collectors were far more efficient than the unglazed ones. Comparison between the 70' glazed single pass and the 70' glazed double pass indicates that at, high air flows and low ΔT, the double pass is much more efficient. At low air flow and high ΔT, there was little to choose between them. In fact, there are indications that at very low air flows, the single pass is the superior collector. The 140' glazed unit is overall more efficient than the 70' one.

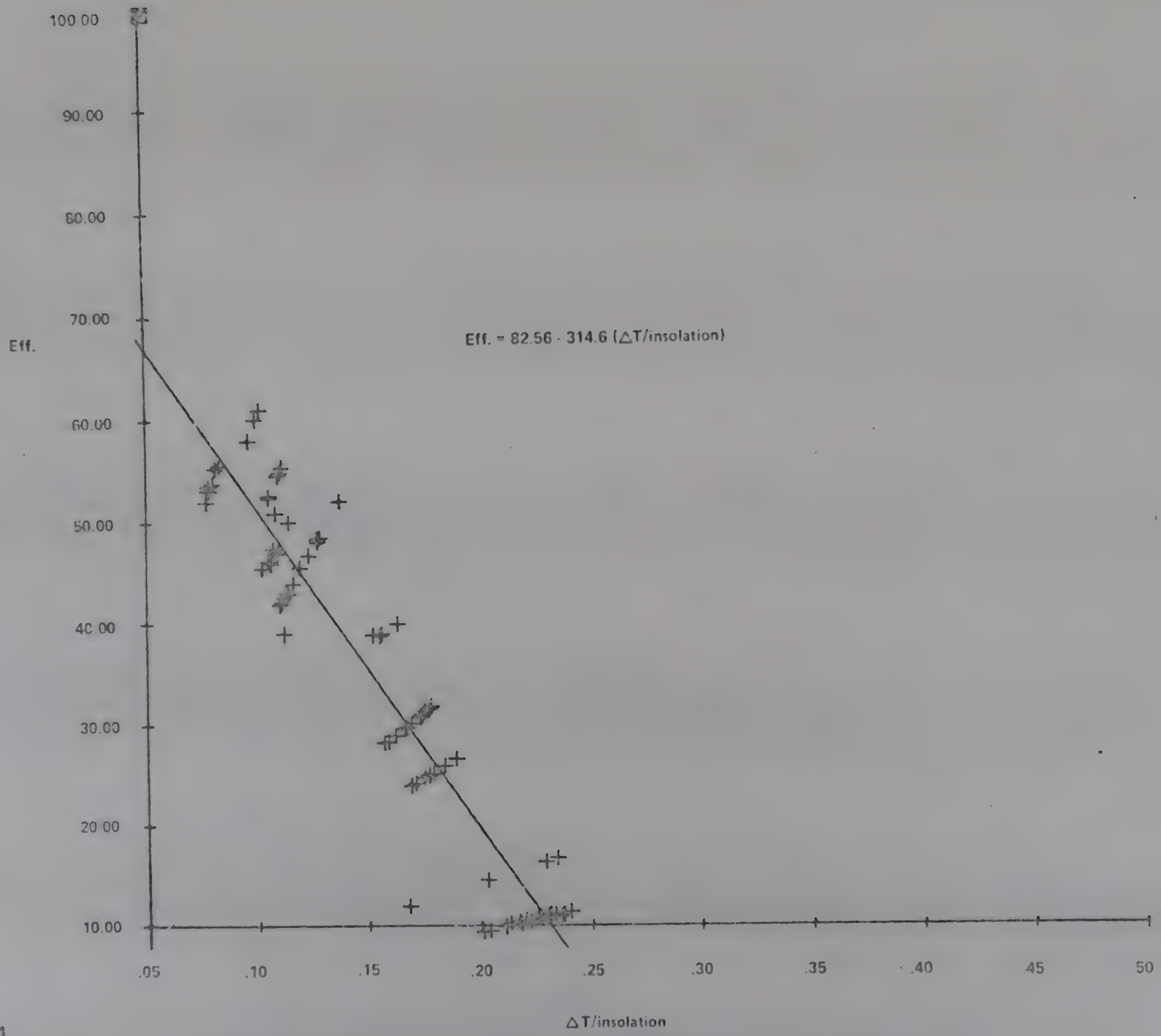

Fig. 4

Relationship between the efficency of the collector and △T/insolation for the 70° unglazed collector.

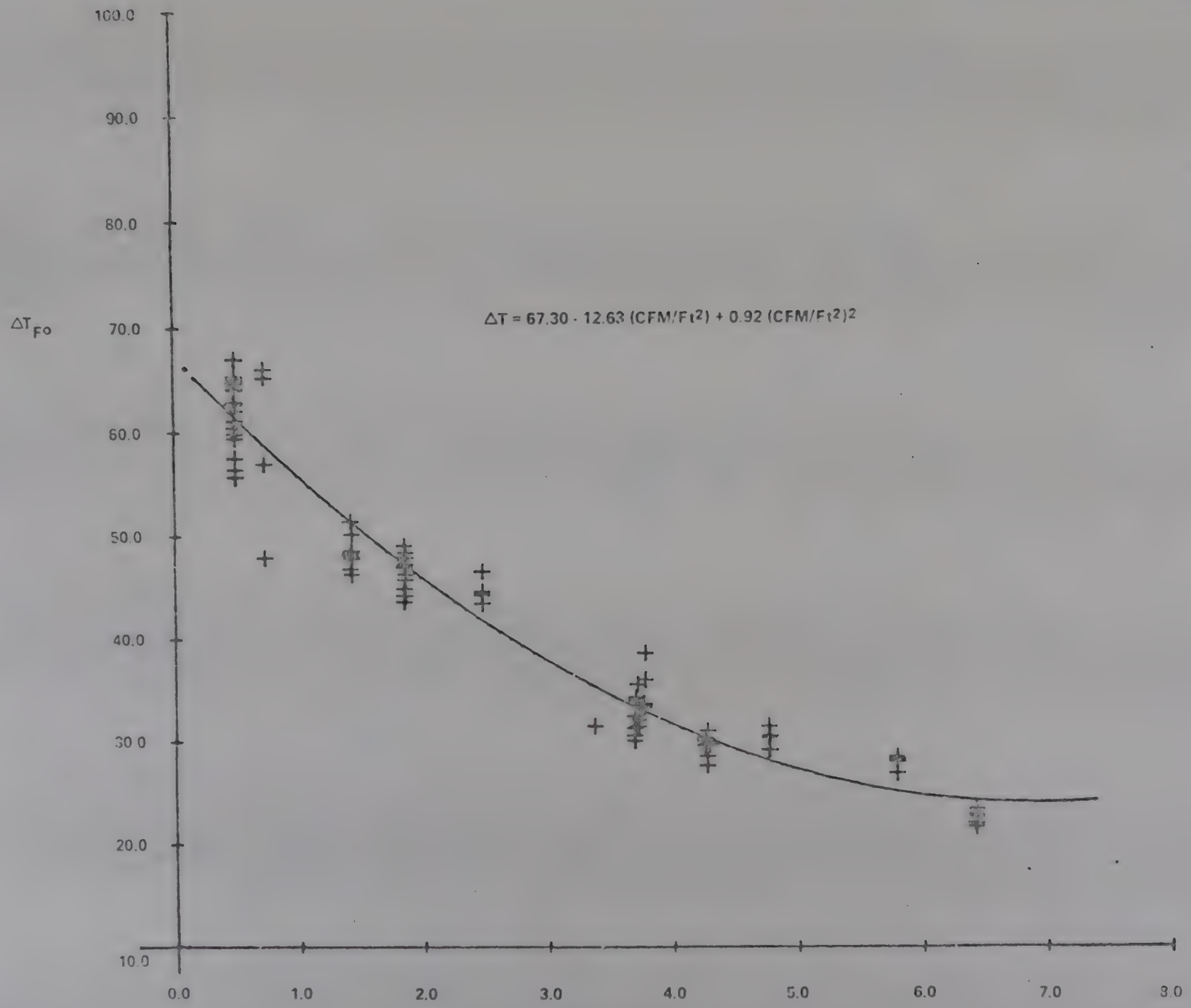

Fig. 5

Relationship between the increase in air temperature thru the collector and the air flow, for the 70' unglazed collect

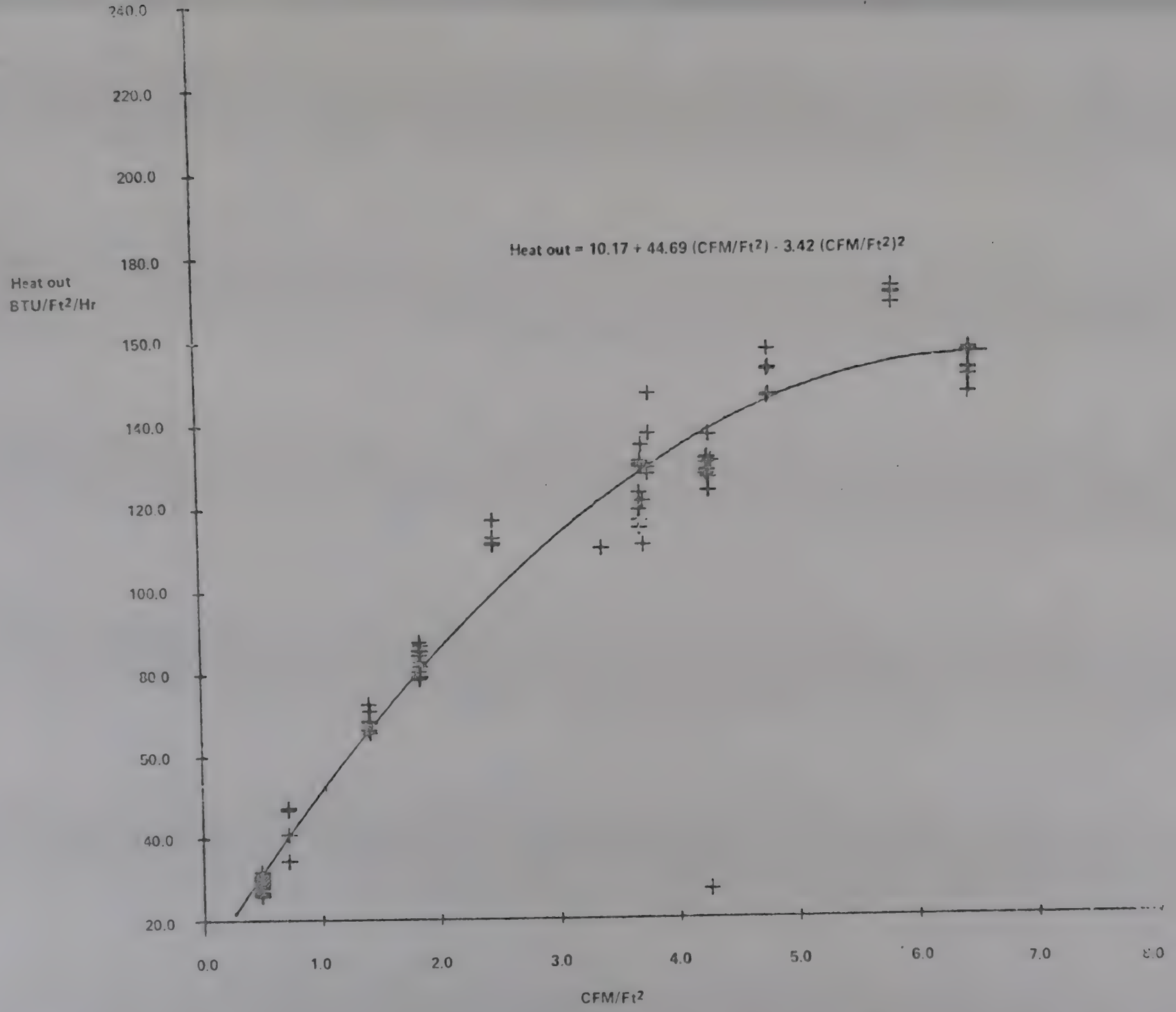

Fig. 6

Relationship between the heat out and the air flow thru the collector, for the 70' unglazed collector.

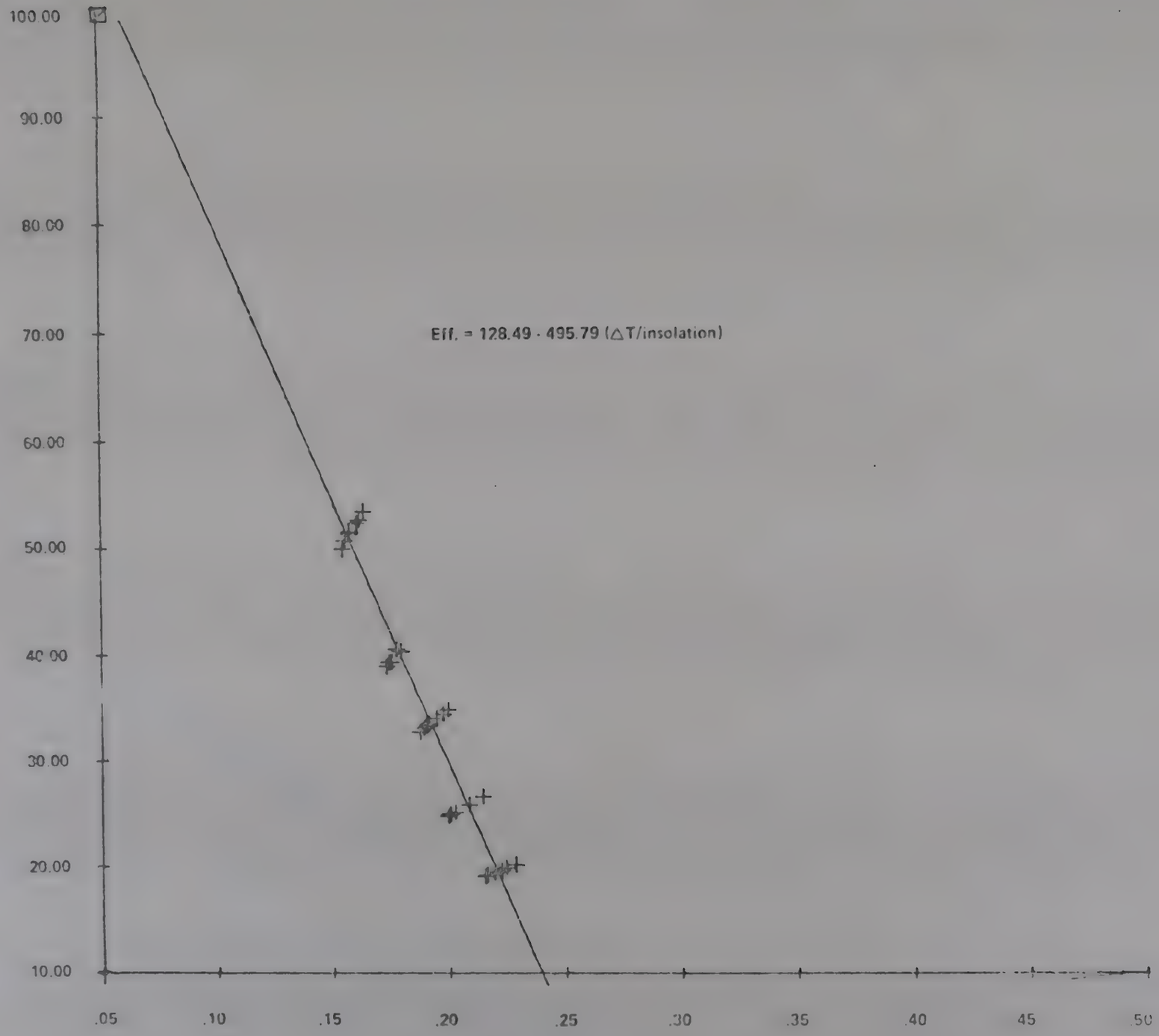

Fig. 7

Relationship between efficency and △T/insolation for the 140' unglazed collector.

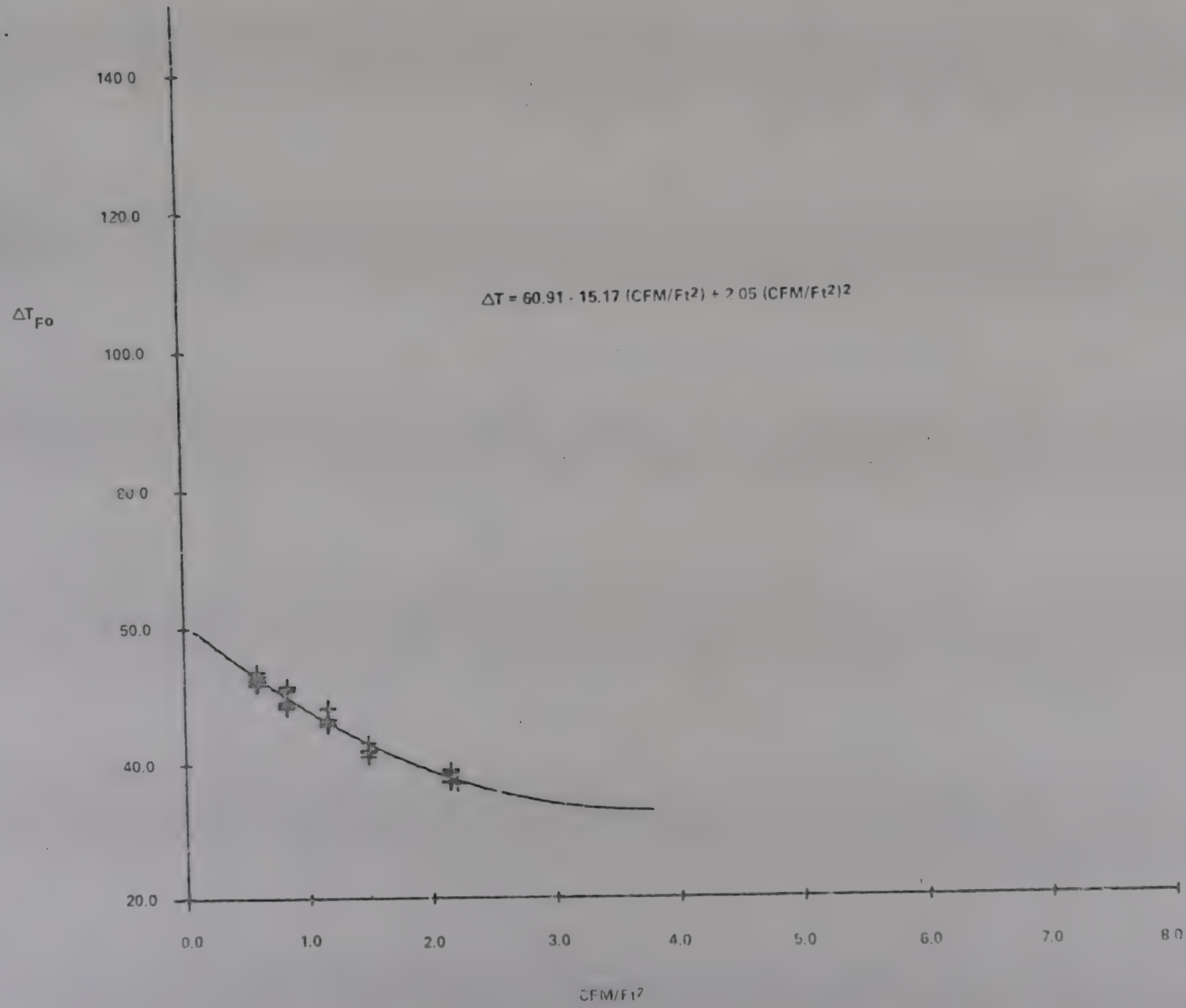

Fig. 8 Relationship between the increase in air temperature thru the collector and air flow, for the 140' unglazed collector.

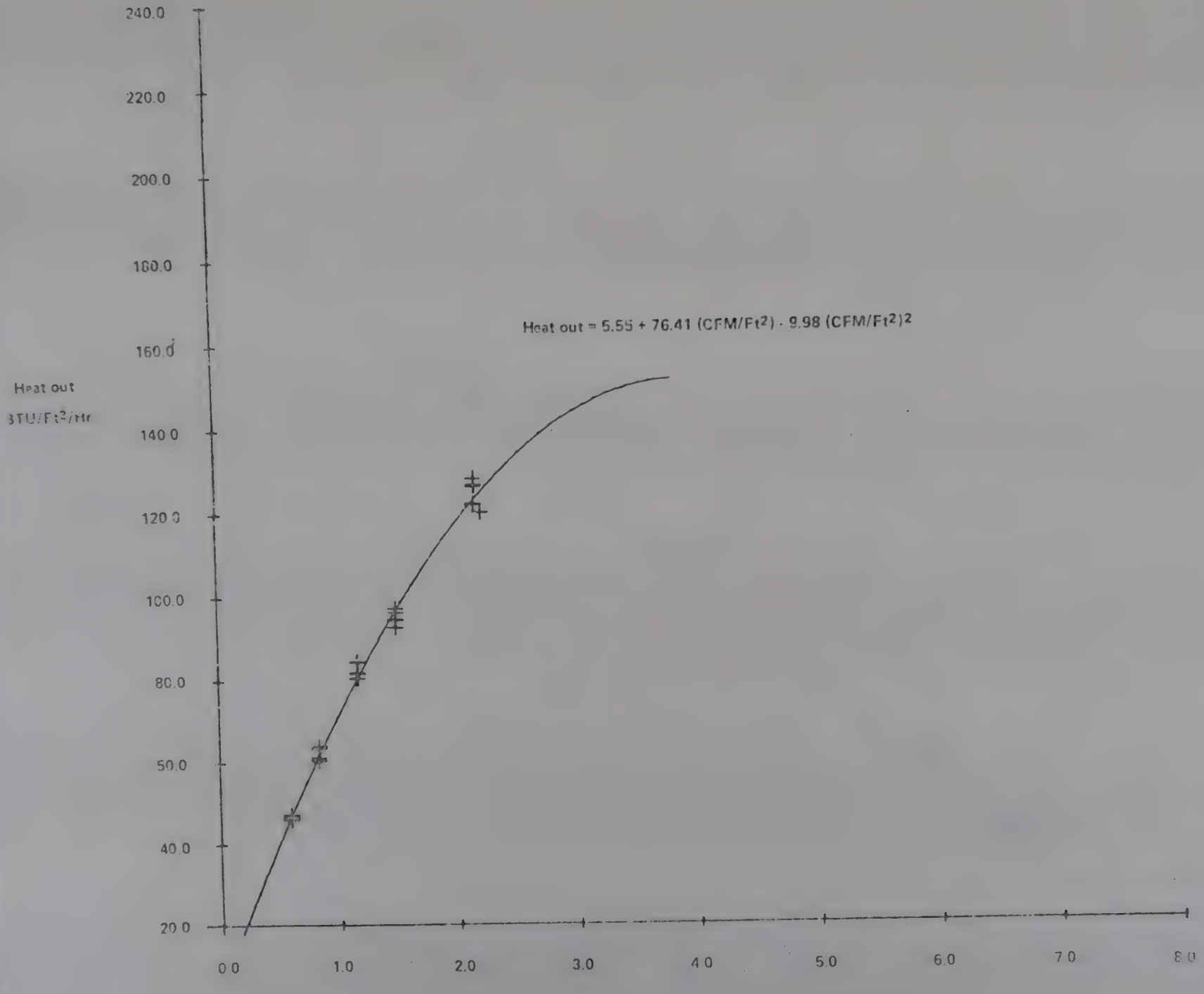

Fig. 9

Relationship between heat out of the collector and air flow for the 140' unglazed collector.

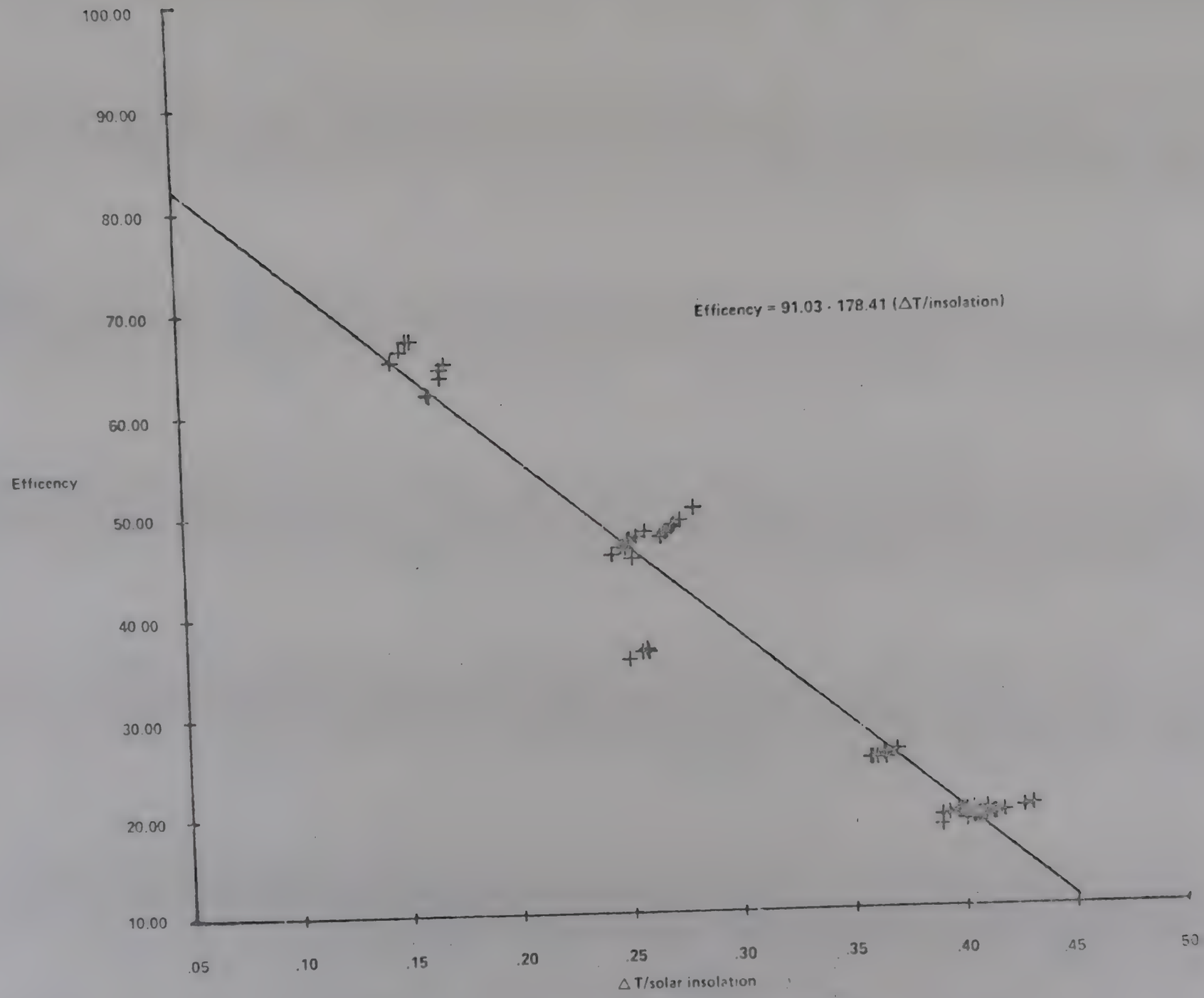

Fig. 10 Relationship between efficency and ΔT/insolation. Seventy foot collector, with one glazing

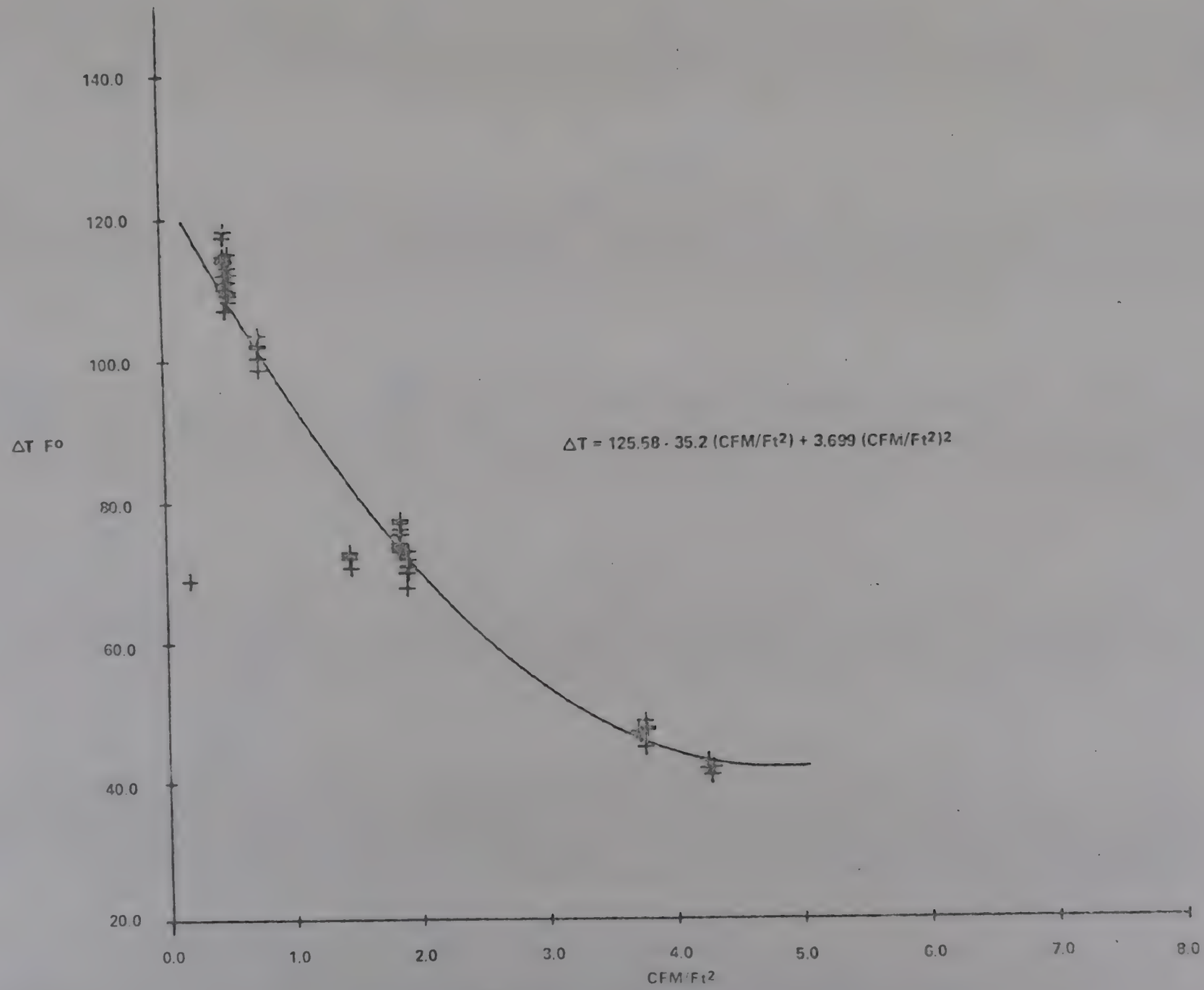

Fig. 11

Relationship between increase in air temperature thru the collector and the air flow thru the 70' collector with one glazing

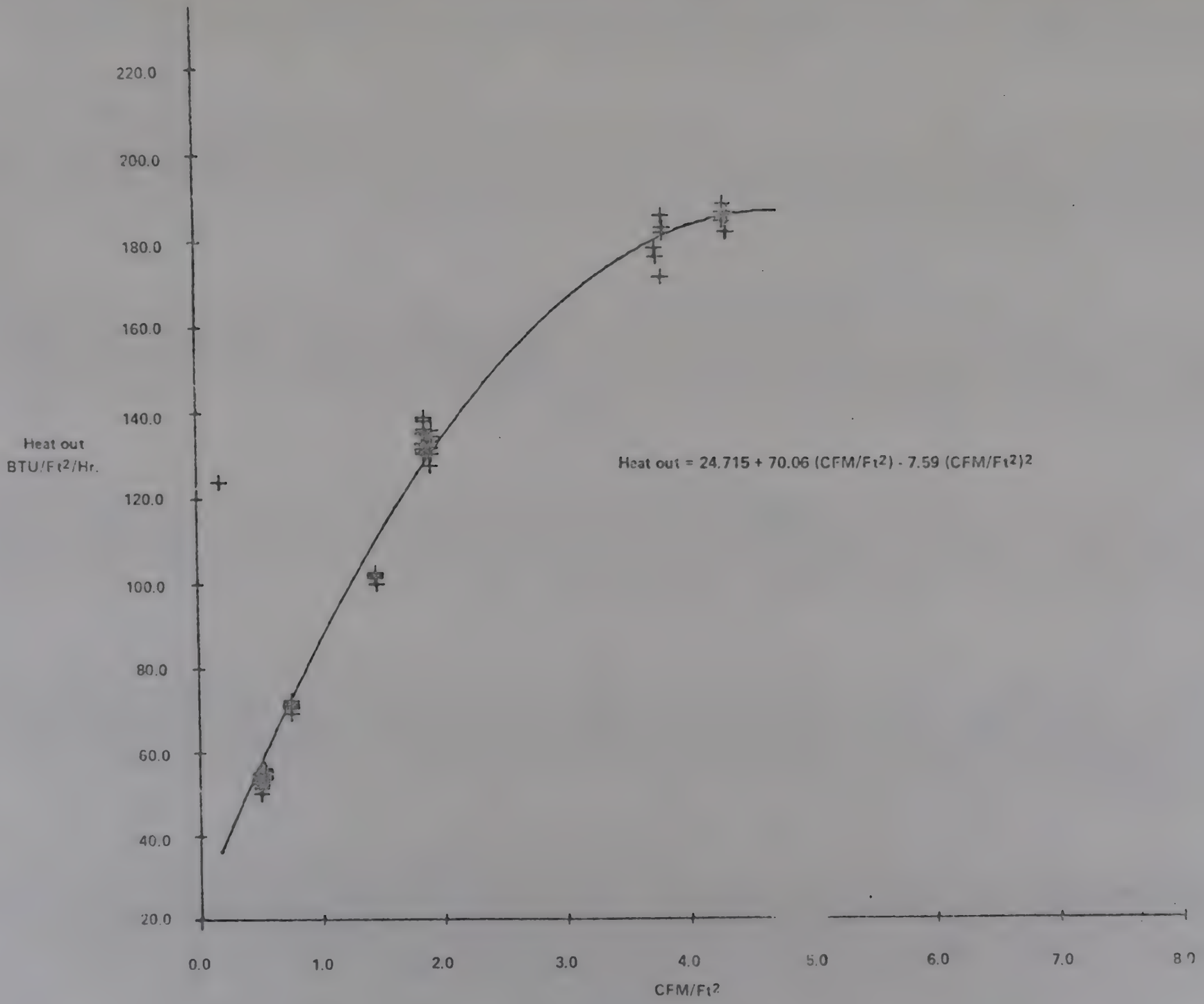

Fig. 12

Relationship between heat out and air flow thru the 70' co with one glazing.

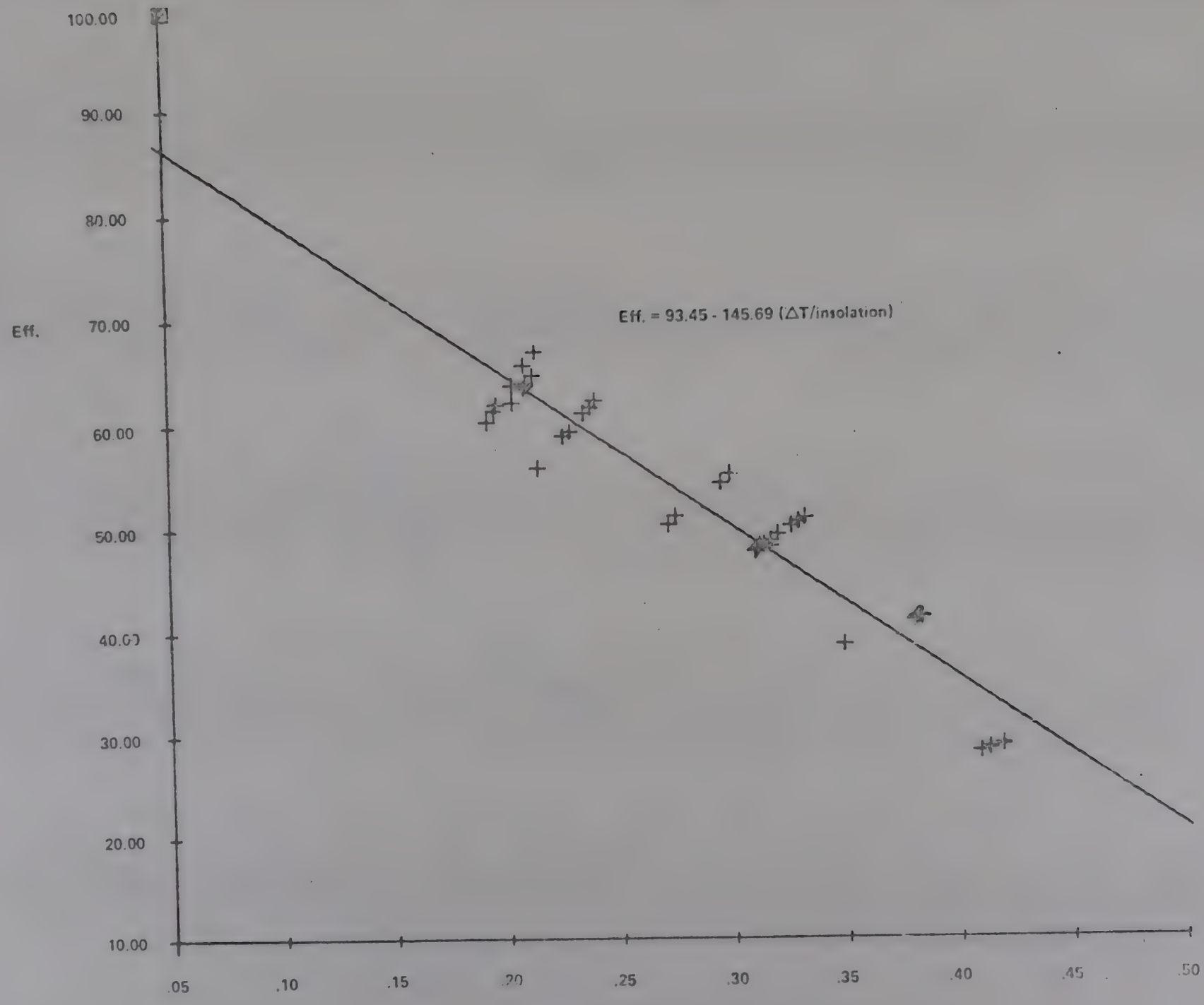

Fig. 13

Relationship between Efficency and ΔT/insolation for the 140' collector with one glazing.

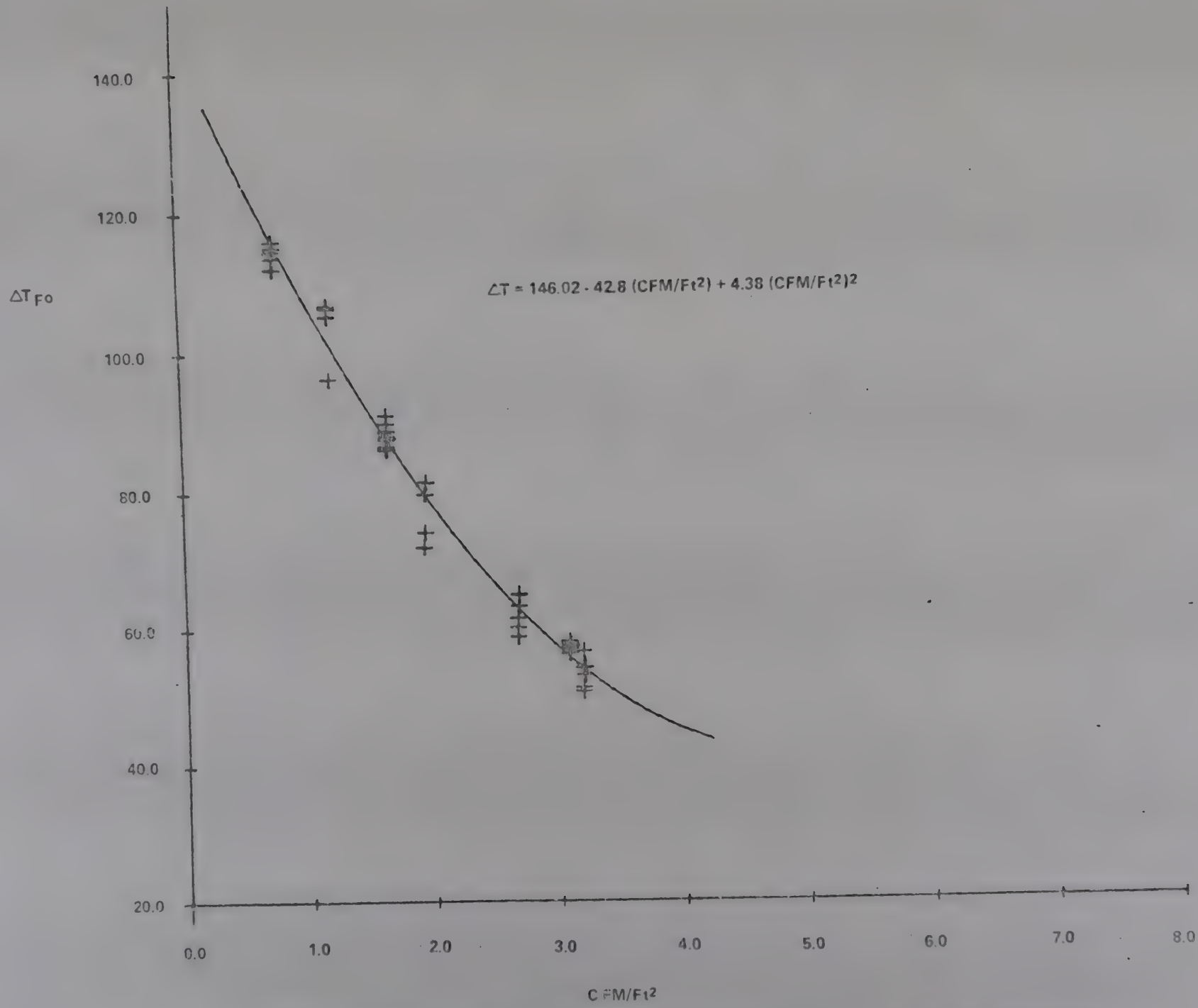

Fig. 14 Relationship between the increase in air temperature thru the collector and the air flow for the 140' glazed collector.

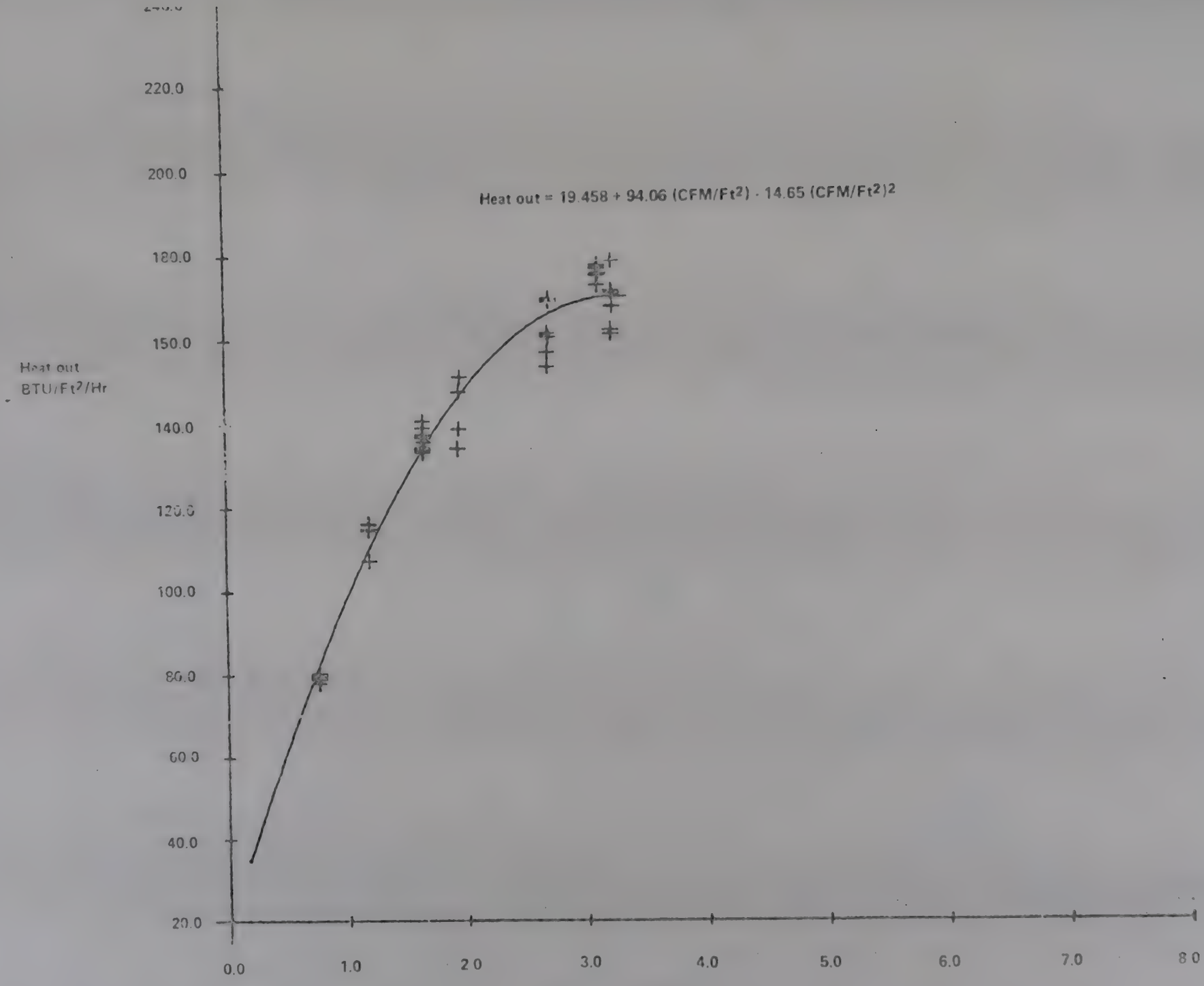

Fig. 15

Relationship between Heat out and Air Flow thru the 70' collector with one glazing.

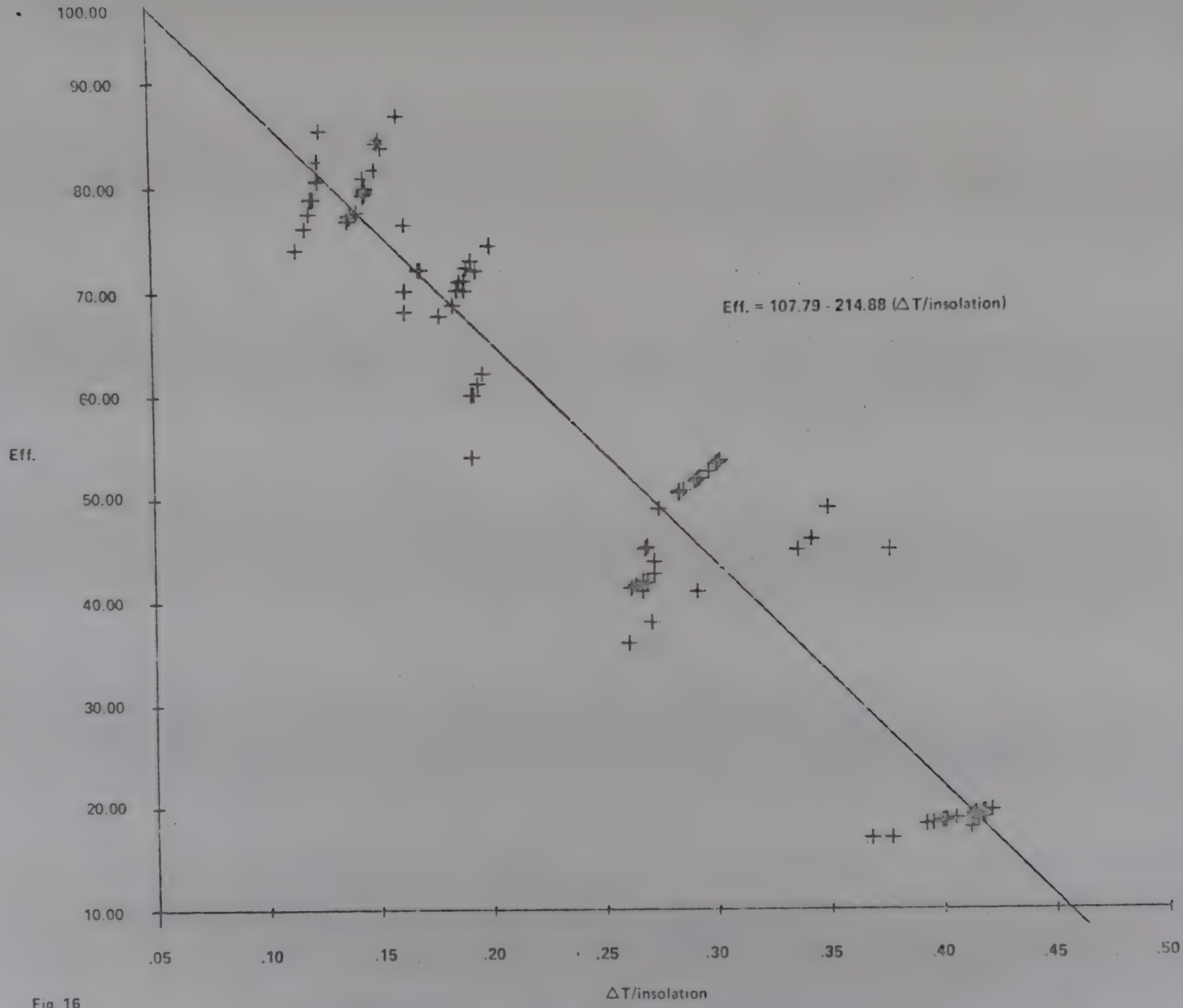

Fig. 16

Relationship between efficency and ΔT/insolation for the 70' double pass collector

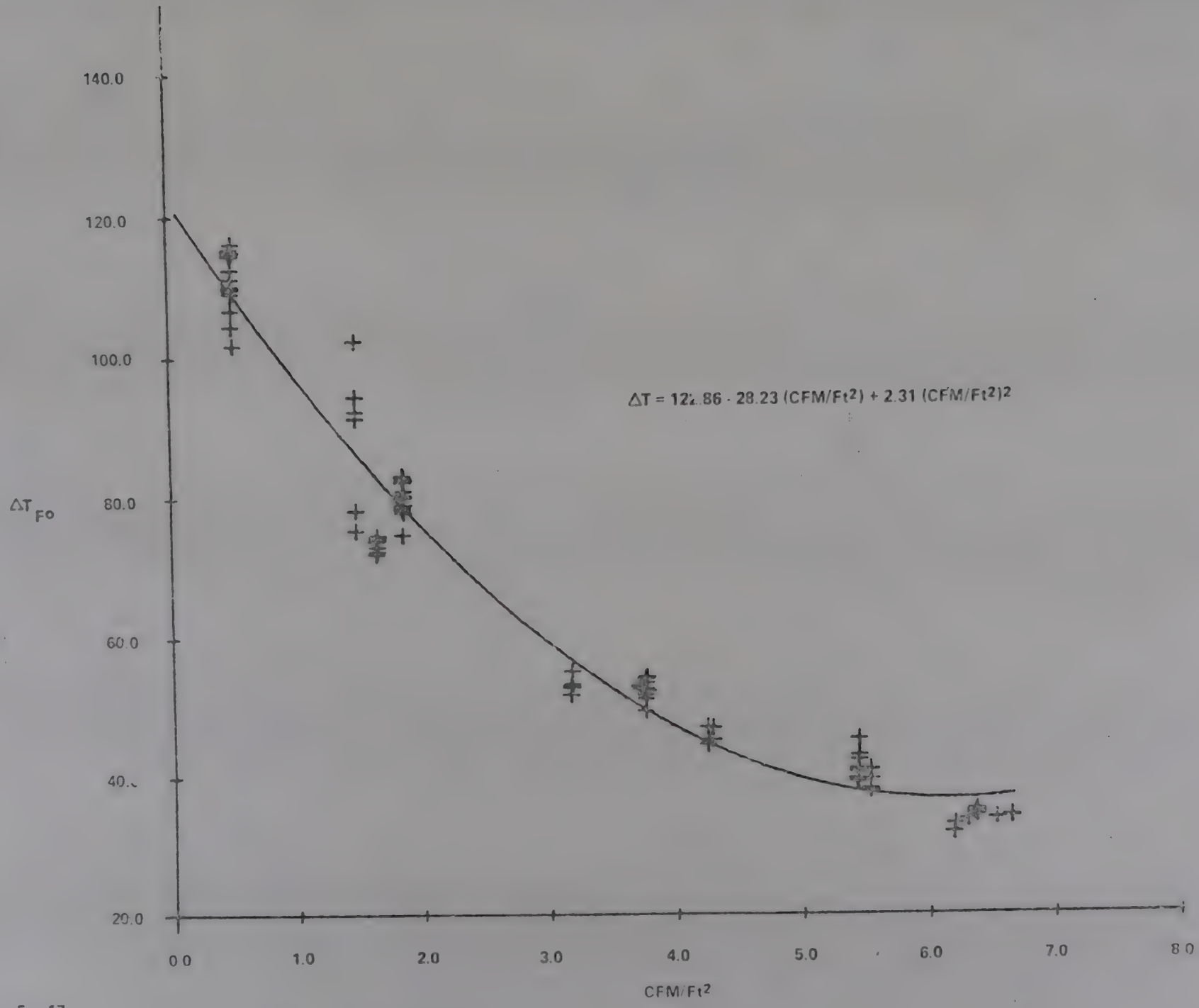

Fig. 17

Relationship between the increase in air temperature thru the collector and the air flow, for the 70' double pass collector.

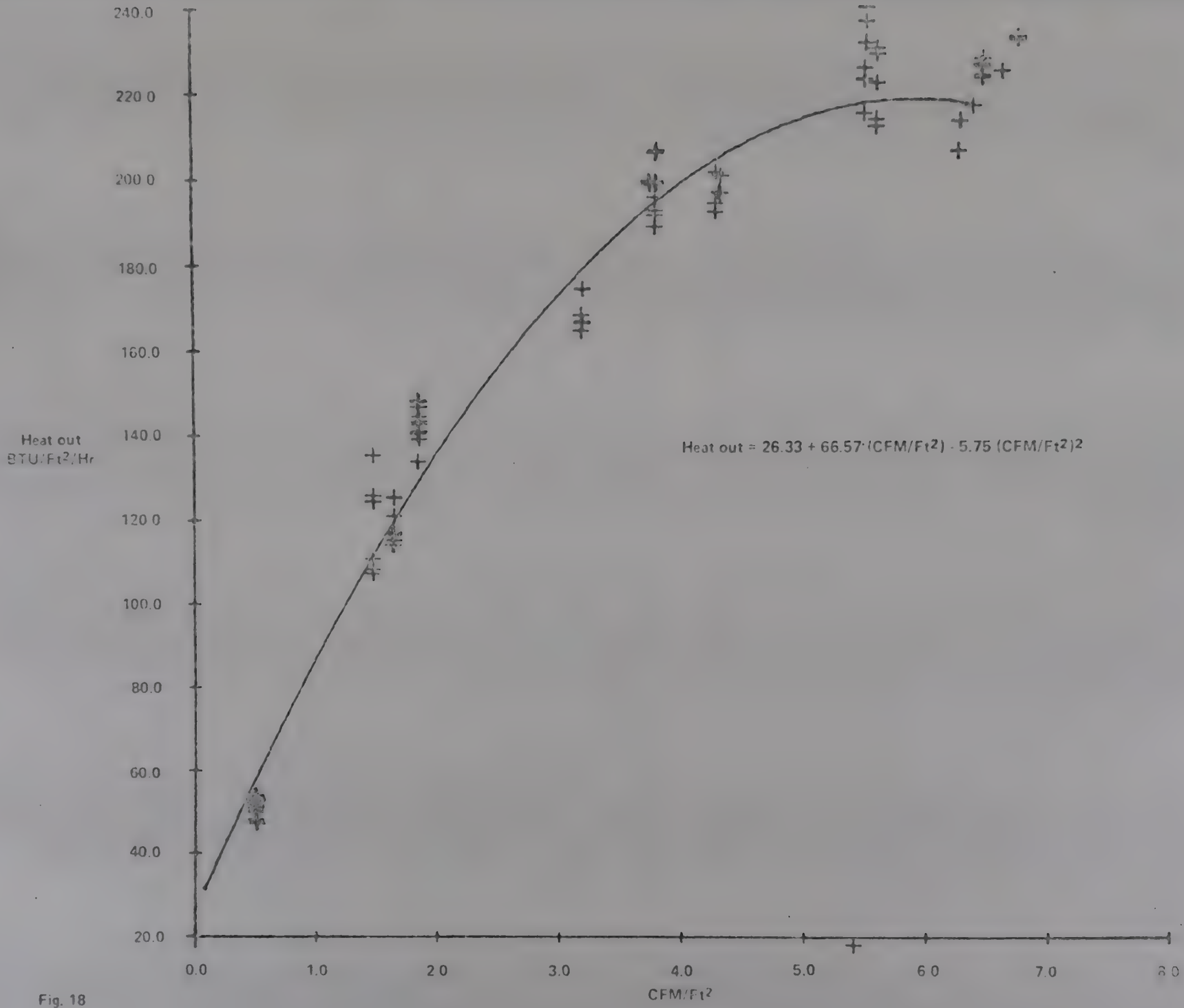

Fig. 18

Relationship between the heat out of the collector and the air flow, for the 70' double pass collector.

EVALUATION OF ALL DAY OPERATION OF A SOLAR COLLECTOR

Examination of the data described previously lead to the decision that the 70' glazed, single pass collector was to be used for further testing. It appeared to be the most promising configuration. The 140' glazed, single pass could also have been used but not enough air could be gotten through this unit to properly test the dehydrator. The 70' collector was operated at varying air flows from early morning until late at night. Unfortunately, weather conditions were such at this time that the tests could not start as early as one would like, but the data can be readily extrapolated. These tests were made between July 1, 1975 and July 5, 1975. The results are shown in Table 1. This again shows that as air volume goes down, the total Btu per day goes down and the ΔT goes up.

These tests were conducted on days when the sky was free of clouds. However, the solar insolation was consistently higher four hours after solar noon than it was four hours before noon. This is undoubtedly due to morning atmospheric conditions. The heat out is also higher after noon than before. This cannot be accounted for by the slightly higher insolation. Rather, it is mainly due to the mass of the collector acting as a heat reservoir.

TABLE I

CFM/ft^2 Air Flow Through Collector	Total Available Between 08:00 and 19:00 Hours. Daylight Saving Time		Average Available Between One Hour Before and After Solar Noon			Instant Values at Three Hours Before Solar Noon			Instant Values at Four Hours After Solar Noon		
	Heat Out Btu/ft^2/Hr	Solar Insolation Btu/ft^2/Hr	ΔT	Heat Out Btu/ft^2/Hr	Solar Insolation Btu/ft^2/Hr	ΔT	Heat Out Btu/ft^2/Hr	Solar Insolation Btu/ft^2/Hr	ΔT	Heat Out Btu/ft^2/Hr	Solar Insolation Btu/ft^2/Hr
0.53	400	2370	111.3	54.7	279.4	76	40	215	49	35	179
0.75	579	2351	100.8	71.4	278.9	68	48	217	66	47	185
1.91	1041	2381	71.3	132.4	282.3	46	90	220	43	82	186
4.28	1417	2350	42.8	185.1	279.2	26	115	208	25	110	170

THE RELATIONSHIP BETWEEN CFM/ft^2 THROUGH THE

SEVENTY FOOT LONG GLAZED COLLECTOR AND THE ENERGY AVAILABLE

ALL-DAY OPERATION

THE DEHYDRATION OF FOOD PRODUCTS USING THE SOLAR COLLECTOR

Tests were made to determine the energy distribution when the solar collector was used as an energy source for a cabinet dehydrator, the design of which is shown in Fig. 19. Carrots were selected as a product to dry because they are available the year round, they are dried commercially in large quantity, and are similar in drying characteristics from batch to batch.

Carrots were purchased from a local wholesale market. They were washed, trimmed, and diced 3/8" x 3/8" x 3/16". After steam blanching, they were spread on wire mesh trays at the rate of 1½ lbs. per square foot. The trays were placed in the solar dryer at solar noon. The unit had been in operation for several hours previous to this and was in equilibrium. Data were gathered in regard to air flows and temperature both in the collector and the dehydrator. The collector configuration used was 70' long, with glazing, single pass. All three collectors were used for a total of 417 square feet of collector surface. The dehydrator was operated at 160°F. If the air from the collectors into the dehydrator was not at 160°F, then supplementary steam heat was supplied to raise the temperature to 160°F. Provisions were made to gather and weigh the condensate from the steam coils so that calculations could be made as to the heat supplied by the collector and heat supplied by the steam. The number of watts needed by the fan motor were also noted so that the heat supplied by the fan could be calculated. The percentage of air recirculated in the dehydrator was varied. The results are shown in Table 2.

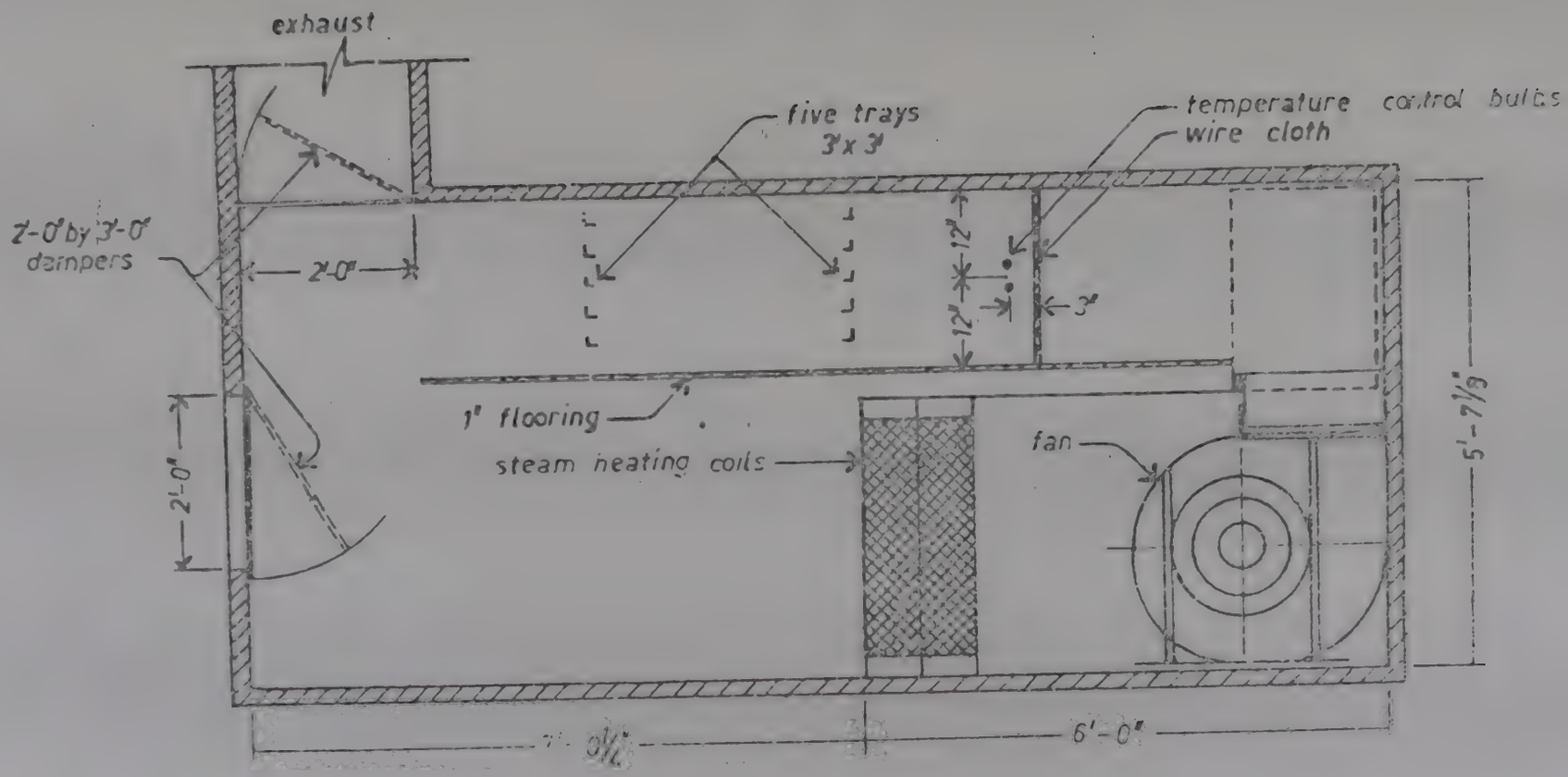

FIG. 19

PLAN VIEW OF THE CABINET DEHYDRATOR

TABLE 2

CFM from collector	% Recir-culation	Lineal Foot per min across tray	Ambient Air Temp.	From Collector		Into The Dehydrater		BTU Added by Fan	BTU Added by Steam	Total BTU Added	Lbs. H2O Evap.	% of Energy Supplied by the Collector
				Air Temp	BTU Added to Ambient Air	Temp.	BTU Added To Ambient Air					
1230	0%	983	81.0	127.3	30,274	126.4	27,642	1400	20,284	49,326	4.05	56%
633	0%	433	72.8	142.8	24,248	140.2	20,602	750	8,102	29,454	[illegible]	[illegible]
410	0%	279	79.1	161.3	18,222	154.6	14,583	510	1,218	[illegible]	[illegible]	[illegible]
1222	18%	1241	74.1	123.9	32,505	122.4	30,114	2,200	23,325	55,139	4.04	[illegible]
632	19%	629	68.3	140.3	24,290	137.7	21,265	981	7,670	[illegible]	[illegible]	[illegible]
410	17%	454	77.0	164.1	18,431	156.7	15,323	510	2,345	18,178	2.68	84%
630	47	960	78.7	141.4	22,550	138.5	19,347	1400	10,347	[illegible]	[illegible]	[illegible]
410	47%	600	75.8	160.9	18,197	154.2	15,142	750	3,668	19,560	3.12	77.4%

EVALUATION OF THE SECOND ONE HALF HOUR OF THE DEHYDRATION OF CARROTS

It will be noted that the temperature of the air leaving the collector is higher than the air entering the dehydrator. This is due to losses through the long duct between these units. Although insulated, it was subject to extensive heat loss. The second half hour of drying was chosen for the evaluation because the initial disturbance to the system caused by inserting a new tray of the product had passed by. At the same time the product was still in the constant rate section of the drying curve. The drying curves are shown in Figs. 20 and 21. The recirculation values are the percentage of the air inside the dehydrator which should have been exhausted after having passed over the carrots but was not discharged. It was instead mixed with the fresh incoming air from the collector. The L.F.M. referred to in the figures is the velocity of the air over the carrots, in lineal feet a minute.

The L.F.M. was the predominant factor in determining the rate of drying in these experiments. It far overshadowed any effect caused by varying the degree of recirculation.

The amount of Btu recoverable by the collectors goes up as the air volume from the collectors goes up. This is due to the higher temperature of the air leaving the collector. However, a penalty was paid in the particular system used for these experiments, in that the rate of drying also went down as the air volume from the collectors went down. This is due to the fact that the same fan that sucked the air through the collector also recirculated the air in the dryer. When the air flow from the collectors was reduced, the velocity of the air over the material being dried was also reduced. In a full scale design this would not be a factor because either a separate blower would be used for the collector and the dryer or design

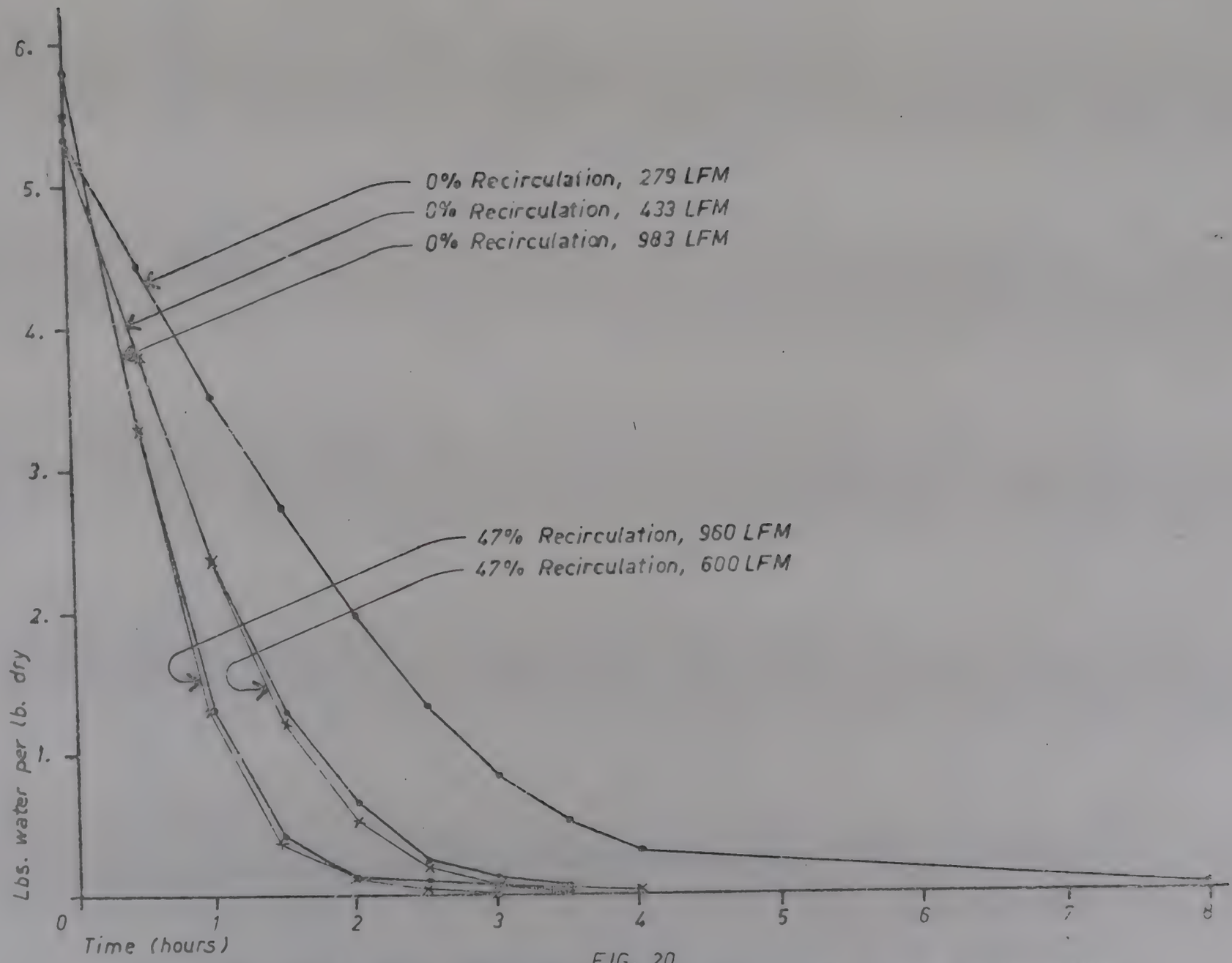

FIG. 20

RELATIONSHIP BETWEEN MOISTURE CONTENT AND TIME IN THE DEHYDRATOR

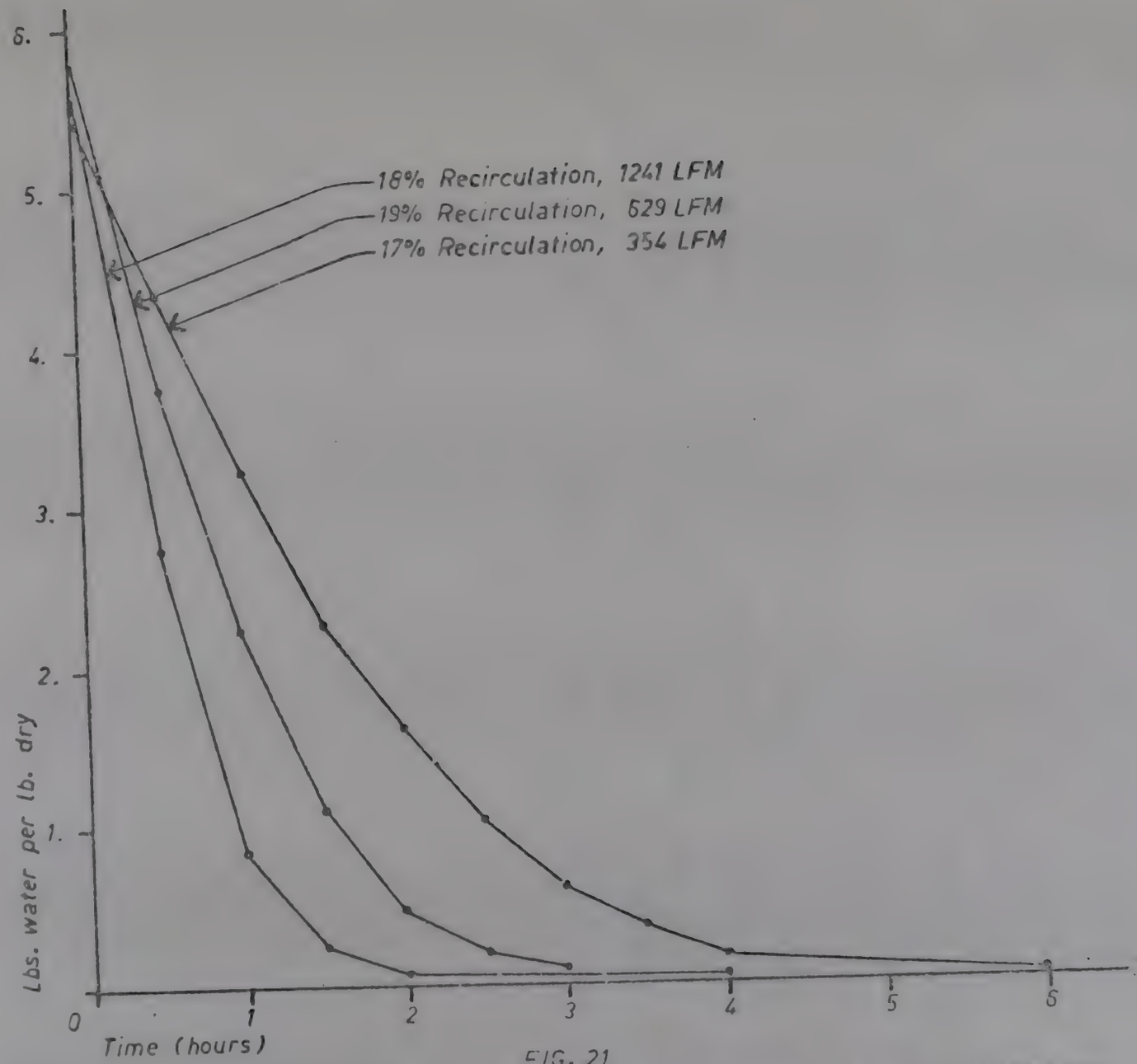

FIG. 21

RELATIONSHIP BETWEEN MOISTURE CONTENT AND TIME IN THE DEHYDRATOR

conditions would be selected to optimize velocity over the product, flow from the collectors and degree of recirculation.

One would expect that as the Btu added to the air by the collector went up that the Btu added by the steam would go down, but this is not true. The reason for this is that the volume of air being discharged from the dehydrator also goes up and, furthermore, the air coming in from the collector is colder, and so requires more energy to heat up. These results point to the need for carefully matching the volume of air from the collector and the volume through the drying section. If you change one you affect many other variables. Experiments on drying other fruits and vegetables were conducted in the unit with the bulk of the energy supplied by the collector. In all cases, the quality of the product was indistinguishable from that of material dried with steam heat only.

DETERMINATION OF THE SIZE OF COLLECTOR REQUIRED TO OPERATE A DEHYDRATOR

The following section is intended as an approximation only. The purpose of including it is to give the non-expert on solar energy or engineering in the commercial dehydration field some idea of what is obtainable from a solar collector. For a more elegant and precise prediction of what is obtainable, when you extrapolate the experimental results to an optimum commercial size unit, see the Appendixes B and C of this report.

A typical truck and tunnel dehydrator of fruits and vegetables will have a hot end temperature of 160°F and this air will be cooled by evaporation of water, radiation, and the warming up of new trays of the product which are regularly added to the tunnel. The discharge temperature would be near 110°F, or a temperature drop of 50°F air temperature. The volume of air blown through the tunnel would be in the order of 20,000 CFM or 1,265 pounds of air per minute. This quantity of air cooling 50°F will evaporate about 12.6 pounds of water a minute or 756 pounds per hour. If there is no recirculation of air and the ambient air temperature is 70°F, then it will require 27,900 Btu/min to heat this air to 160°F, or 40,000,000 Btu per day per tunnel. This energy could be supplied either by fossil fuel, by solar collectors, or by a combination of both. Table 3 shows the values obtained when these energy sources are mixed with the air volume requirements.

It must be emphasized that the values in Table 3 should be evaluated in the following light.

1. The area of the commercial collector was made up of units of the same area and dimensions as those used in the laboratory experiments.
2. That the collectors were flat plate, single glazed, black painted, and horizontal.
3. The unit was constructed in San Luis Obispo and operated in July in clear weather.
4. Loss in the duct work is similar to that of the laboratory experiments.
5. The heat added by the fan is not taken into account.

It would be expected that a carefully designed commercial unit would have the size of the air passages through the collectors optimized so as to increase the efficiency a few per cent. Broader and possibly longer units would also increase the efficiency by reducing heat loss from the edges and more effective heat transfer. Slanting the collectors so that they faced the sun at a better angle would increase the efficiency at this time of year and this latitude (35^{o}) by 8-10%. However, it would increase the non-collecting area of the collector and reduce the collection of diffuse light at those times when there was a cloud cover over the sun. The total effect of these modifications would probably allow a 20-25% reduction in the size of the collectors given in Table 3.

The values in Table 3 were obtained in the following manner. It is assumed that the size of the collector is such that 100% of the energy will be supplied by the sun for one hour before and after solar noon. The rest of the time supplementary heat will be required. First the ΔT needed to heat ambient air at $70^{o}F$ to the desired discharge temperature is determined. Then by consulting Fig. 11 the CFM/ft^2 air flow is determined. The

TABLE 3

Average Temperature Out of Collector at Noon ± 1 hour	From Fig. 11 and 12 Characteristics of Collector to Give at Noon the Indicated ΔT		Size of Collector Needed to Deliver 20,000 CFM at Indicated ΔT at Noon	Btu from this Collector Per Min at Noon	Btu/ft^2 Per Day from Fig. 22	Total Btu Per Day Available (Millions)	Percent of Total Heat Supplied by Collector
	CFM/ft^2	$Btu/ft^2/hr$					
160°F 90°ΔT	1.15	95	$17,391 ft^2$	27,535	752	13.0	[illegible]
140°F 70°ΔT	2.0	135	$10,000 ft^2$	22,500	1049	10.5	[illegible]
120°F 50°ΔT	3.3	173	$6,060 ft^2$	17,473	1333	8.0	[illegible]

Values are directly taken from the experimental results. They are for a tunnel dryer requiring 20,000 CFM @ 160°F, no recirculation, ambient air @ 70°F. It requires 27,535 Btu per minute or 40 million Btu per tunnel per day to operate.

CFM/ft^2 is entered into Fig. 12 to find the heat out of the collector in Btu/ft^2/hr. Once the CFM/ft^2 is found, then by dividing that value into the CFM needed by the tunnel the area of the collector is determined.

This will provide the necessary energy for the two hour period around solar noon. The energy that a collector of this size would supply between the hours of 0800 and 1900 Daylight Saving Time can be determined by consulting Fig. 22, obtained by plotting the data from Table 2. This value multiplied by the area of the collector will equal the total Btu/day available.

The results indicate that 32% of the energy of denydration can be supplied by a dryer of this design. It also points up the fact that if one were satisfied with a 20% replacement of fossil fuel with solar energy then a collector of 63% of the size needed to gather 32% of the energy from the sun would be needed.

The results of a similar, partly completed, calculation are shown in Table 4. However, a one hundred and forty foot long, two feet wide collector was used. As can be seen, there is more energy collected per square foot of surface than with the seventy feet long collector. The penalty you pay for this improvement is that the power requirement for the air blower goes up sharply. At some point the increase in blower horsepower is greater than the energy gain from increased collector length. What this optimum is can be calculated by the methods described in Appendixes B and C of this report.

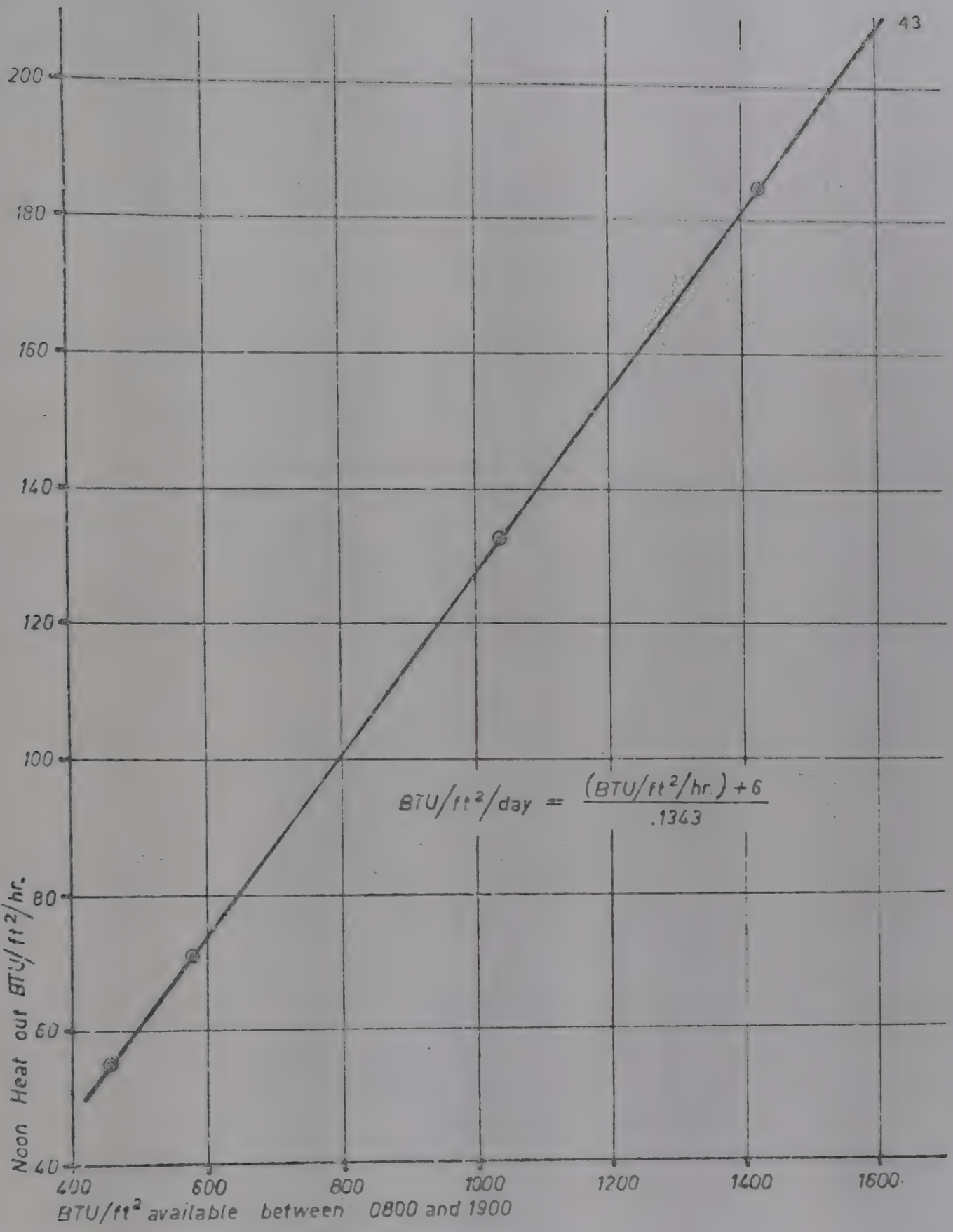

FIG. 22

RELATIONSHIP BETWEEN BTU/ft²/hr. AT NOON AND THE BTU/DAY AVAILABLE FROM A 70' x 2' GLAZED COLLECTOR

TABLE 4

Average Temperature ^{o}F Out of the Collector at Noon	From Fig. 14 and 15 Characteristics of Collector to Give the Indicated ΔT		Size of Collector Needed to Deliver 20,000 CFM	Btu/ft^2 Per Min. at Noon from Collector
	CFM/ft^2	$Btu/ft^2/hr$		
$160^{o}F$ ($\Delta T 90^{o}$)	1.55	130.0	$12,903 ft^2$	27,535
$140^{o}F$ ($\Delta T 70^{o}$)	2.33	159.1	$8,583 ft^2$	22,761
$120^{o}F$ ($\Delta T 50^{o}$)	3.49	169.3	$5,730 ft^2$	16,170

Values are directly taken from the experimental results. They are for a tunnel dryer requiring 20,000 CFM @ $160^{o}F$, no recirculation, ambient air @ $70^{o}F$. It requires 27,535 Btu per minute per tunnel to operate.

DISCUSSION AND CONCLUSIONS

There seems to be no reason why solar collectors cannot be used to heat air for food dehydration. The main problem is the high capital cost investment, but as will be pointed out in the appendix written by TRW, the gap between amortized capital costs for solar energy systems and current rates for the purchase of fossil fuels is closing rapidly. The most economical use of solar energy at the present time is its use as a preheater for a predominantly fossil fuel energy system. But this picture could change quickly. If natural gas becomes unavailable and other fuels continue to escalate in price, the construction of solar collector and storage systems for 24 hour operations becomes viable.

Workable systems might also include heat exchangers to recover waste heat. The drying process itself might be modified in two ways to adapt itself to optimized solar characteristics. Foods could be dried at lower than normal temperatures and/or the drying process could be interrupted at night. Both possibilities present bacteriological problems that must be considered. Previous work has indicated that for the majority of foods, 132°F is probably the lowest safe temperature. Many foods, however, such as walnuts and grains, are dried at temperatures as low as 110°F. For these purposes, relatively small collectors operating at high air flow rates would be sufficient. Current practice for most fruits and vegetables favors temperatures of 160°F or more. In addition to bacteriological problems, stopping the drying process at night would necessitate serious increases in drying machinery as well as major schedule changes.

As shown in Appendix B, experimental collector performance results with unglazed and single glazed collectors with single pass air flow are in substantial agreement with predictions based on standard collector analysis pro-

cedure referenced therein. The predicted increase in performance due to changes in the ratio of collector length to air passage depth at a fixed temperature rise was substantiated by the experiments. These results, along with the measured pressure loss data correlated in Appendix B, give a firm basis for collector geometry optimization. With known collector capital costs, fan electricity costs, and so on, these results allow calculation of the operating conditions and collector configuration that will minimize system life cycle costs.

Although not compared with predictions, test results with double-pass air flow (see Appendix B) show performance gains relative to single pass flow only at relatively low collector air temperatures. This may be a viable operating mode for air preheating purposes, but is detrimental to performance at higher operating temperatures.

ACKNOWLEDGMENT

I would like to acknowledge the extensive help of Professor Edgar Carnegie. He supervised the construction of the collector and the installation of the instrumentation. He also contributed a great deal to the success of the project by his suggestions and advice.

BIBLIOGRAPHY

1. Szulmayer, W. (1971). From Sun-drying to Solar Dehydration. 1. Methods and Equipments. Food Technology in Australia 23, 440-443.

2. Baird, C.D. and Bagnall, L.O. (1975) Solar Crop Drying in the Sunshine State. Presented at the American Society of Agricultural Engineers Meeting, Davis, California, June 22-25.

3. Selcuk, M.K., Ersay, O., and Akyurt, M. (1974). Development, Theoretical Analysis and Performance Evaluation of Shelf Type Solar Driers. Solar Energy 16, 81-88.

4. Akyurt, M. and Selcuk, M.K. (1973). A Solar Dryer Supplemented with Auxiliary Heating Systems for Continuous Operation. Solar Energy 14, 313-320.

5. Lawand, T.A. (1966). A Solar-cabinet Dryer. Presented at the Solar Energy Conference, Boston, Massachusetts, March, 21-23.

6. Phillips, A.L. (1965). Drying Coffee with Solar-heated Air. Solar Energy 9, 213-216.

7. Read, W.R., Choda, A., and Copper, P.I. (1974). A Solar Timber Kiln. Solar Energy 15, 309-316.

8. Buelow, F.H. (1961). Drying Crops with Solar Heated Air. Presented at the Solar Energy Conference, New Mexico, April 10.

9. Peterson, W.H. (1973). Solar Heat for Drying Shelled Corn. Presented at the ASAE Meeting, Regina, Saskatchewan.

10. Löf, G.O.G. (1962). Recent Investigations in the Use of Solar Energy for the Drying of Solids. Solar Energy 6, 122-128.

APPENDIX A

DATA ACQUISITION SYSTEMS

Edgar Carnegie

Agricultural Engineering Department

California Polytechnic State University

APPENDIX A

DATA ACQUISITION SYSTEMS

Edgar Carnegie

Agricultural Engineering Department

California Polytechnic State University

In evaluating any thermal system, temperatures at many locations as well as other data must be determined, in order to know the heat movement within a system. Manual recording was unsatisfactory, as requiring too much time and not accurate enough. Several systems were investigated including data loggers and data acquisition systems with micro processors. A Hewlett Packard 3050 A data acquisition system was finally chosen (Fig.1). This system allows for flexibility of random access to any channel at any time and also the capability of doing much of the number crunching that is necessary in the evaluation of a solar collector while the collector is in operation.

The programs for this system were loaded on four magnetic cards. The first card set up the subroutines that the main program will call. For example, subprogram titled "Time." A subroutine that calls the clock to obtain the time in months, days, hours, minutes, and seconds that a particular activity is taking place and loads this into an assigned memory in the calculator. Another subroutine "Temp" is a subroutine that converts voltages from the DVM to temperature and degrees Fahrenheit. The next programmed card sets up the memory locations and the channels that will be used by the various transducers that are connected to the scanner. The main program is stored and loaded on the last two cards. The main program (Fig. 2) starts the scanner at an assigned time and scans through

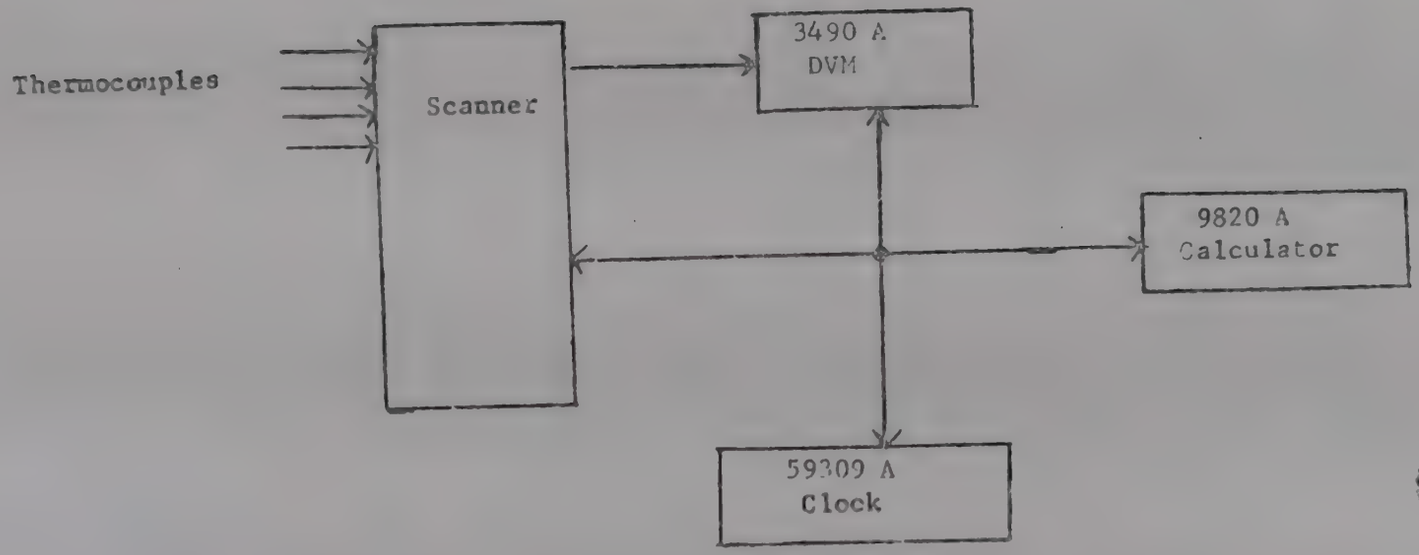

Figure 1

HP 3050 A Data Acquisition System

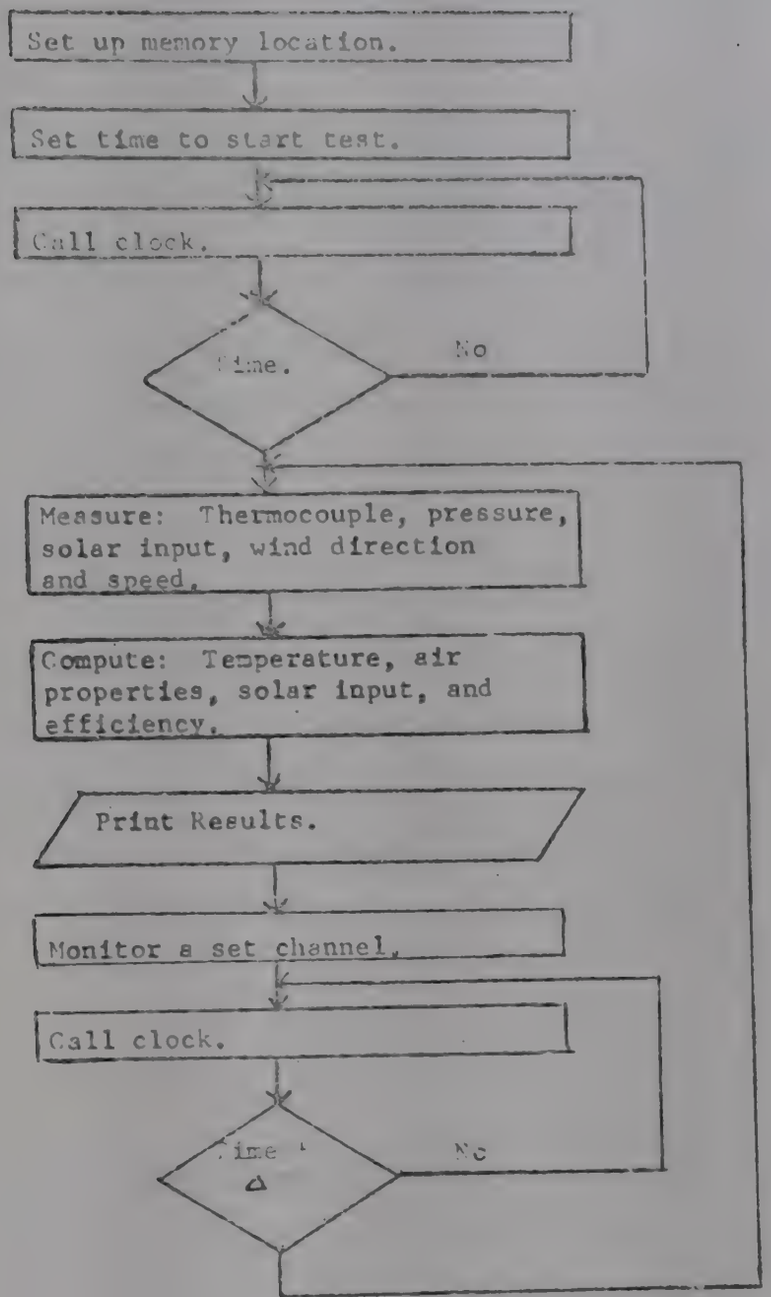

Figure 2

Flow chart of solar collector data acquisition system.

TR 1539
3/3/83

all the temperature channels five times and stores the average temperature which is then printed out as a channel and temperature. The program then loads the dry bulb and wet bulb temperatures and calculates psychrometric information on the incoming air to the collector. The calculator then calls for the measurement of the orifice meter, which was built according to ASME standard 19.5. Using standard orifice equations, the calculator then calculates the air flow through the collector. The calculator then measures the signal from the solar pyrometer and computes the Btu's per hour per square foot from the sun and then calculates the efficiency of the collector. It then calls for the information from the wind speed and direction transducers and prints out all the information (Fig. 3). The system is then put into a monitoring mode where it will monitor a predetermined channel and display the value waiting for the time to cycle again.

THERMOCOUPLES

The bulk of the transducers used in this system were copper-constantan thermocouples. Thirty surface measuring thermocouples and twelve air measuring thermocouples were used in each collector. The surface thermocouples were epoxied into a dimple 1/4 inch in diameter and 1/8 inch deep forced into the sheet metal of the collector. This appeared to give good surface contact and a true temperature of the surface of the collector. The air thermocouples were placed in the center of a 5/8 inch diameter polished aluminum tube to shield the thermocouples from the affects of radiant heat. In order to insure adequate air flow past the wick for the wet bulb temperature, a small

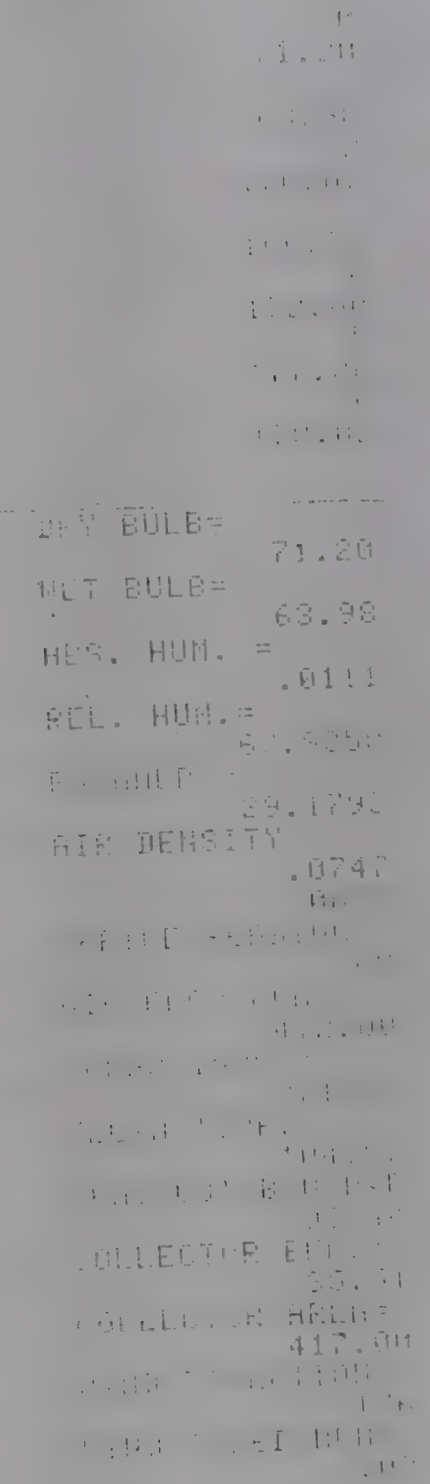

Figure 3

Typical Readout from the

Data Collector

fan was used to pull the air over the wet and dry bulb thermocouple at a fixed rate. This unit was placed at the entrance of the collector in order to obtain information on the air coming into and being heated by the solar collector. Eighteen thermocouple leads were bundled together and wrapped in aluminum foil and fed through a 3/4 inch black plastic pipe to each of the three insulated junction boxes on each collector. The leads were then connected to the thermocouples on the collector in the junction box. The aluminum shields were connected to the junction and grounded. This was done to minimize the affect of induced signals. The leads were then brought to the site of the data acquisition system where a male copper-constantan plug was placed on the end of each lead. A patch panel was then connected to an ice bath reference junction and also connected to the scanner. In this way, any thermocouple could be easily connected to any channel to give complete freedom for the experiments that were run. A grid of averaging thermocouples was also used in the duct work and in the dehydrator themselves. The averaging thermocouples were arranged in a grid pattern and connected in parallel.

CALCULATIONS

The following are the calculations which were programmed into the calculator in order to evaluate the incoming signals.

1. The psychrometric calculations start by obtaining the pressure of saturated steam from a fifth order Polynomial Regression,

$$Ps = 1.9068 \times 10^{-2} + 1.2669 \times 10^{-3}t + 1.3528 \times 10^{-5}t^2 + 4.3002 \times 10^{-7}t^3 + 2.1633 \times 10^{-10}t^4 + 2.1644 \times 10^{-11}t^5$$

where: Ps is the saturated steam pressure in psia

t is the temperature in degrees Fahrenheit

2. The pressure of the moisture in the air is calculated by

$$Pw = Ps(wb) - \frac{14.696 - Ps(wb)}{2830 - 1.44t(wb)} [t(db) - t(wb)]$$

where: Pw is the moisture pressure in the air in psia

wb stands for wet bulb

db stands for dry bulb

3. The absolute humidity or humidity ratio is then found.

$$H = \frac{.622 \times Pw}{14.696 - Pw}$$

where: H is the humidity ratio in pounds of water/pounds of dry air

4. The Relative Humidity can easily be calculated at this time from RH = Pw/Ps

where: RH is the Relative Humidity

5. The amount of heat in the air, Enthalpy, is calculated by

$$h = .24t(db) + H[1060.8 + .444t(db)]$$

where: h is the enthalpy of the air in Btu/lb of air

6. The air density is then obtained with the use of the ideal gas law plus the density of the water vapor in the air by

$$\alpha = \left(\frac{(14.7 - Pw)}{.37041[t(db) + 460]}\right)\left(1 + \frac{H}{RH}\right)$$

where: α is the density of the air in pounds/ft^3 at the wet and dry bulb conditions

The density of the air can now be determined with the relationship

$$\frac{\alpha\ 1}{t_1 + 460} = \frac{\alpha\ 2}{t_2 + 460}$$

for any temperature in the system.

7. Air rates were calculated with the use of standard orifice equations

$$CFM = \frac{5.98217 \times C \times d^2 \sqrt{P/\alpha}}{\sqrt{1 - B^4}}$$

where: $C/\sqrt{1 + B^4}$ is the discharge coefficients for a square-edged orifice for a given B ratio

B^4 is the ratio d/D

d is the diameter of the orifice

D is the diameter of the pipe

P is the pressure drop across the orifice in inches of water

A third order polynomial regression was obtained for the discharge coefficients for the two orifices used for the 6 inch orifice.

$$\frac{C}{\sqrt{1 + B^4}} = .63737 - 5.5846 \times 10^{-5}V + 7.7037 \times 10^{-8}V^2 - 2.2578 \times 10^{-11}V^3$$

and for a 9 inch orifice

$$\frac{C}{\sqrt{1 + B^4}} = .77697 - 4.599 \times 10^{-5}V + 1.3759 \times 10^{-8}V^2 - 1.1017 \times 10^{-12}V^3$$

where: V is the velocity of the air in the 12 inch air duct.

8. The heat collected from the solar collector was obtained

$$Q = \frac{(h_2 - h_1) \times 60 \times CFM \times \alpha}{A}$$

where: Q is the heat from the collector in $Btu/ft^2/hr$

A is the area of the collector in ft^2

9. The efficiency of the collector is obtained by

eff = Q/Is

where: Is is the solar insolation in $Btu/ft^2/hr$

APPENDIX B

COMPARISON OF PREDICTED SEAD COLLECTOR PERFORMANCE WITH EXPERIMENTAL RESULTS

Philip Niles

Environmental Engineering Department

California Polytechnic State University

Comparison of Predicted SLAD Collector Performance with Experimental Results

Philip Niles

1. INTRODUCTION

To be able to predict design and performance data for solar collectors of a similar configuration to those tested, but of possibly different size and operating at different flow rates and environmental conditions, it is necessary to extrapolate from known data points and/or use theoretical relations developed in the literature.

This report compares a portion of the experimental results described in the first section with what would be expected on the basis of the Hottel-Whillier-Bliss theoretical analysis procedure (see [2], [3]). Fig. 1 shows a cross-section of the collectors tested when using a single-glazing of Kalwall fiberglass-reinforced polyester sheet. For unglazed tests, the Kalwall and associated steel and wood supports were removed. The collectors were run in single-pass fashion (air flows in air channel only) in the unglazed tests, and single-pass and double-pass (air first flowing under glazing and returning through air-channels) in the single-glazed tests. Seventy-foot and one hundred and forty-foot collectors were tested in these configurations.

Few of the assumptions required in the theory can be explicitly verified due to the inability to independently vary most of the parameters. However, a comparison between the overall efficiency predictions and the experimental efficiency data shows whether or not the design parameter assumptions as a whole result in reasonably accurate performance predictions.

Because of the expected strong influence of solar-absorber to cooling-air

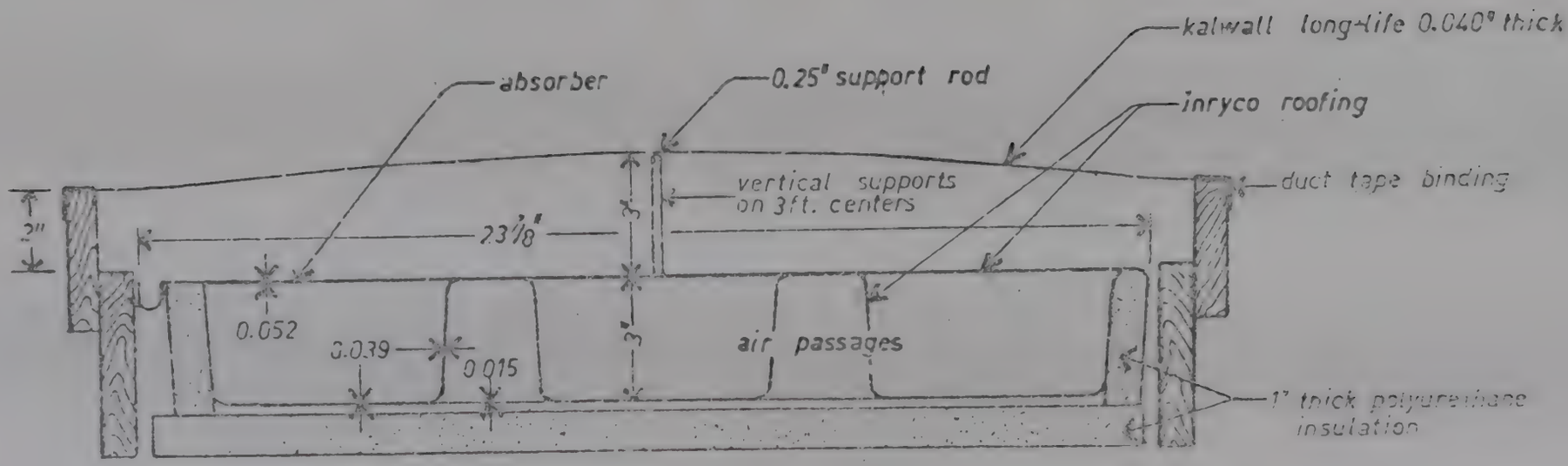

ALL METAL SURFACES PAINTED WITH BLACK NEXTEL
TOTAL FLOW AREA = 0.441 ft²
COLLECTOR HORIZONTAL WITH AIR FLOW NORTH TO SOUTH

Fig. 1
SINGLE GLAZED COLLECTOR CROSS-SECTION Scale ½" = 1"

heat transfer on predicted collector efficiency (and thus collector cost) and fan power (and thus operating cost), the tests were designed to make use of two different lengths of collector of the cross-section showing in Fig. 1. This gave the ability to obtain the same overall air temperature rise through the same shape collectors with two different flow velocities, and thus convective heat transfer coefficients, while keeping other independent variables constant.

2. PERFORMANCE RESULTS

Fig. 2 shows measured and calculated efficiencies as a function of the ratio of air temperature rise to insolation normal to the collector.

The data points shown are for tests made within 2 hours of solar noon, during which time the incidence angle of the sun on the collector was always less than 34^{o} during the May 25 to August 9 period for which data is reported. Insolation during these test was between 260 and 301 Btu/hr-ft^2, and wind velocities were generally light with gusts to 6 mph.

The basis for the theoretical curves in Fig. 2 is discussed in section 3 below.

Fig. 3 compares the data taken with a 70 ft collector in double-pass operation with that for the single-pass 140 ft collector from Fig. 2. These two sets of data were compared because of comparable pressure drops that occured in each when operating at the same flow rate of air. Thus they represent collectors of identical geometry and fan horsepower, but different air flow routes.

Fig.4 shows day-long collector performance for July 2, 1975. Numerical integration of this data showed a useful heat collection of 597 Btu/day-ft^2 with a total insolation of 2381 Btu/day-ft^2, for a day-long average efficiency of 597/2381 = .251 or 25.1%. The peak efficiency at solar noon was 27.5%

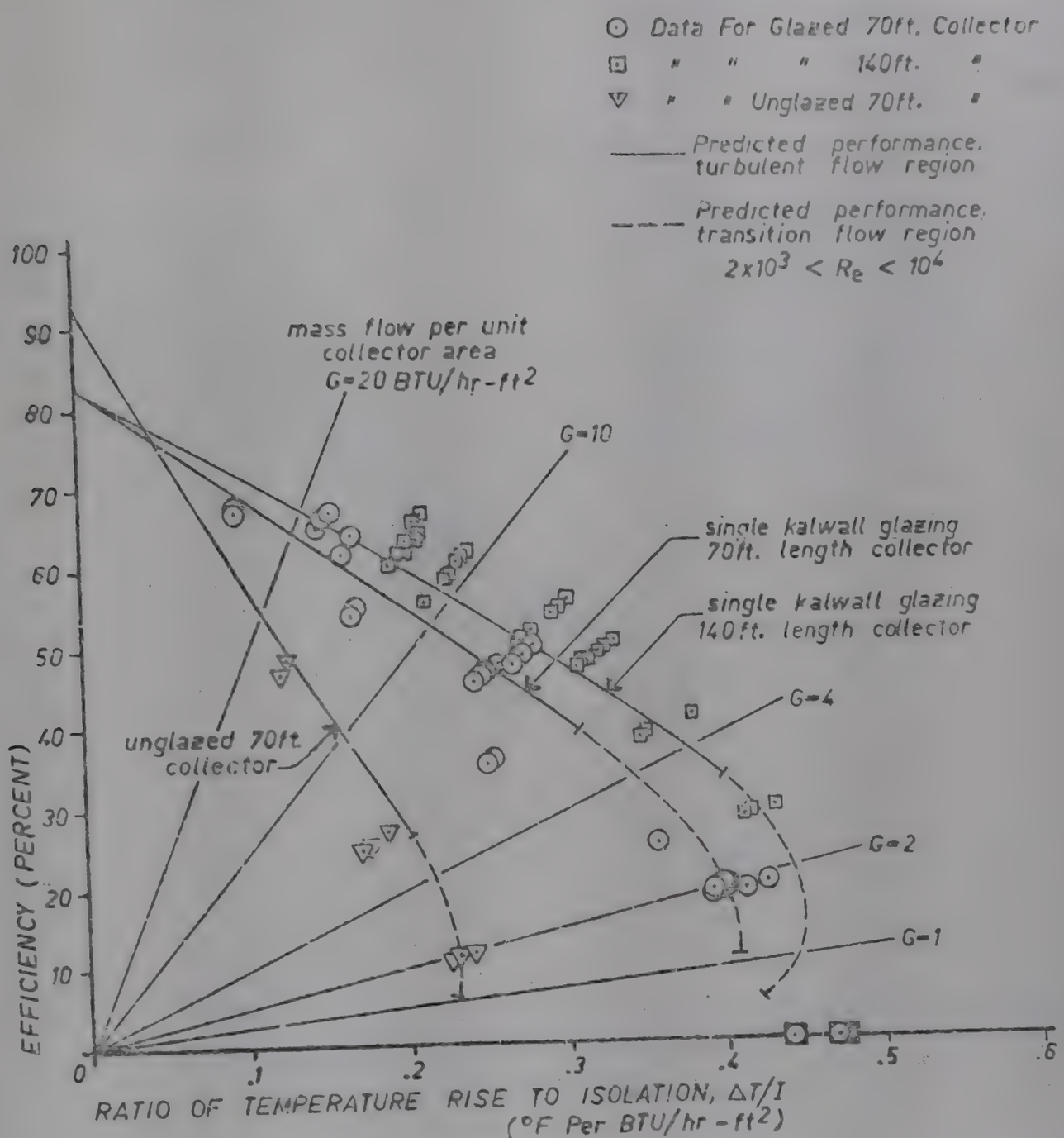

Fig. 2

Theorical And Experimental Collector Performance For Single Pass Operation

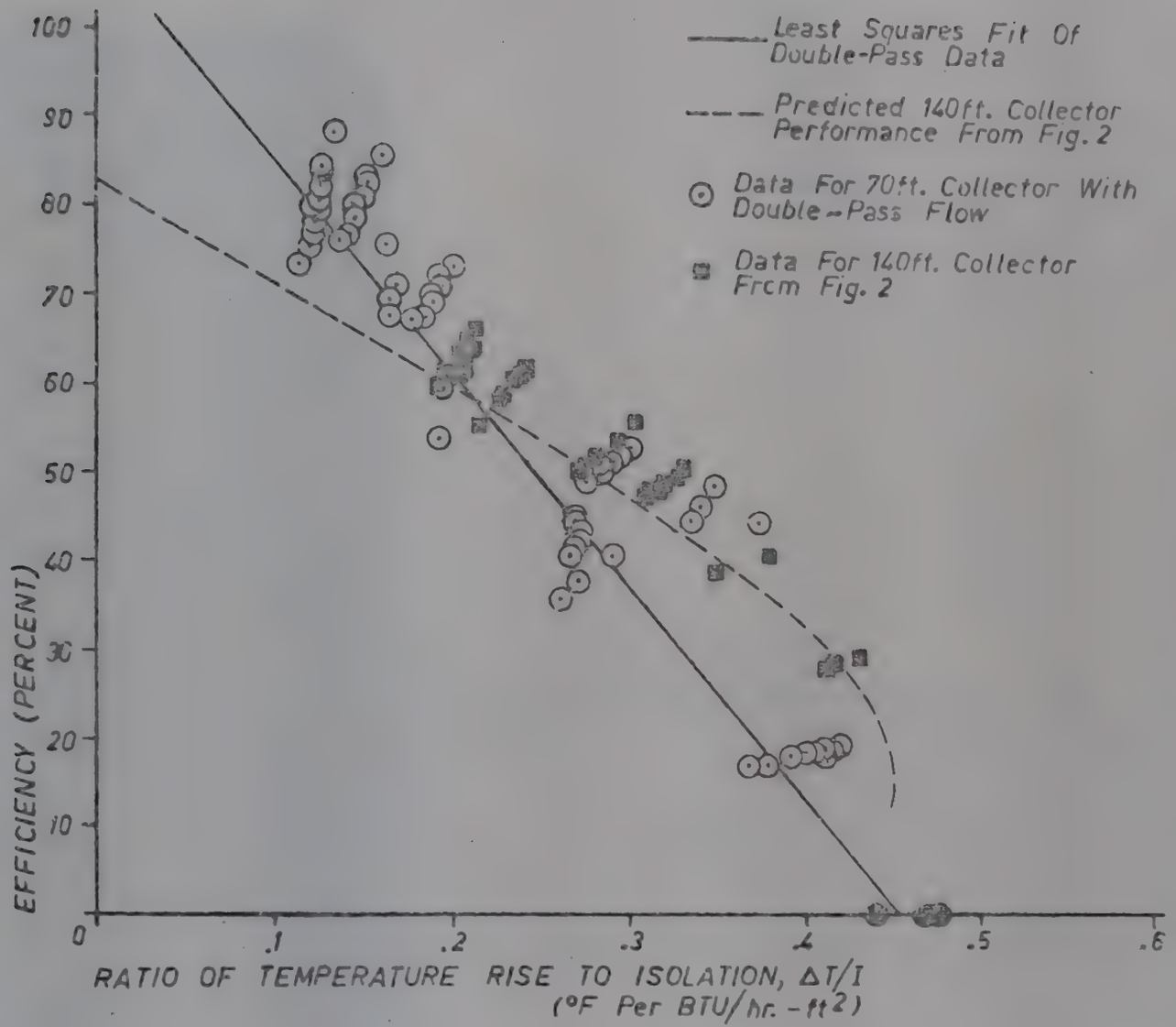

Fig. 3
Comparison Of Single And Double Pass Performance

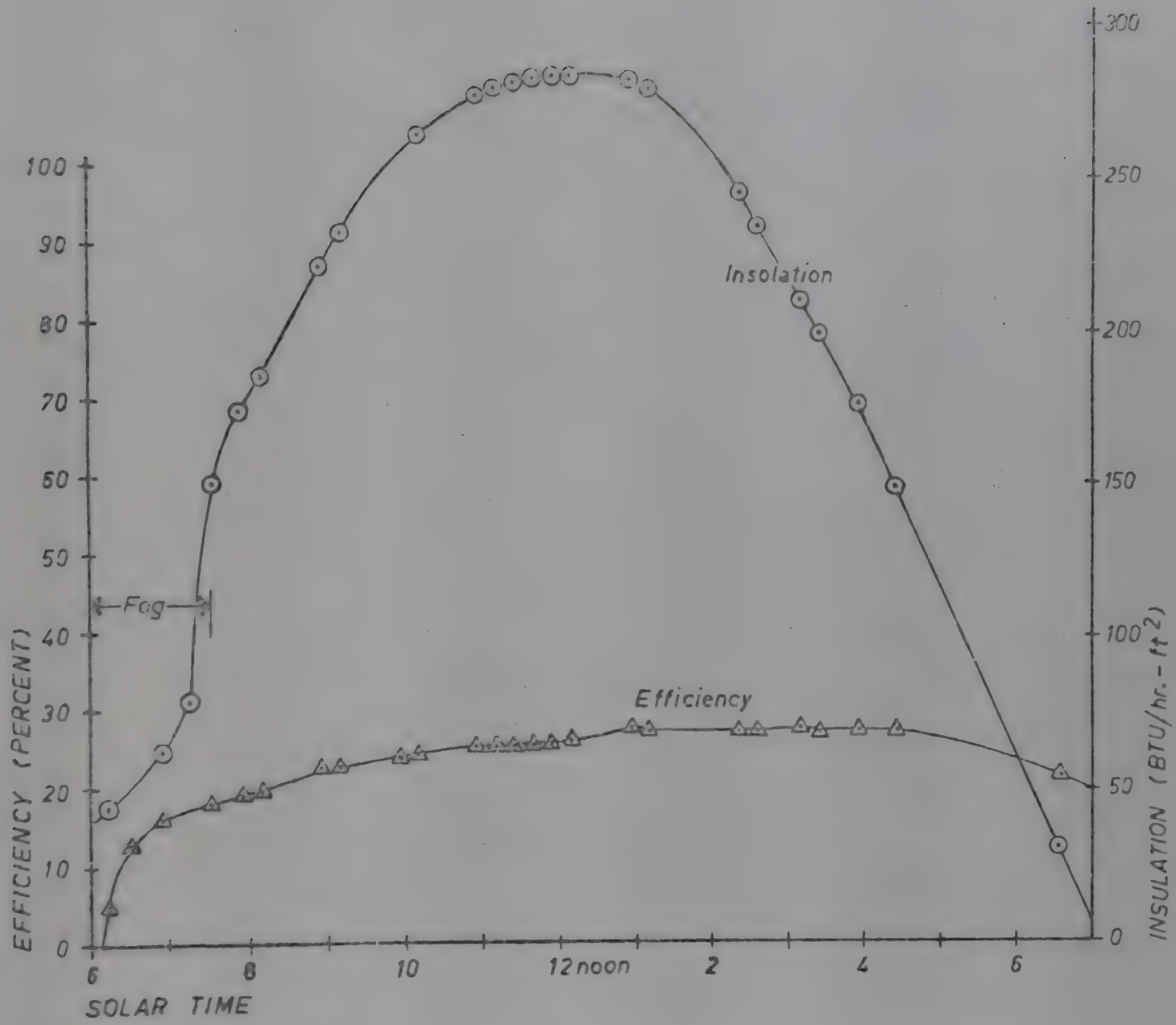

Fig. 4
Day-Long Performance For July 2, 1975

yielding a ratio of average to peak efficiency of

$$\frac{\eta_{ave}}{\eta_{peak}} = \frac{.251}{.275} = .91$$

Similar calculations on a number of days corroborated this value within about 2 percentage points.

3. BASIS OF PERFORMANCE PREDICTIONS

It can be shown by elementary energy balances (for example, see Threlkeld [1]) that the temperature rise of ambient air passing through a solar collector having uniform flow beneath a flat-plate absorber is given by

$$t_o = t_a + (\tau\alpha)\, I\varepsilon/U_F' \qquad (1)$$

Where:

$$\varepsilon = 1 - \exp\left[-\frac{U_F'}{G\, C_p\, (1 + U_F/hk)}\right]$$

t_a = ambient air temperature, ^oF

t_o = air temperature leaving collector, ^oF

$(\tau\alpha)$ = effective transmittance-absorptance product of cover and absorber combination, and essentially equal to the fraction of incident solar radiation that is absorbed by the absorber plate.

I = total (direct plus diffuse) insolation normal to the collector, Btu/hr-ft^2.

U_F = combined convection and radiation heat loss coefficient between absorber and the outdoor environment, Btu/hr-ft^2-^oF.

h = convection heat transfer coefficient from the inside wall of a circular duct (of equivalent hydraulic diameter to the

collector air channel) to the air flowing through the channel, Btu/hr-ft^2-^{o}F.

k = factor by which h is increased to account for heat transfer augmentation due to fins attached to the absorber plate, and due to radiation across the air channel.

U_F' = $U_F + U_B (1 + U_F/hk)$, is the effective heat loss coefficient including the losses through the insulation around the air channel.

U_B = overall heat conductance between the moving air and the outside environment via the insulated air channel walls. This was estimated to be 0.24 Btu/hr-ft^2-^{o}F (based on absorber area) for the configuration shown in Fig. 1.

Cp = specific heat of air taken as 0.24 (1 + 0.45w) Btu/lb-^{o}F, where w is the absolute humidity (lb water/lb air).

G = mass flow rate of air per unit area of collector surface exposed to the sun, lb/hr-ft^2.

Equation (1) is essentially that derived by Bliss [2] and Whillier [3], except for the method of including heat losses through the insulation. Since the useful heat output is G Cp (t_o - ta), then the instantaneous collector efficiency can be written

$$\eta = G \ C_p \ (t_o - t_a)/I \qquad (3)$$

Using (1), this becomes

$$\eta = \frac{G \quad Cp \ (\tau\alpha)\varepsilon}{U_F'} \qquad (4)$$

The average absorber plate temperature Tpa is required to determine U_F and can be determined from a relationship derived similar to (1),

$$Tpa = Ta + \frac{(\tau\alpha)I}{U_F'}\left(1 - \frac{G\ Cp}{U_F'}\ \varepsilon\right) \qquad (5)$$

Except for the explicit dependence of Tpa on I, and thus U_F on I, the efficiency predicted by (4) is only dependent on the ratio (to - ta)/I, and thus for a given flow rate, $\Delta T/I$ and η should be constant all day long for a given collector except for effects of large solar incidence angles and shading during early morning and late afternoon hours.

a. Determination of U_F: In the unglazed configuration. U_F was taken as the sum of the convective loss (1 + .3 V(mph)) Btu/hr-ft^{2}-^{o}F from Whillier [5], and the radiant loss to the atmosphere. The effective sky temperature for radiation was assumed to be 20°F below ambient, a value consistent with the "typical-atmosphere" correlation of Bliss [4] at the ambient dewpoint temperatures experiences during the test period. When single-glazed with a layer of Kalwall as shown in Fig. 1, U_F was taken as the sum of the conductance through the glazing as determined by equation 3.9 of Whillier [5], and the overall conductance through the 2-inch high wood glazing supports. The latter was calculated to be 0.07 Btu/hr-ft^{2}-°F based on the absorber area. To solve equation 3.9 [5] it was assumed that the black painted absorber and glazing emissivities were 0.95 and 0.9 respectively for thermal radiation. The Kalwall transmissivity to thermal radiation was assumed to be zero.

b. Determination of h and k. The convective heat transfer coefficient h was estimated using Reynolds analogy in the form $(St)(Pr)^{2/3} = f/8$, where the Moody friction factor f was determined from pressure drop measurements. Fig. 5 shows the experimental values of f plotted versus Reynolds number with properties evaluated at the average film temperatures in the collector. This figure shows the f values to generally be somewhat higher than was

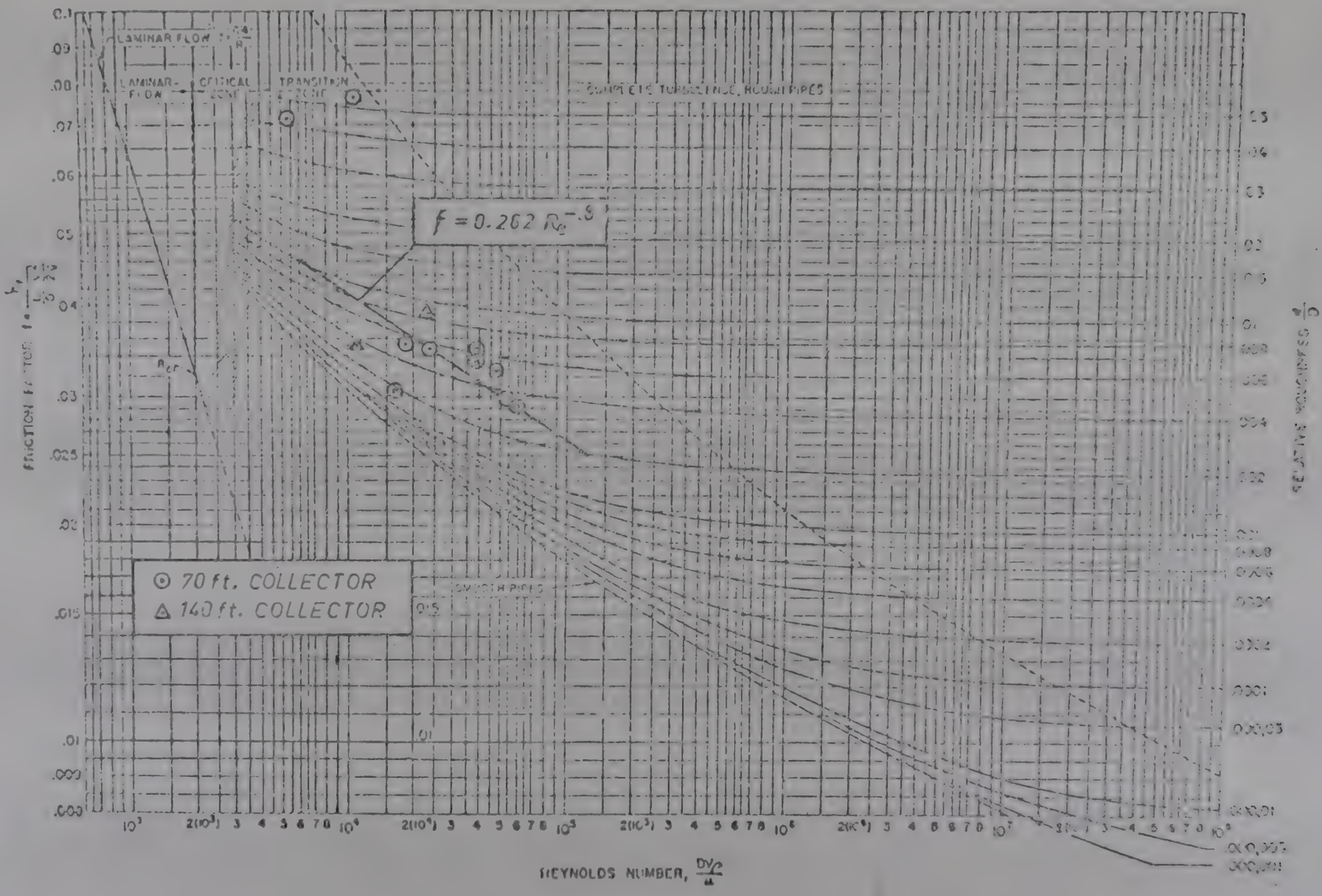

Fig. 5

Experimental Friction Factors Plotted On Moody Diagram (from [8])

expected for commercial galvonized duct for which ASHRAE suggested using a relative-roughness (see Fig. 5) of 0.003. It should be noted in this respect that the metal decking used had mechanically dimpled surfaces on vertical portions, apparently for structural reasons. The data for f was represented by the equation $f = 0.262\ Re^{-.8}$ for use in the heat transfer analysis. Substituting this into the above heat transfer equation yielded

$$Nu = 0.033\ Re^{0.8}\ Pr^{1/3} \qquad (6)$$

This equation was used to evaluate the coefficient h with all properties evaluated at the film temperature.

A hydraulic diameter of 0.28 ft was calculated for the air channel. The average flow velocity for the total channel cross-sectional area was used in calculations.

It should be noted that equation (6) was used in determining h for all the predictions of Fig. 2, even though at the low flow rates the Reynolds numbers correspond to the transition flow region.

It was estimated through fin and radiation heat transfer calculations that the channel in Fig. 1 would have 40% higher heat transfer from the absorber surface to the cooling air than would be expected if the fins and metal bottom did not conduct heat and were totally reflective to thermal radiation. Thus, a value of k = 1.4 was assumed. Although calculated for mid-range performance conditions, this value was used for all predictions.

c. Determination of $(\tau\alpha)$. A $(\tau\alpha)$ of 0.93 was assumed for the unglazed configuration with the flat-black painted absorber. In the glazed configuration this was modified as described by Whillier [5] to include the glazing transmissivity (measured with an Epply pyranometer as 0.88 for the 0.040 inch

Kalwall), cover reflections and cover solar heating (together increasing $(\tau\alpha)$ by about 1½%), and shading (primarily due to the center support rod) of about 1%. Together these factors reduce $(\tau\alpha)$ to 0.83 for the glazed collector cases.

All calculations were based on a wind velocity of 2 mph, and ambient temperature of 70 ^{o}F, and an insolation of 275 Btu/hr-ft^2.

4. DISCUSSION OF RESULTS AND CONCLUSION

A. Single-pass Operation. Comparing the experimental results with the predictions in Fig. 2 shows substantial agreement, with the theoretical predictions slightly optimistic in the unglazed case, and perhaps slightly pessimistic in the single-glazed cases. A number of possible parameter adjustments in the theoretical model could be made to account for the differences, but withoutexperimental verification with independently changed parameters, what adjustments are necessary in the model are not apparent.

The predicted increase in performance due to the increase in collector length (and thus flow velocity for a given $\Delta T/I$) from 70 ft to 140 ft is seen to be comparable to that which occured in the experiments, verifying the strong dependence of efficiency on flow velocity.

It may be noted that favorable agreement occured between the predicted and experimental results at the low flow rates corresponding to transition region flow, although fully turbulent convection was assumed in the predictions.

No experimental or theoretical results were obtained in the laminar flow region, although no-flow experimental results were obtained as shown on the abscissa of Fig. 2.

Because of the relatively close agreement between the experimental results and the predictions, it is felt that the theoretical methods used are sufficiently accurate to use on advanced planning of facilities wherein these type of collectors are desired.

Based on the theoretical equations, the losses through the insulation

and through the sides of the space between the glazing and absorber had a substantial effect on the performance. If the insulation were perfect (infinite thermal resistance), the efficiency curves for the single-glazed 70-foot case would be raised 7 efficiency points at a flow rate of 4 lb/hr-ft^2. If the sidewalls under the glazing were perfectly insulated, an additional 2 percentage points would be added. For the 140-foot collector, both insulation improvements would increase the efficiency by about 12 percentage points at G = 4.

B. Double-pass Operation. The comparison in Fig 3 between double-pass flow results and single-pass flow results (for the same flow pressure loss in each case) indicates that the double-pass configuration had a lower efficiency when operating with high temperature rises ($\Delta T/I > 0.2$) and higher efficiency at low temperature rises ($\Delta T/I < 0.2$). These results are qualitatively in agreement with the prediction made by Close [6] who predicted similar consequences in comparing a single-pass glazed collector to one with parallel flow under the glazing and in the air channel.

C. Day-long Efficiencies. Useful for design purposes, the day-long efficiencies were found to be within about a percentage point of 91% of the peak efficiency on a number of clear days. This number agrees with that suggested by Whillier [5] (see his equations 3.7 a and b) to account for the decrease in performance during the early morning and late afternoon.

D. Optimization of Collectors. As discussed in an earlier report [7] and substantiated in the tests reported herein, for a particular collector cross-section (such as Fig. 1) and temperature rise ($\Delta T/I$), the collector efficiency increases as the air velocity through the collector increases. Thus, for a given Btu output, the collector capitol costs would decrease with increasing air velocity. However, as the velocity increases, the fricitional pressure loss through the collector increases, taking more fan

power to drive the air and thus counteracting the cost savings accruing from the increased collector efficiency. This suggests that there is an optimum velocity that will minimize total ownership and operating costs. At what velocity (and corresponding collector length) this optimum occurs depends strongly on collector material and fabrication costs as well as system and electrical cost, temperature rise desired, operating days per year, and local environmental and insolation conditions.

This was the basis for the length optimization study done formerly [7], which led to the selection of the collector lengths tested. Because the test data reported here is in substantial agreement with performance assumed in that study, the optimum lengths reported there are still valid for the conditions assumed. It was assumed that electricity cost was 3 cents/KW-hr, with collector (and associated system) costs of 10 dollars per square foot of collector surface. Fan efficiency was assumed to be 70%, with collector operation of 12 hours per day over a 200 day per year season, during which the daily insolation was 2200 Btu/ft^2. Capital costs were assumed to be 20% of collector costs per year. Translating the optimum length result from the 1½ inch deep air channels studied in [7] to the 3 inch channels actually tested, shows that for a noon air temperature rise of 60 ^{o}F, an optimum length collector would be about 200 feet long. For a noon temperature rise of 130 ^{o}F, an optimum length of near 800 feet was indicated.

These results indicate somewhat longer collections than those tested are optimum because of the increase in channel depth tested over that for which the optimization study was made. Pending more detailed cost studies, these results are felt to be representative of the lengths of collectors required in crop drying applications for the channel depth assumed. Of course, decreasing channel depth will roughly proportionally decrease the optimum length required.

The optimization results assumed the geometry of Fig. 1 is fixed. However, of course, other configurations using other materials may lead to more cost effective collectors. In particular, air ducts made of a lighter gauge metal, possibly corrugated, and possibly surfaced in a selective fashion are felt to have promise. Depending on the temperature rise desired, double-glazing may also be cost-effective. Considerable interest is also being directed toward transparent air-inflated air-channels where the absorbing surface is at the bottom of the air channel. With inflatable glazing, this configuration would eliminate the need for costly energy-intensive metallic components.

REFERENCES

1. Threlkeld, J.L.; Thermal Environmental Engineering: 2nd Ed., p. 424, 1970.

2. Bliss, R.W.; "The Derivations of Several "Plate-Efficiency Factors" Useful in Design of Flat-Plate Solar Heat Collectors"; Solar Energy, vol. 3, p. 55, 1959.

3. Whillier, A.; "Black-Painted Solar Air Heaters of Conventional Design"; Solar Energy, vol. 8, No. 1, p. 31, 1964.

4. Bliss, R.W.; "Atmospheric Radiation Near the Surface of the Ground: A Summary for Engineers"; Solar Energy, vol.5, No. 3, p. 103, 1961.

5. Whillier, A.; "Design Factors Influencing Solar Collector Performance"; Chap. III of Low Temperature Engineering Applications of Solar Energy, American Society of Heating, Refrigeration and Air-Conditioning Engineers, Inc., New York, 1967.

6. Close, D.J.; "Solar Air Heaters For Low and Moderate Temperature Applications"; Solar Energy, vol. 7, No. 3, p. 117, 1963.

7. Niles, P.W., Pohl, J.G.; "Task 5 - Economic and Technical Feasibility of Solar Food Dehydration Systems. An Evaluation of a TRW Proposal", Appendix H of Research on the Application of Solar Energy to the Food Drying Industry, 3rd Quarter Progress Report, NSF/RANN/SE/GI 42944/PR/74/3, Oct. 1974.

8. Moody, L.B.; "Friction Factors for Pipe Flow"; Trans. ASME, vol. 66, p. 671, 1944.

Bibliography of other Reports Generated

1. NSF/RANN/SE/ERT 7419063/PR 74/2
2. NSF/RANN/SE/ERT 7419063/PR 74/3
3. NSF/RANN/SE/ERT 7419063/TR 74/4
4. NSF/RANN/SE/ERT 7419063/PR 74/4
5. NSF/RANN/SE/ERT 7419063/PR 75/1
6. NSF/RANN/SE/ERT 7419063/PR 75/2

Distribution List

Number of Copies	
5	Lloyd Herwig, Director Advanced Solar Energy Research & Technology National Science Foundation Washington D. C. 20550
10	Alex Schwarzkopf Program Manager Office of Public Technology Projects National Science Foundation Washington D. C. 20550
35	George S. James Information Programs Manager Advanced Energy Research & Technology National Science Foundation Washington D. C. 20550
14	One each to the following CPSU faculty/ staff: T. Lukes, H. Boroughs, E. Carnegie, P. Niles, J. Pohl, J. C. Gibson, H. Jones, L. MacDonald, D. Gerard, P. K. Phillips, G. Hasslein, R. Valpey, C.McKibbin, A. Amaral
6	One each to the Industry Advisory Board members
6	Jack M. Cherne TRW, Systems Application Center One Space Park 01 - 1010 Redondo Beach, California 90278
1	Sid Sternberg National Science Foundation California Institute of Technology, Thomas Lab Pasadena, California 91109
1	Dr. Ed Berry National Science Foundation Western Regional Office Room 214, 831 Mitten Road Burlingame, California 94010

NSF/RANN/GRANT ERT 7419063

RESEARCH ON THE APPLICATION OF SOLAR ENERGY TO THE FOOD DRYING INDUSTRY

FINAL REPORT

OCTOBER 1975

By

Jack M. Cherne Manager, Solar Energy

and

Rim A. Kaminskas Project Engineer

TRW REPORT NO. 27319-6002-RU-00

Prepared for

CALIFORNIA POLYTECHNIC STATE UNIVERSITY

San Luis Obispo California

TRW

SYSTEMS AND ENERGY

ONE SPACE PARK • REDONDO BEACH • CALIFORNIA

NSF/RANN/GRANT ERT 7419063

RESEARCH ON THE APPLICATION OF SOLAR ENERGY TO THE FOOD DRYING INDUSTRY

FINAL REPORT

OCTOBER 1975

By

Jack M. Cherne Manager, Solar Energy

and

Rim A. Kaminskas Project Engineer

TRW REPORT NO. 27319-6002-RU-00

Prepared for

CALIFORNIA POLYTECHNIC STATE UNIVERSITY

San Luis Obispo California

TRW

SYSTEMS AND ENERGY

ONE SPACE PARK • REDONDO BEACH • CALIFORNIA

CONTENTS

		Page
1.	INTRODUCTION	83
2.	EXPERIMENTAL SOLAR FOOD DRYING FACILITY	84
3.	SOLAR SYSTEM PERFORMANCE	92
4.	ANALYSIS OF A FULL SCALE DEMONSTRATION SYSTEM	98
5.	THE SOLAR DEHYDRATION PLANT	102
	5.1 Solar System Operation	102
	5.2 Solar System Description	103
	5.3 Solar Collector Performance	104
	5.4 Thermal Storage	105
	5.5 Reasons for Differences Between Earlier and Current System Performance Predictions	105
	5.6 Potential Energy Savings	106
6.	APPENDIX	107

ILLUSTRATIONS

		Page
1.	Solar Dehydration Facility at Cal Poly	85
2.	TRW-Cal Poly Solar Collector During Installation (Without Glazing)	85
3.	Cabinet Dehydrator at Cal Poly Solar Test Facility	85
4.	Collector Operating Modes	86
5.	Block Diagram of Experimental Solar Dehydration Facility at Cal Poly	86
6.	Solar Crop Drying Roof Plan and Details	88
7.	Solar Crop Drying Structural Details	89
8.	Solar Crop Drying Ductwork and Details	90
9.	Solar Crop Drying Collector Plans and Sections	91
10.	Cal Poly Collector Test Data	93
11.	Cal Poly Collector Test Data	94
12.	Cal Poly Collector Test Data	95
13.	Cal Poly Collector Efficiency	96
14.	Total Heat Collected During One Day and Temperature Rise as a Function of Air Flow Rate	96
15.	Comparison Between Cal Poly Collector Efficiency, Predicted Efficiency of Optimized Collector and Buelow's Efficiency	97
16.	Comparison of Performance Indexes for Oil-Fired Steam Production and Solar System	100
17.	TRW-Cal Poly Solar Collector Design	103
18.	Solar Dehydration Facility	103
19.	Block Diagram of System Operation	104
20.	Energy Distribution for a Typical 24-Hour Cycle	105
21.	Air Collector Thermal Model Flow Diagram	109
22.	Fan Power Program Flow Diagram	110

ACKNOWLEDGEMENTS

The work described in this report is based on the analysis and design of the solar energy system designed by TRW under subcontract to California Polytechnic State University, San Luis Obispo. Cal Poly is performing this research under a grant from the National Science Foundation (Grant ERT 7419063, formerly GI 42944).

This research program was under the direction of the Principal Investigator, Thomas M. Lukes, of Cal Poly. The data presented herein are based on tests performed on the complete food dehydration system at Cal Poly by Prof. Lukes.

The design of the full scale solar collectors and their integration into the food drying building was under the direction of Robert Schoof assisted by Ron Corey and Charles Weisenburger.

ABSTRACT

This report summarizes the work performed on tasks 6, 7, 9 and 10 on the "Application of Solar Energy to the Food Drying Industry" Program. This work was performed between October 1974 and August 1975 under a subcontract from the California Polytechnic State University. The objective of these tasks was to

- Design a laboratory-sized version of the produce dehydration plant.
- Assist Cal Poly in the operation of the laboratory experiment.
- Assist Cal Poly in the analysis of the experimental data.
- Develop the basis for a proof-of-concept plant which would be designed, built and tested during a later Phase.

During this time an experimental solar food dehydration system was designed, constructed at the Cal Poly Campus and tested. The test results indicated that the solar system operates considerably better than was predicted during earlier stages of this program and that use of solar energy is economically feasible for food dehydration, as well as other industrial applications requiring low grade heat.

1. INTRODUCTION

The food dehydration industry in the United States produces about 325 billion pounds of dried food products per year and consumes about 150 trillion BTU in the dehydration operation. Dehydration is performed primarily for food preservation purposes. Typical products include dried potatoes, rice, prunes, onions, garlic, corn, apples, dairy products, vegetables, etc. The specific technique used for dehydration varies with each product, but fundamentally, the process is the same for all: the product is prepared and placed on conveyor belts, bins, or trays and heated air is blown over the product until it is dry.

The food dehydration industry has historically used natural gas to provide heat for dehydration. Now the natural gas supply will be reduced, or possibly cut off entirely, in approximately five years to industrial users to save it for use in homes. As a result, the dehydration industry will be faced with finding a new source of energy to stay in business. The alternatives are heating oil, LNG, electricity, coal and solar energy.

When a dehydration plant manager is faced with a decision as to which one of these systems to install, he will, most likely, do it on the basis of cost and future availability of the energy source.

2. EXPERIMENTAL SOLAR FOOD DRYING FACILITY

An experimental solar drying facility was constructed at the Cal Poly Campus. The purpose of this facility was to obtain test data on the solar system performance and to experiment with actual drying of produce using solar energy. Photographs of the installation are shown in Figures 1, 2 and 3.

The facility consists of three solar collectors mounted on top of a building connected to a laboratory cabinet dehydrator. Each collector is 2 feet wide by 70 feet long. The ducting is arranged so that the collectors can be operated one at a time, two or three in parallel, and two in series. They also are designed so that they can be used unglazed, or glazed with various plastic materials. In addition, the collectors were designed so that they could operate in single pass, double pass and convection recovery modes are illustrated in Figure 4.

As can be seen from the photographs in Figures 1, 2, and 3, this position is not optimum from performance point of view. It would have been desirable to incline the solar collectors so that they receive maximum sunshine during the operating season. However, the horizontal position was a compromise to comply with Cal Poly campus aesthetic guidelines. Since system testing has been performed during summer months, the collector performance was not affected significantly.

The collectors were connected to a laboratory type dehydrator. The air was drawn through the air collectors, preheated by the solar energy and after entering the dryer, heated additionally when required by a steam-heated exchanger. A diagram showing the experimental setup is shown in Figure 5.

No thermal storage was provided because, at the time when the system was designed, it was thought that storage would not be economically justifiable. In retrospect, this decision was wrong. It turned out that crushed rock thermal storage would have been desirable to experiment with. However, since there is ample data on crushed rock thermal storage systems, system performance with storage can be predicted with suffucient confidence to design a full scale system for demonstration.

Figure 1. Solar Dehydration Facility at Cal Poly

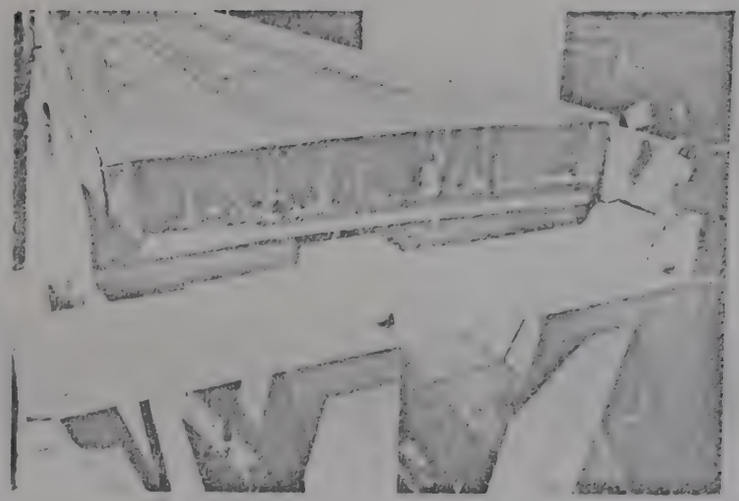

Figure 2. TRW-Cal Poly Solar Collector During Installation (Without Glazing)

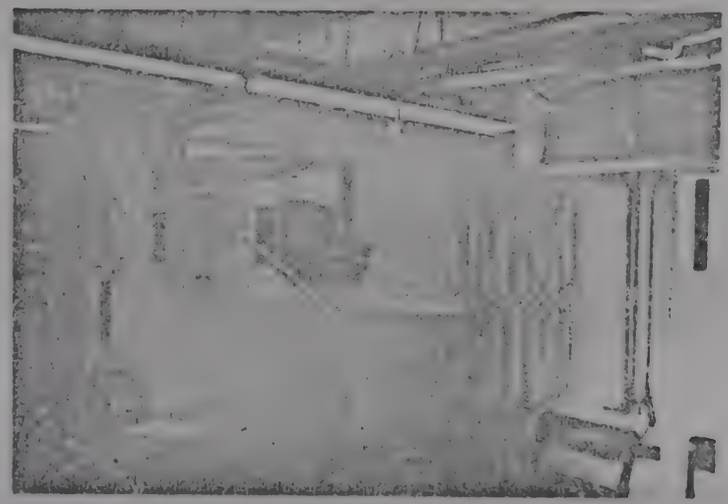

Figure 3. Cabinet Dehydrator at Cal Poly Solar Test Facility

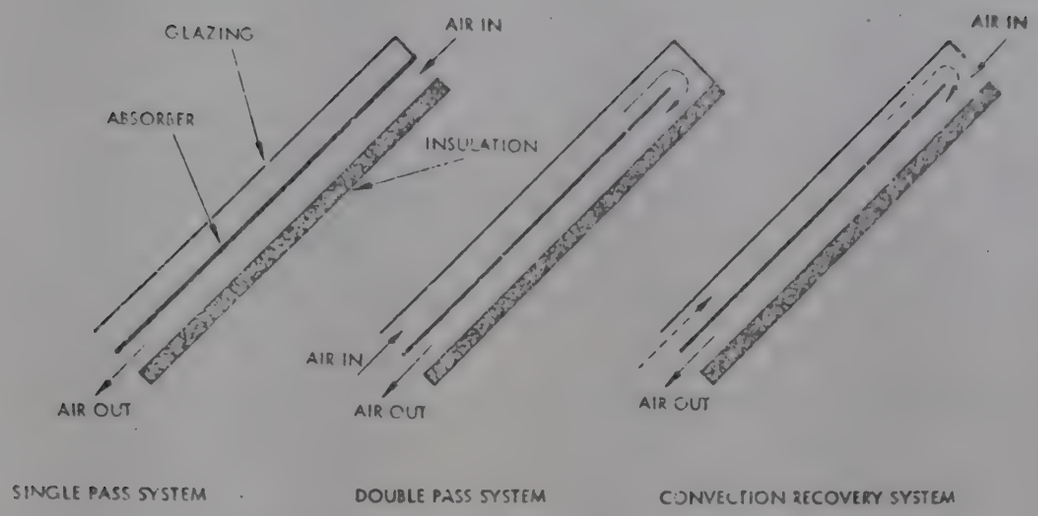

Figure 4. Collector Operating Modes

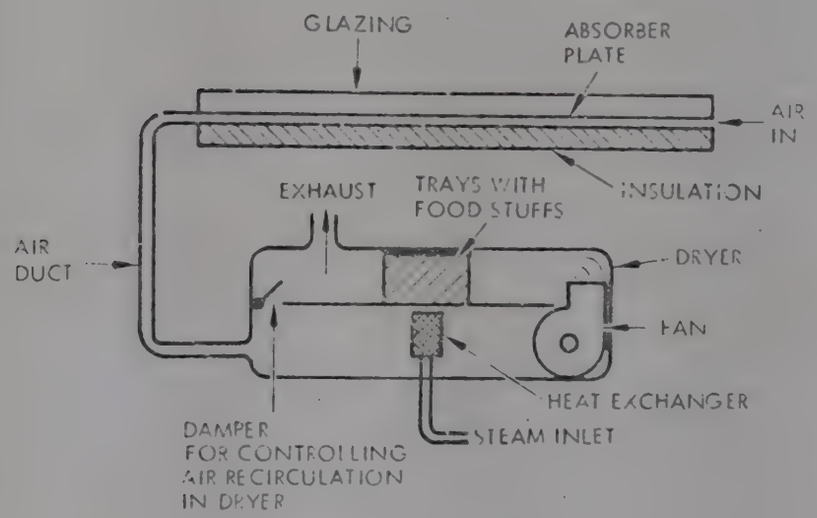

Figure 5. Block Diagram of Experimental Solar Dehydration Facility at Cal Poly

The entire solar collection system as well as the dehydrator were instrumented so that air temperatures, air flow rates, pressure drops (as well as temperatures of various parts of the collectors) could be monitored and recorded. The test data provided collector efficiency measurements at various configurations and air flow rates. In addition, several types of food-stuffs were dehydrated in the laboratory dryer to gain operating experience with the solar system as well as to evaluate dehydrated product quality.

Construction details of the experimental solar drying facility are shown in Figures 6 through 9.

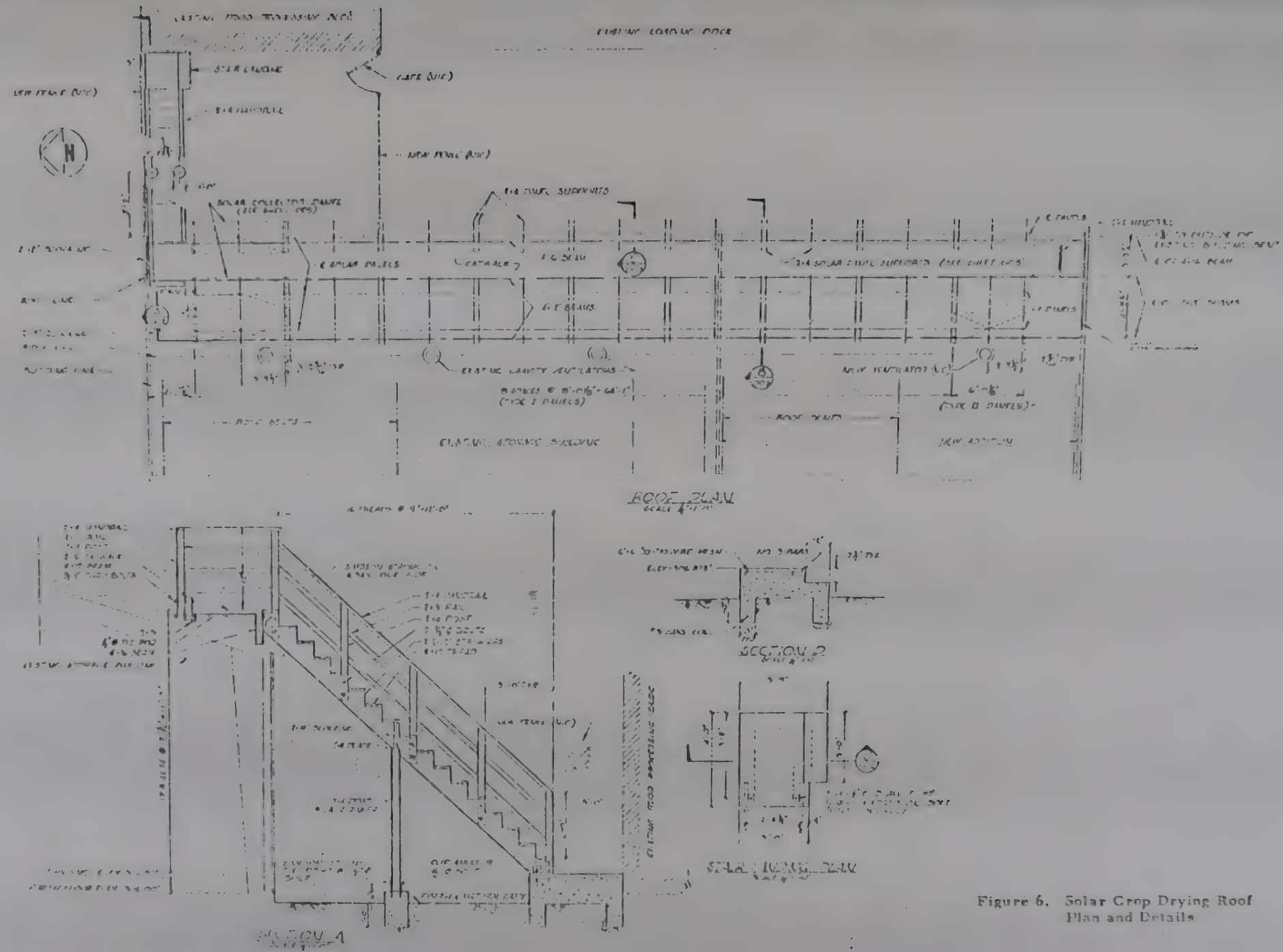

Figure 6. Solar Crop Drying Roof Plan and Details

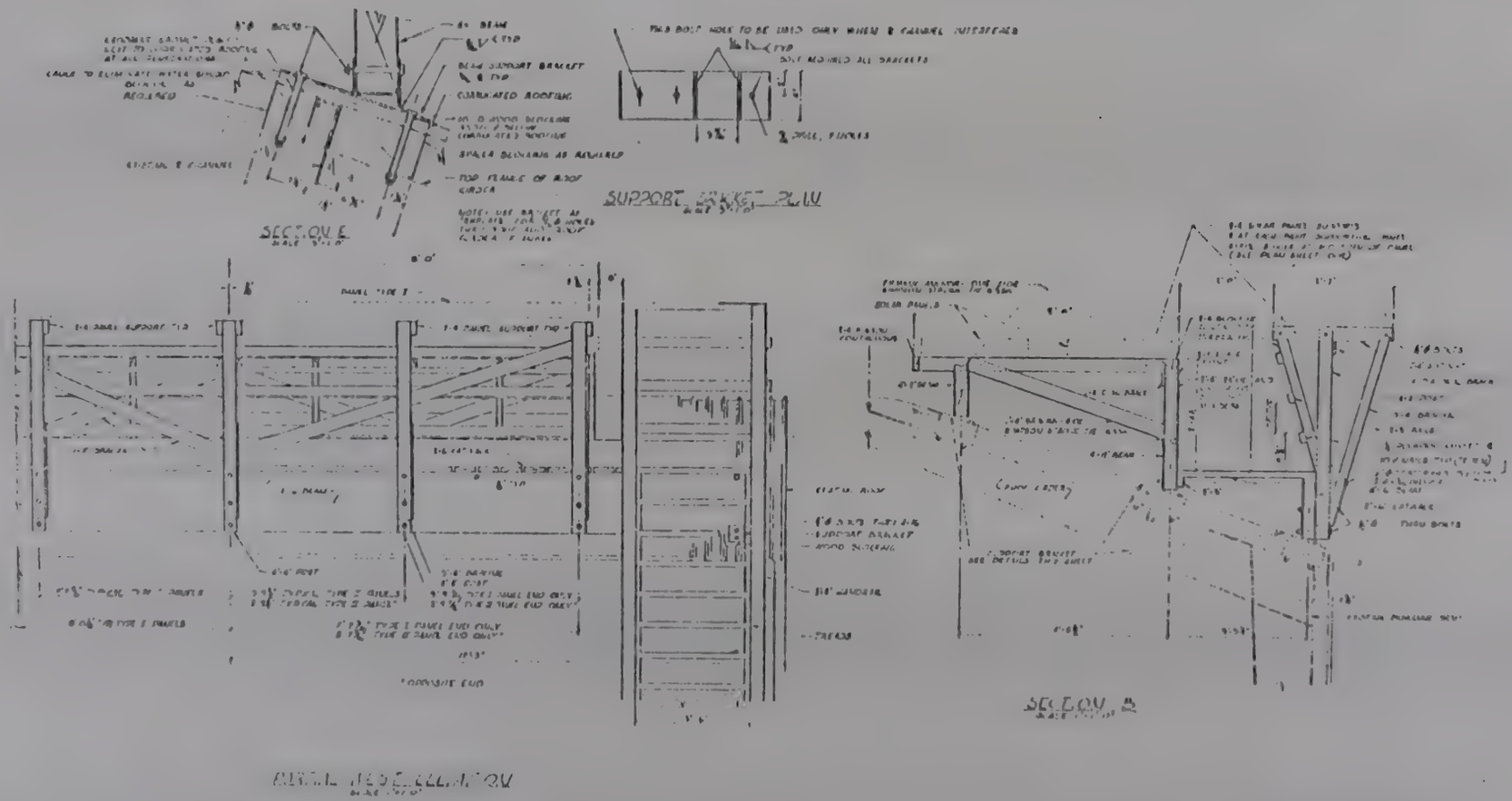

Figure 7. Solar Crop Drying Structural Details

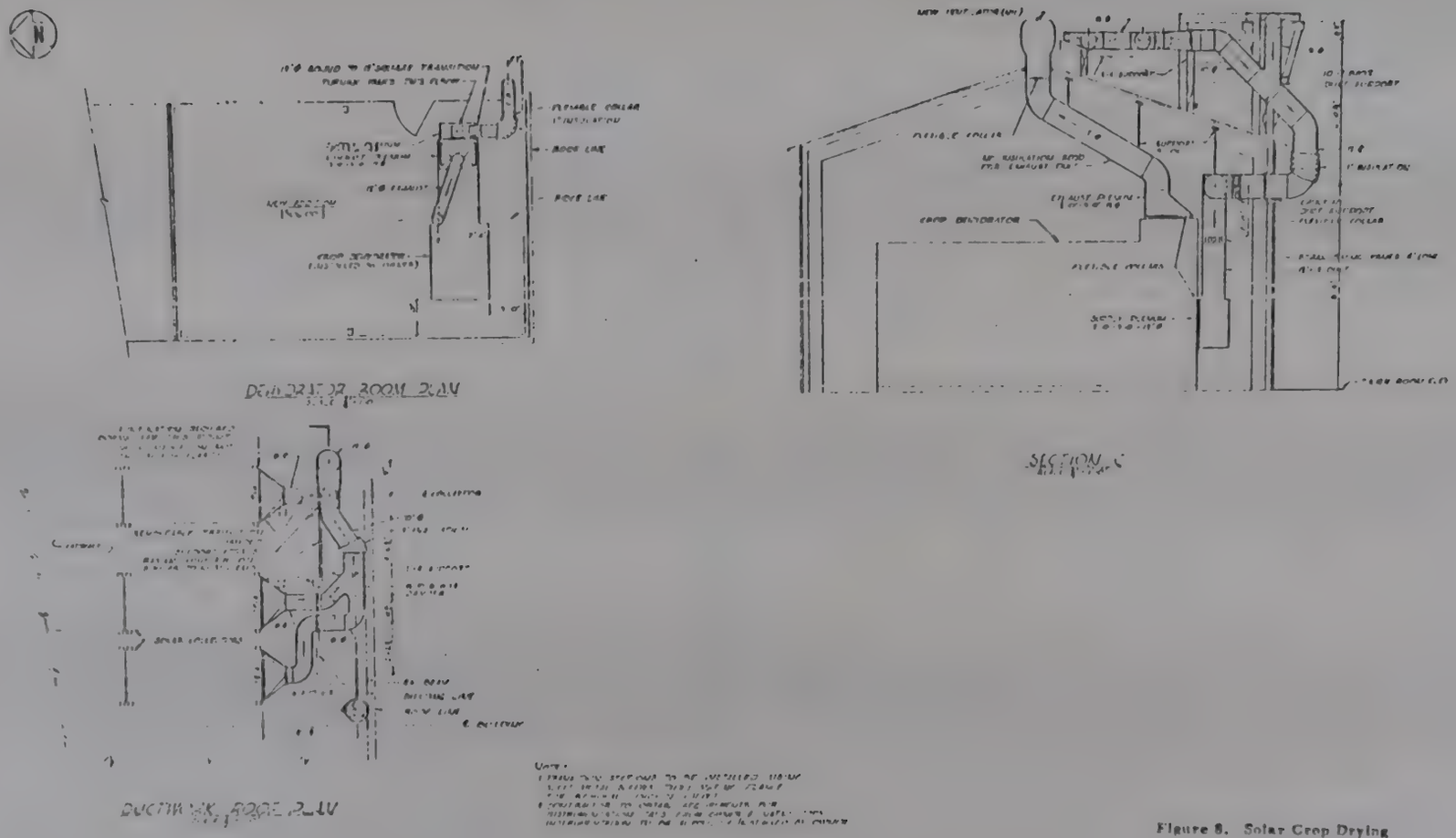

Figure 8. Solar Crop Drying Ductwork and Details

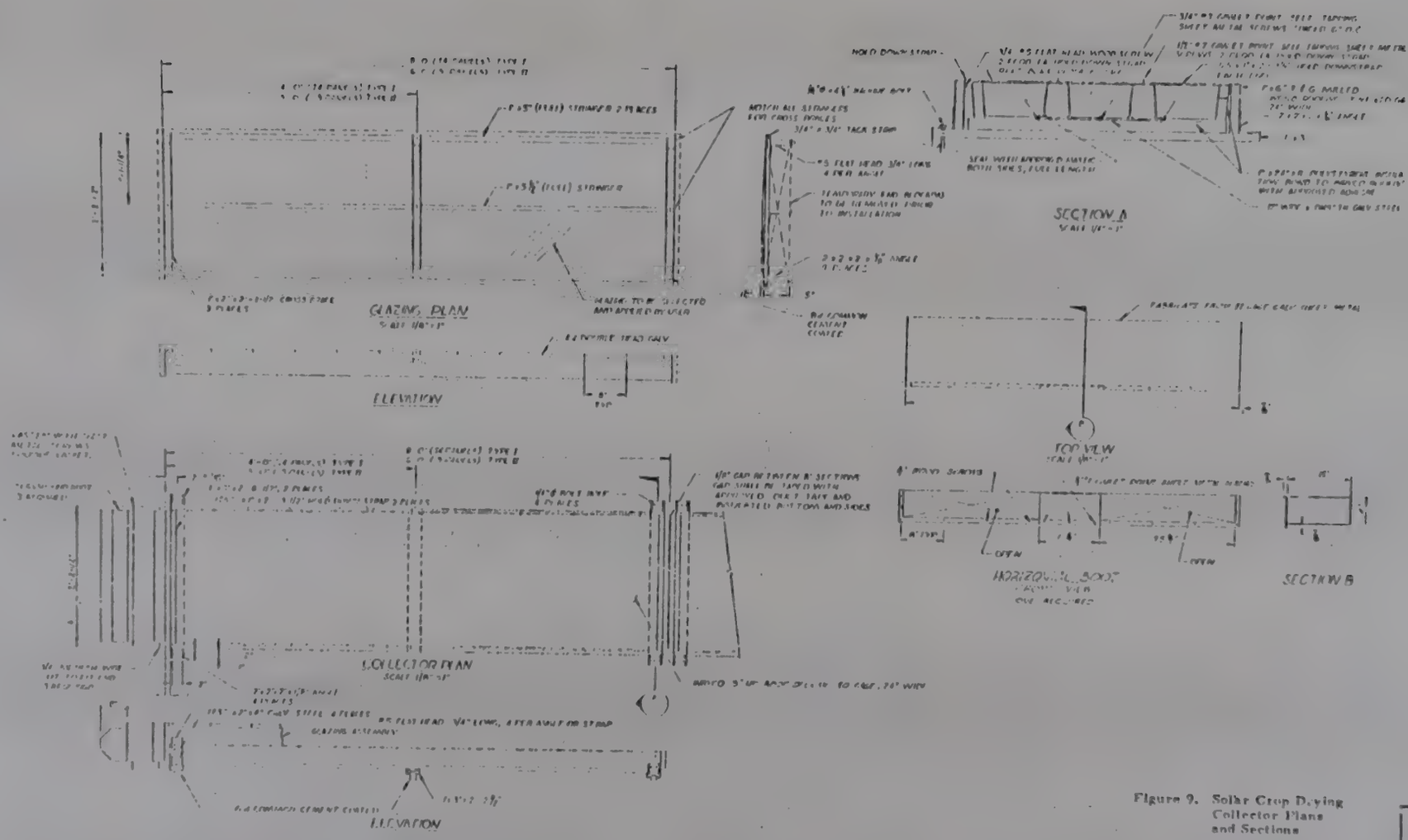

Figure 9. Solar Crop Drying Collector Plans and Sections

Reproduced from best available copy.

3. SOLAR SYSTEM PERFORMANCE

Extensive tests have been performed with the experimental solar food dehydration system. For detailed description of test procedures and results the reader is referred to the reports prepared by the principal investigator, Tom Lukes of Cal Poly. The following sections describe only the highlights of the test data and TRW's assessment of the results, especially as they pertain to performance predictions of a full scale plant. The collector configuration for which the data is presented was a 70 ft long collector in a single pass system using Kalwall glazing.

Figures 10 through 12 show insolation (Q in), solar collector energy output (Q out) and air temperature rise ΔT in the collector as a function of time of the day for air flow rates of 0.53, 0.74, and 1.9 cfm/ft^2, respectively.

The efficiency of the Cal Poly collector is presented in Figure 13.

The Cal Poly collector was originally intended to be used as an air preheater supplying only (on the order of) 25% of the dehydrator energy needs and, therefore, was optimized to operate at relatively small ΔT, high efficiency, and high air flow rates. However, very encouraging test data obtained at lower flow rates, in the range of 0.5 to 1.5 cfm/ft^2, brought out the possibility of operating the solar collector at a ΔT in the neighborhood of 100°F and thus supply a large part of the energy requirements of a dehydrator. However, to improve heat transfer from the collector surfaces to the air at these air flow rates, the duct sizes in the collector would have to be made much smaller to increase the air velocity. It is estimated that optimization of the duct sizes for flow rates in the range 0.5 to 1.5 cfm/ft^2 should improve the collector efficiency by about 10%. An additional 5% improvement in heat output could be obtained by inclining the collector from the horizontal position used at the Cal Poly facility to the appropriate angle facing south. The predicted efficiency of such an optimized collector is also shown in Figure 13. The computer models used to predict the collector performance are described in the Appendix. These models will be used to optimize the configuration of the collector for a full-scale demonstration.

Figure 14 presents the daily collector output in terms of Btu/ft^2-day and maximum ΔT (at noon) as a function of air flow rate in the collector. Data are given for the Cal Poly collector as is, as well as predictions for

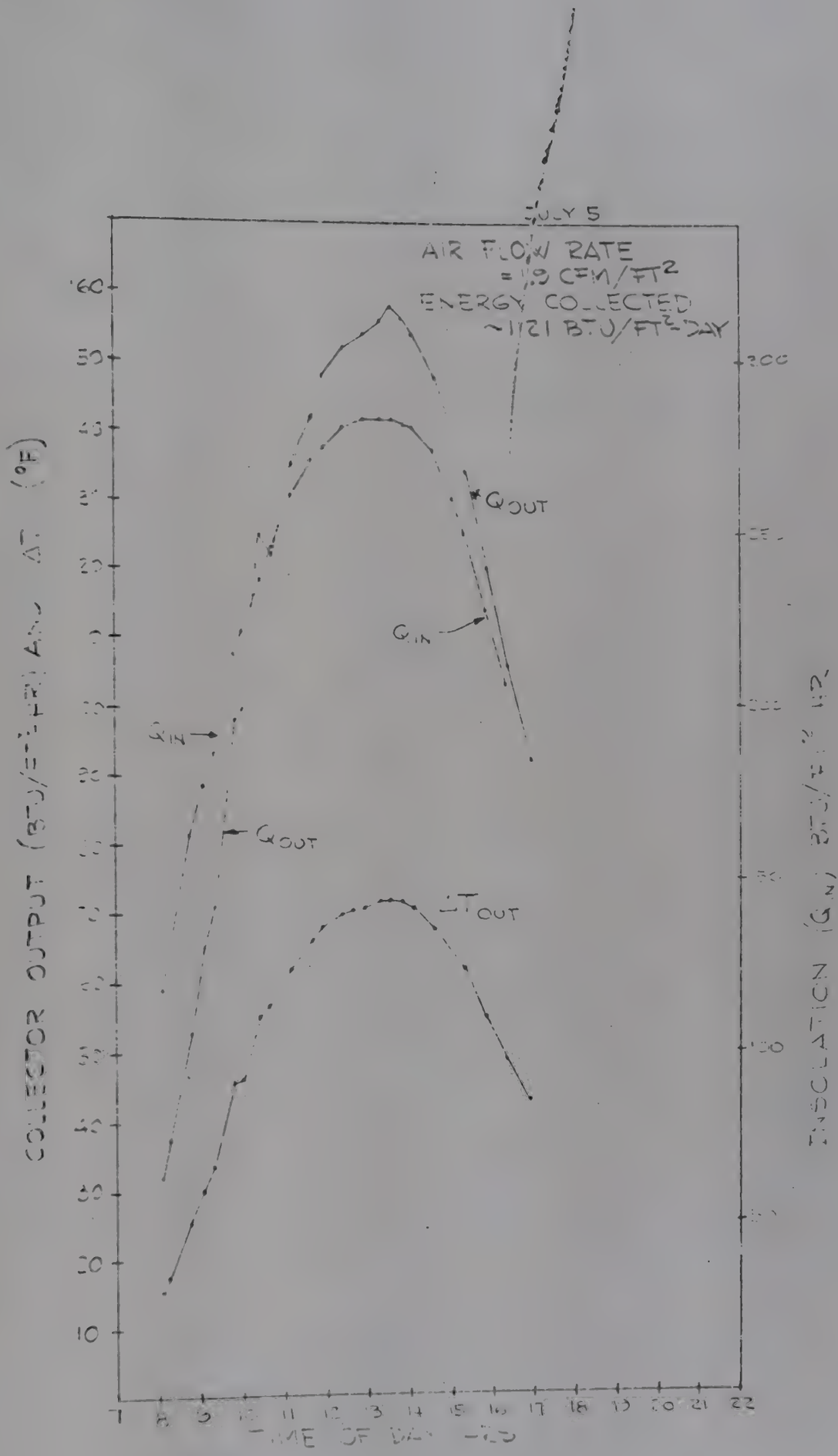

Figure 10. Cal Poly Collector Test Data

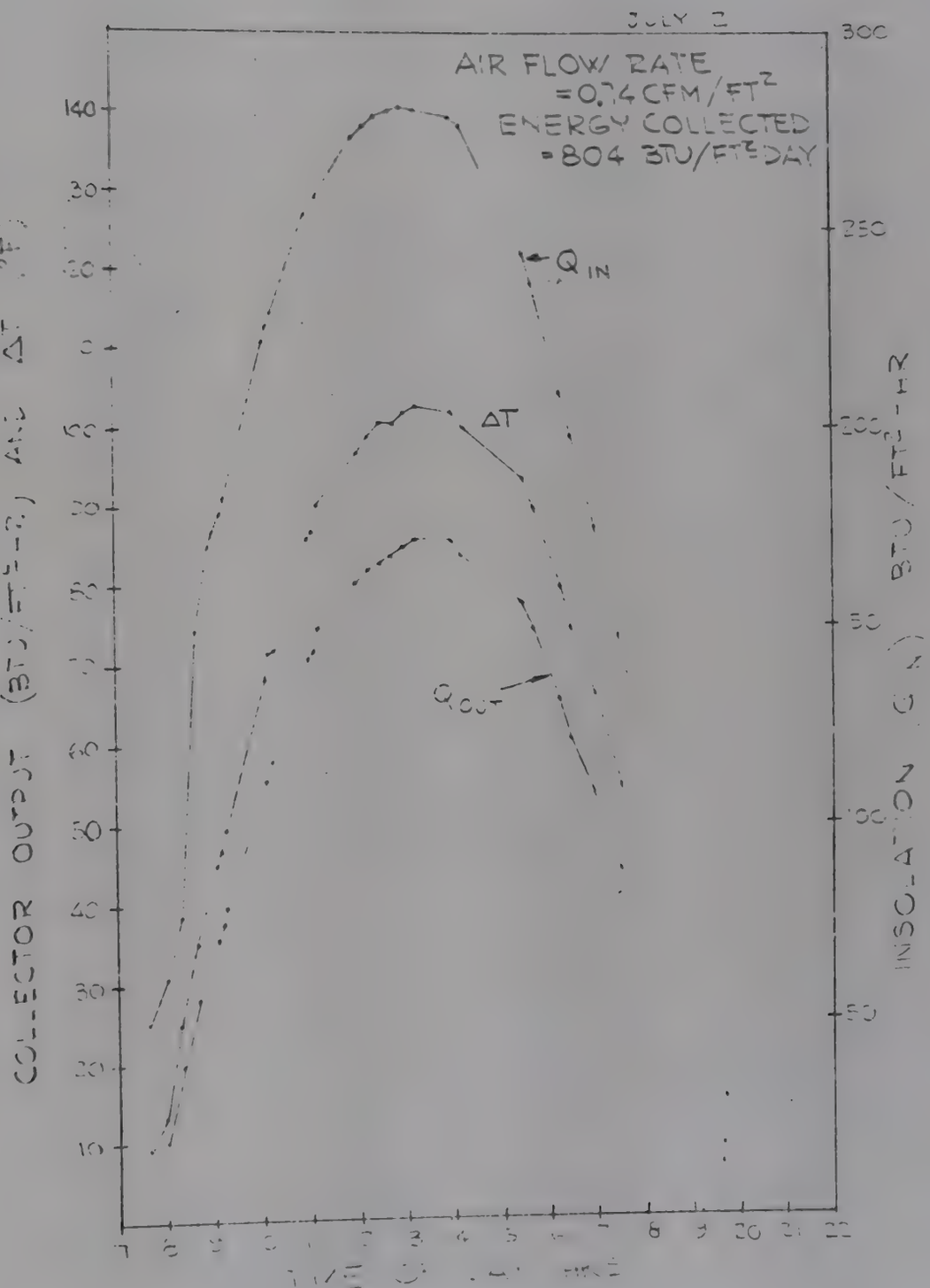

Figure 11. Cal Poly Collector Test Data

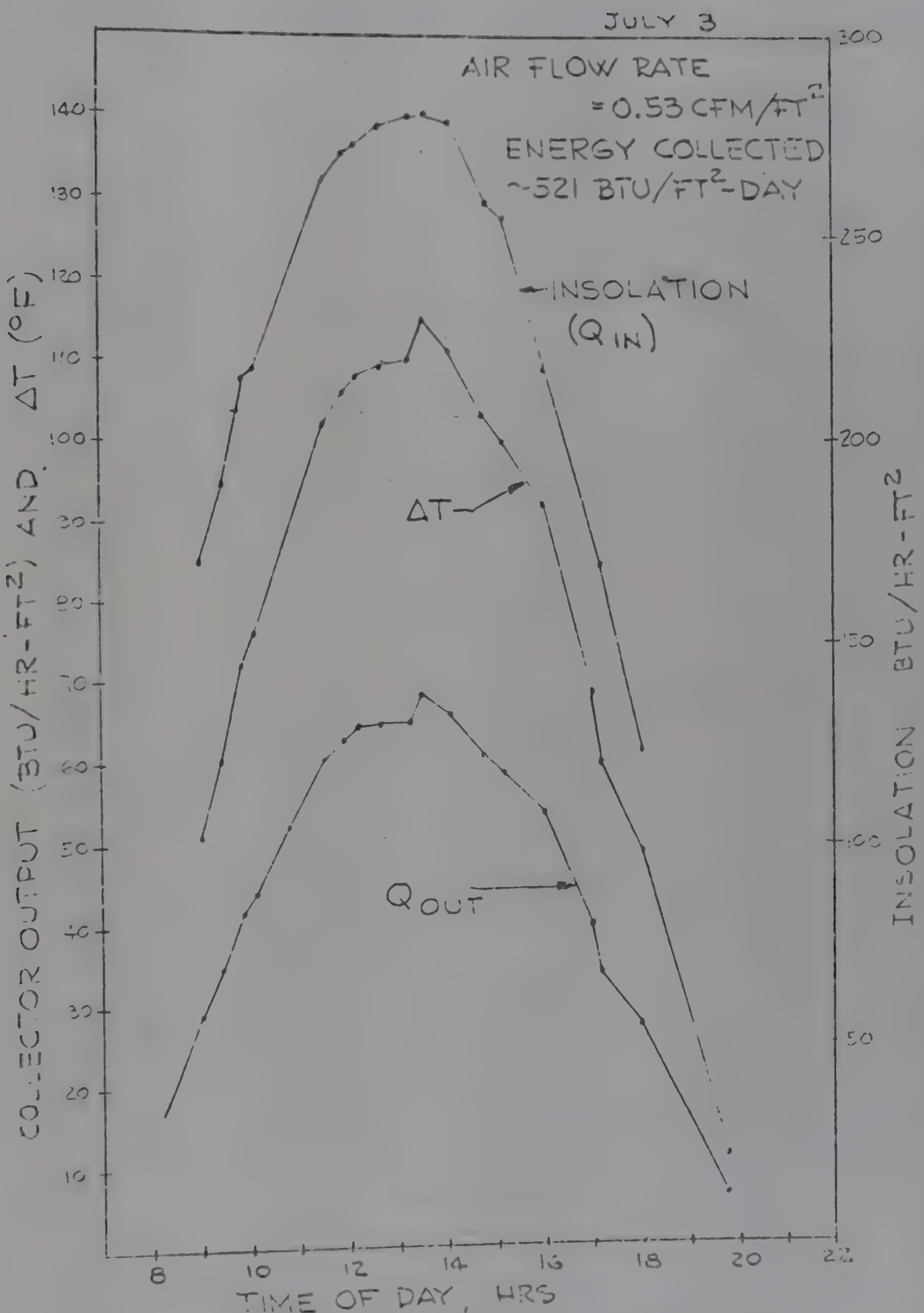

Figure 12. Cal Poly Collector Test Data

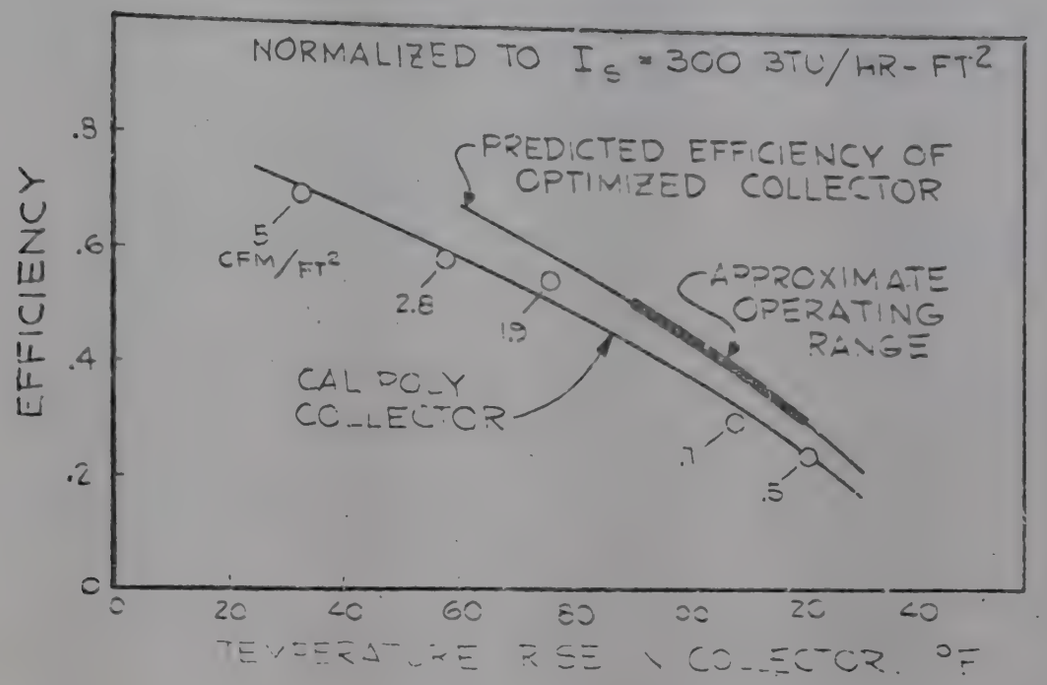

Figure 13. Cal Poly Collector Efficiency

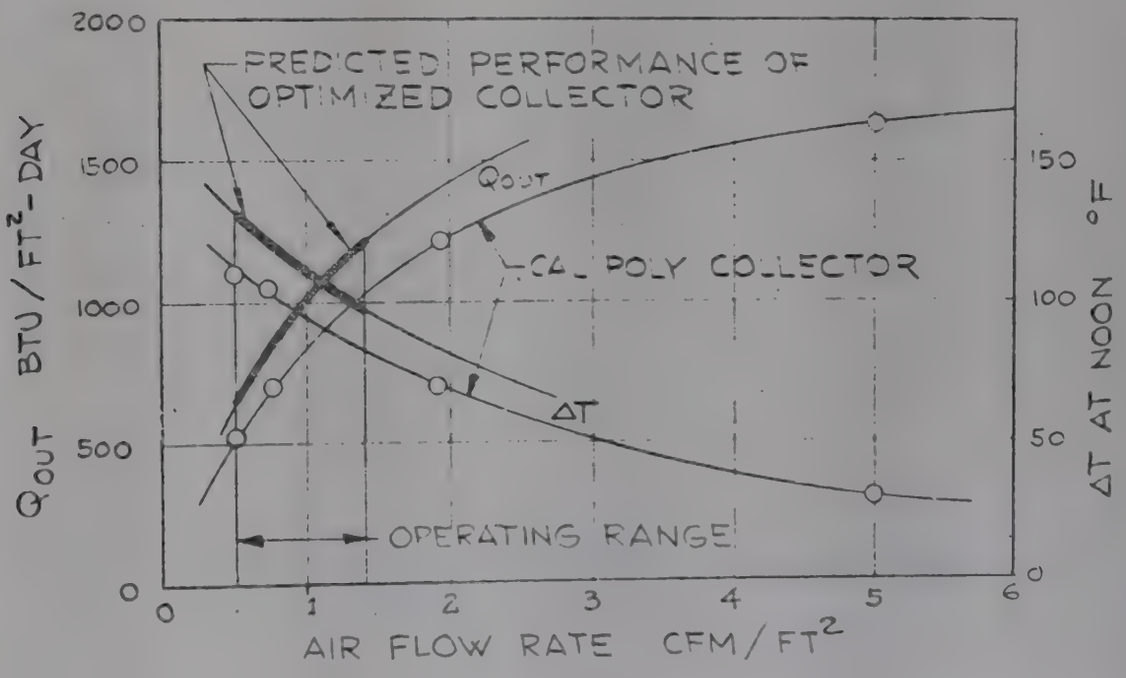

Figure 14. Total Heat Collected During One Day and Temperature Rise as a Function of Air Flow Rate

a collector with optimized duct sizes and inclination. The "operating range" is for a system which would be capable of supplying about 75% of the energy needs of a dehydrator. Average daily output of such collector would be about 880 Btu/ft^2 and an operating temperature (air supplied to the dehydrator) of 160°F.

Figure 15 presents a comparison between Cal Poly collector efficiency, predicted efficiency of optimized collector, and Buelow's[1] efficiency. The latter efficiency was used for the majority of the computer calculations performed at the beginning of the program and explains the pessimistic results that were reached at that time. Note that the predicted efficiency of an optimized collector at 100°F ΔT is almost twice as large as Buelow's prediction.

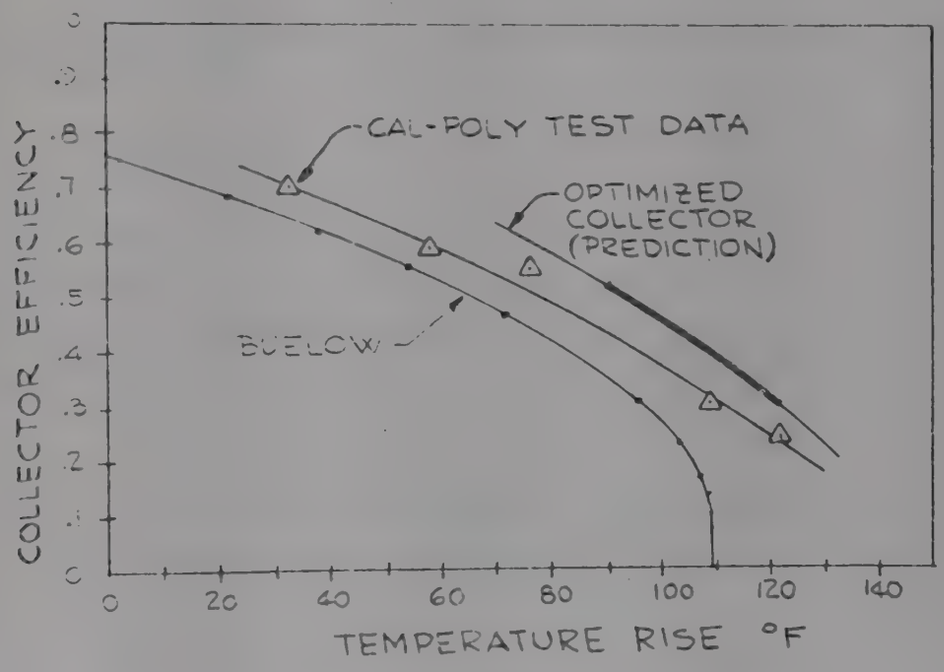

Figure 15. Comparison Between Cal Poly Collector Efficiency, Predicted Efficiency of Optimized Collector and Buelow's Efficiency

(1) Frederick H. Buelow, "Drying Crops with Solar Heated Air," Paper presented at the United Nations Conference on New Sources of Energy, 10 April 1961.

4. ANALYSIS OF A FULL SCALE DEMONSTRATION SYSTEM

Production food dehydration plants use natural gas for an energy source due to its low cost. Propane is an emergency fuel but its cost is of the order of four times that of natural gas. Now that natural gas is in short supply and may be curtailed for industrial use, alternate fuels must be found for the food dehydration industry. The alternatives are:

- Heating Oil – Burn oil to generate steam which, in turn, is used to heat air for dehydration (direct burning of oil to heat the air is not acceptable due to the possible contamination of foods).
- Imported LNG – Could be used as a direct substitute for natural gas.
- Electricity – Use electricity to heat the air directly.
- Coal – Burn coal to generate steam to heat the air for dehydration.
- Solar Energy – Use solar energy to heat the air for dehydration.

The choice of which one of these systems to install will most likely be on the basis of cost and future availability of the energy source. To compare the cost of these systems on common grounds, we use a performance index criterion. The performance index is expressed as

$$\frac{\text{Btus delivered to the dehydrator per day}}{\text{Capital investment} + \text{operating cost in terms of equivalent capital}^{*}} \quad \text{(Btu/\$ - day)}$$

*Operating cost includes fuel costs and maintenance. Equivalent capital is the mortgage that would be paid off with the money spent on operating expense. We use 10-year mortgage of 10% interest rate. For example, if the operating cost is $5000 a month for fuel and maintenance, the equivalent capital is $378,330, or monthly payment of a $378,330 10-year mortgage at 10% interest rate would be $5000 a month.

Basically, the performance index gives the number of Btus that a heating system will provide per day per dollar invested in the system. The higher the performance index, the more economical the system is.

For a Cal Poly-TRW designed solar system, we know from the test data and performance predictions that the system will deliver 880 Btu/sq ft of collector area per day at the design air flow rates. The collector cost is $4.18/sq ft (installed with ducting), plus 0.73 for thermal storage. Thus, the total solar system cost is $4.91/sq ft. Since the operating cost for solar systems is very small (we will neglect it here), the performance index for the solar system is thus (880 Btu/day/$4.91 = 180 Btu/$-day.

The performance indexes for the other systems are given below:

- Oil-Steam – The performance index depends on the price of oil, as shown in Figure 16.

  At $16/bbl, the performance index is 200 Btu/$-day
  $22/bbl, the performance index is 150 Btu/$-day
  $25/bbl, the performance index is 130 Btu/$-day

- Electrical Heating – The performance index is 110 Btu/$-day (at 2.5 cents/kw hr).

- LNG – The performance index is 210 Btu/$-day (at 38 cents/therm).

- Coal-Steam – Very difficult to predict for the southwestern region, because coal is not used and prices are not well established. However, it appears to be in the neighborhood of 300 Btu/$-day.

The following conclusions can be drawn from the data given above:

- The solar system will become competitive with oil when oil prices increase to $17/bbl. At the time of this writing, imported oil is at $14/bbl and President Ford's surcharge has brought it up to $16/bbl. As a result of policy changes made during a recent OPEC meeting (June 1975), the oil prices are expected to rise another 30 to 35%, which will bring the prices to $21 to $22/bbl. At this price range, a solar system can comfortably compete with oil.

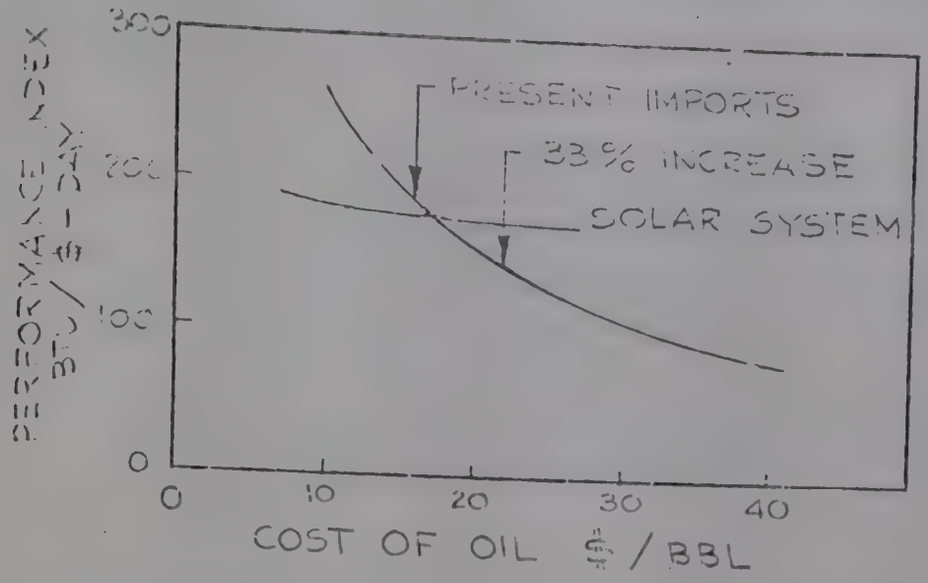

Figure 7. Comparison of Performance Indexes for Oil-Fired Steam Production and Solar System

Figure 16. Comparison of Performance Indexes for Oil-Fired Steam Production and Solar System

- Electric heating at 2.5 cents/kw hr is already more expensive than solar heating.

- LNG at 38 cents/therm. is still the most economical fuel (next to coal) for dehydration. However, a 16% increase in the LNG price will make the costs equal to solar system costs. In addition, since LNG is imported from Algeria, there is some uncertainty about its future availability.

- Coal-fired steam plants appear to be the most economical to use for dehydration providing that:

  (1) Coal at the price range of $40/long ton becomes available in the Southwest.

  (2) Environmental polution problems can be resolved.

  (3) The dehydration plants are near a railroad track to deliver the coal. (Most of the existing dehydration installations in California area are not close to rail lines.)

Based on these comparisons, it appears that solar systems will become quite competitive with fossil fuels in the very near future for dehydration as well as numerous other industrial and residential heating applications. In addition, there are two more considerations in favor of the solar systems.

- The solar system economics stated in this report are based on the performance of existing experimental hardware built at Cal Poly. We believe that performance improvements and/or cost reductions will occur as a result of work performed under this and related programs. These improvements should reduce the cost of solar Btus even further.

- Finally, the Government is planning an incentives program to encourage the use of solar energy. When these incentives are instituted, the solar systems will be even more desirable.

5. THE SOLAR DEHYDRATION PLANT

A typical industrial dehydrator unit (conveyor or tunnel dehydrator) handles about 400 lb of wet produce an hour and requires about 2500 Btu and 2000 cubic feet of air to evaporate a pound of water (at 40% efficiency). Since most of the weight in the produce is water (about 90% for vegetables), the dehydrator requires nearly 1.0 million Btu per hour. The corresponding air flow requirement is 800,000 cubic feet of air per hour or 13,000 cfm.

The typical drying temperature used in commercial dehydrators is in the area of 180°F. However, the work performed by Cal Poly under this grant indicates that the drying temperature can be reduced to about 160°F without significantly increasing dehydration costs or affecting the product quality. Since solar system efficiency is considerably better at 160°F than at 180°F, we chose the former as the operating temperature for purposes of illustration. The exact determination of the operating temperature, however, would require additional system analysis and optimization.

5.1 SOLAR SYSTEM OPERATION

From the previous paragraphs, we see that to satisfy the energy needs of a typical dehydrator, the solar system should produce about 13,000 cfm of air heated to 160°F. Since industrial dehydration plants typically operate continuously, day and night, seven days a week, this energy needs to be supplied continuously. It would require approximately 25,000 square feet of solar collector to heat this quantity of air to 160°F. A bin approximately 16 feet in diameter and 30 feet high, filled with 6000 cubic feet of crushed rock, would provide thermal storage. The collectors would be of the general type developed by Cal Poly and TRW under this research program (see Figure 17). The system could be installed at an existing dehydration facility and connected to a production dehydrator. The solar system would be designed to supply approximately 20 million Btu/day, or about 75% of the energy needs of the dehydrator. An artist's concept of such a solar food dehydration facility is shown in Figure 18.

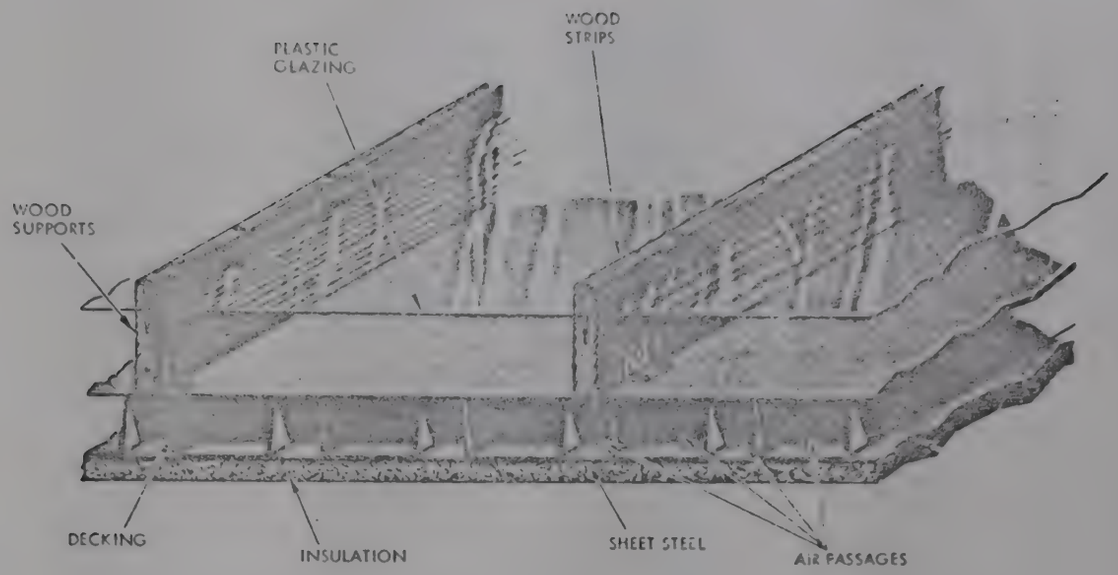

Figure 17. TRW-Cal Poly Solar Collector Design

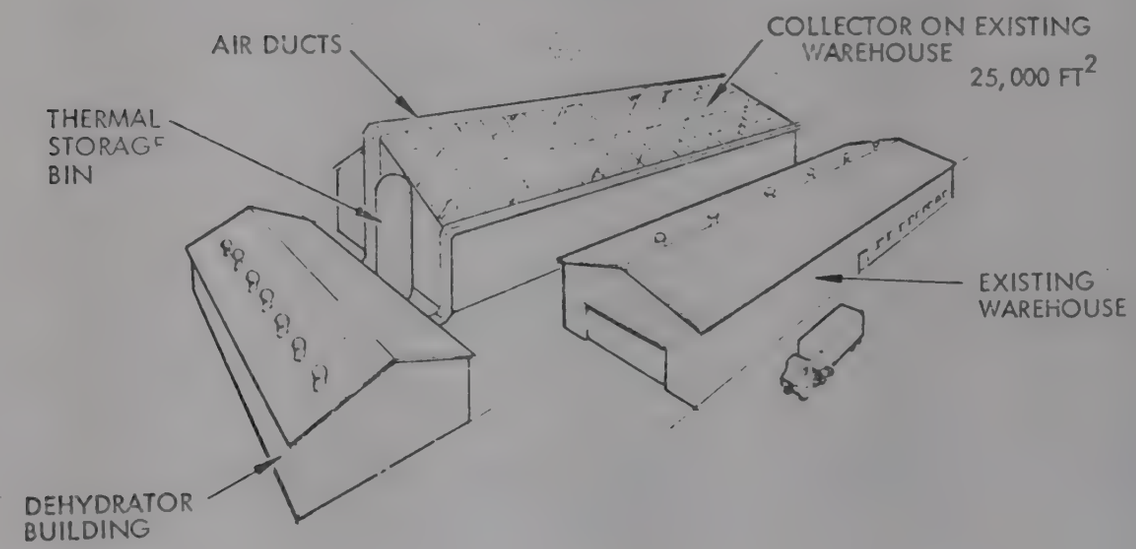

Figure 18. Solar Dehydration Facility

A block diagram of a solar system which would be capable of supplying a large part of the energy requirement at an industrial food dehydrator is shown in Figure 19. The system contains a solar collector, thermal storage, two air fans, interconnecting ducting and several dampers. The system has three operating modes.

(1) Drying Using Solar Collectors and Auxiliary Heat – Fresh air is passed through the collectors, preheated and then supplied to the dehydrator (for additional

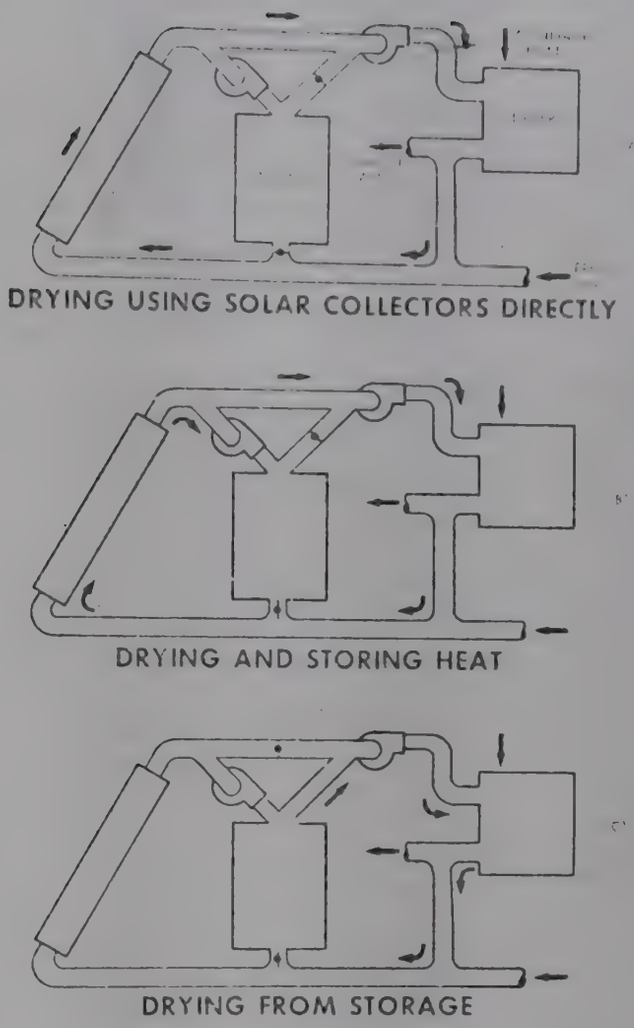

Figure 19. Block Diagram of System Operation

heating using conventional means). This mode is used whenever insufficient sunshine is available to heat the air to the full drying temperatures.

(2) Drying and Storing Heat – This mode is used when the collector starts collecting more energy than is required by the dehydrator. At this time, a variable speed storage fan is started and increases the air flow in the collectors to maintain a constant air output temperature. Part of the air (13,000 cfm) goes to the dehydrator and the rest is passed through the thermal storage to store heat for later use.

(3) Drying from Storage – This mode is used in the evening after the sun sets and the solar collector no longer can supply the energy requirements of the dehydrator. Then the air is drawn through the storage, heated and supplied to the dehydrator. The solar collector remains inoperative during this time.

. A plot showing the operating modes and energy distribution during a typical 24-hour cycle is shown in Figure 20.

We expect that more than 75% of the energy needs of the dehydrator could be provided using this system. The remaining 25% (primarily during early morning hours) will come from conventional sources such as oil-fired steam, LNG, or electricity.

5.2 SOLAR SYSTEM DESCRIPTION

Solar Collector – As mentioned earlier, the solar dehydrator system would use on the order of 25,000 square feet of the TRW-Cal Poly designed collector. As described in prior reports the collector is made up of standard Ryerson steel decking panels which serve as the air ducts, plastic glazing, and insulation on the bottom and sides. The collector will also serve as the roof of the building. The estimated cost of this collector is $4.78/sq ft installed. Since conventional roofing used on industrial buildings costs about 60 cents/sq ft installed, the delta cost attributable to the collector is $4.18/sq ft.

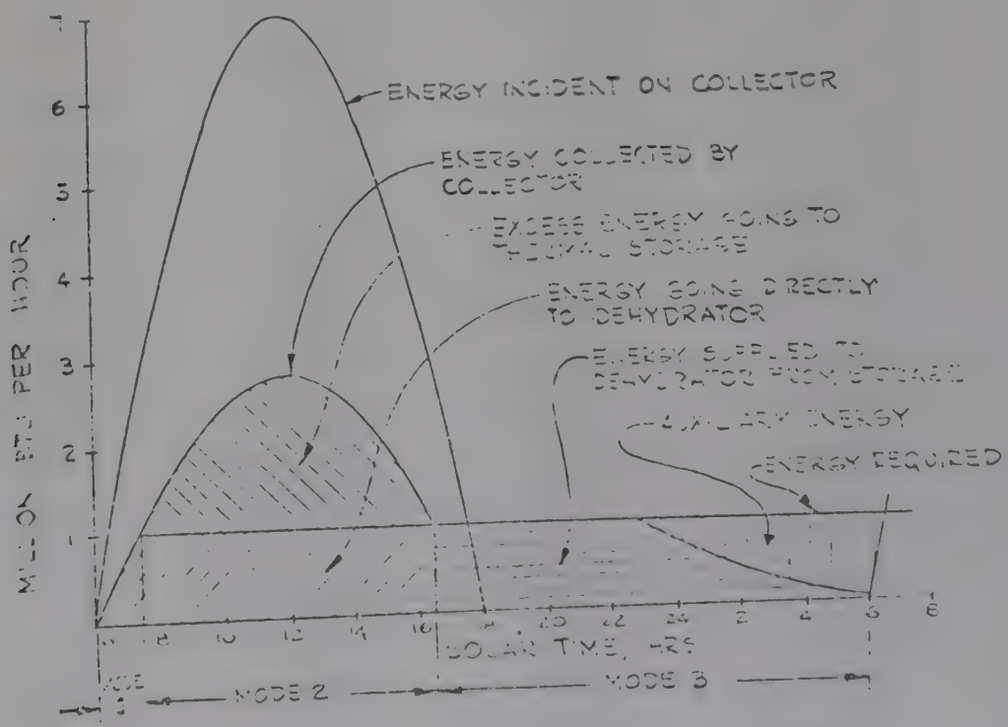

Figure 8. Energy Distribution for a Typical 24-Hour Cycle

Figure 20. Energy Distribution for a Typical 24-Hour Cycle

The efficiency of the TRW-Cal Poly collector as an air heater is given in Figure 13. However, several changes and improvements could be incorporated in the new collector to be used for the full-size dehydration plant. These are:

(1) Decrease the duct sizes. The TRW-Cal Poly collector was designed to operate at high air flow rates (~4 cfm/sq ft) and high efficiency at a low temperature rise. The collector for a full size dehydration plant would require flow rates in the range of 0.5 to 1.4 cfm/sq ft and large temperature rise (~90°F ΔT). Thus it would be necessary to reduce the duct sizes to improve heat transfer between the collector and the air. A decrease in duct size is estimated to provide approximately 10% improvement in the collector efficiency.

(2) The TRW-Cal Poly collector used standard off-the-shelf steel decking panels. We propose to redesign these panels to use lighter gauge metal, provide for easy air-tight sealing, as well as choose duct sizes which optimize heat transfer and pressure drop. Once the tooling is made (the decking sections are roll-formed), the cost of the panels for the solar collector should be less and the collector should be lighter than the conventional decking used in the TRW-Cal Poly collector.

5.3 SOLAR COLLECTOR PERFORMANCE

Data obtained during a typical one-day test run of the TRW-Cal Poly collector are shown in Figure 12. The data give solar energy input, collector output, and outlet air temperature. For this run the air flow rate was constant at 0.53 cfm/sq ft. The total energy collected was about 520 Btu/sq ft-day, and the maximum air temperature rise was about 115°F. Test points obtained in similar tests but at other flow rates are shown in Figure 14. Also shown in Figure 14 are performance predictions of the redesigned and optimized collector. As mentioned before, by redesigning the duct sizes we expect to improve heat transfer giving about a 10% increase in heat collection efficiency. Another 5% improvement will be obtained by tilting the collectors at the proper angle to the sun (Cal Poly collectors are horizontal). Thus a total improvement of about 15% over the Cal Poly collectors is expected. With these improvements, the collector daily output is expected to be about 600 Btu/day-sq ft at 0.5 cfm/sq ft and 1150 Btu/day-sq ft at 1.4 cfm/sq ft. The daily average is expected to be about 880 Btu/-sq ft.

APPENDIX

Air Collector Thermal Model

The air collector thermal model is a detailed model of an air collector which is used to determine the efficiency of a solar collector as a function of a wide variety of design parameters.

The model runs on TRW's SINDA thermal analyzer program and will analyze collectors for varying duct sizes, duct materials, number of glazings, solar insolation, collector flow rate and wind velocity. Thermodynamic properties of air are stored within the program and are used to accurately determine forced and free convection modes of heat transfer. The collector is divided into ten (10) sections within the model and each section is, in turn, divided into ten (10) thermal nodes. The collector temperature distribution and directions of heat flow are calculated within the program.

Fan Power Program

The fan power program is used to determine fan power requirement and resultant pressure drop as a function of duct height, width, length and volumetric flow rate.

The program is written in Fortran IV and runs on the TRW Time-share system. The program calculates the duct hydraulic diameter, air velocity, Reynold's number, friction factor, pressure drop, mass flow rate and fan power requirement. Loops are set up within the program to facilitate parametric runs.

When used in conjunction with the air collector thermal model, the fan power program may be used to optimize solar air collectors.

The enclosed flow diagrams, Figures 21 and 22, show the detailed operation of each program.

Reproduced from
best available copy.

Figure 22. FAN POWER PROGRAM FLOW DIAGRAM

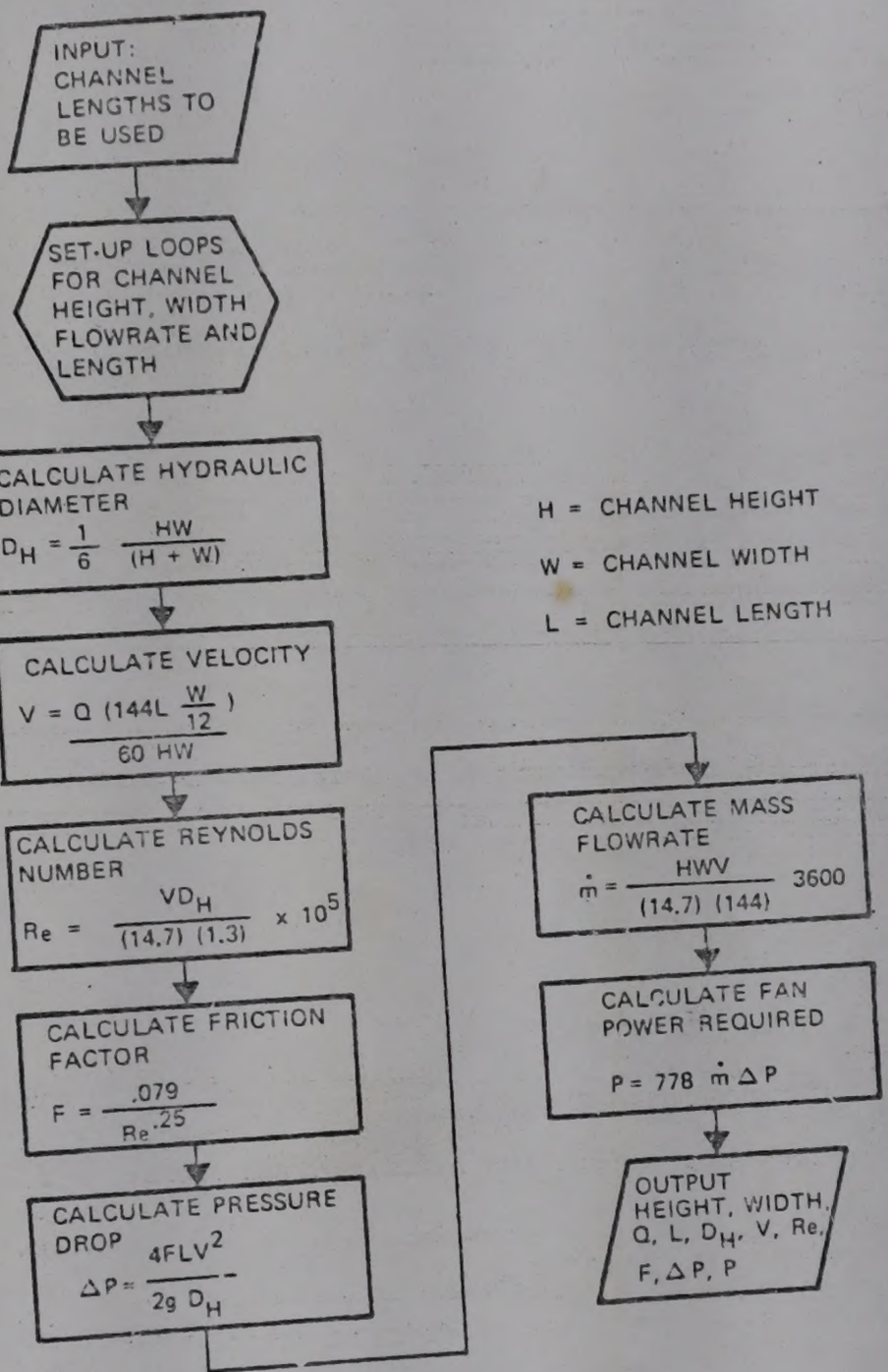
INPUT: CHANNEL LENGTHS TO BE USED
SET-UP LOOPS FOR CHANNEL HEIGHT, WIDTH FLOWRATE AND LENGTH
CALCULATE HYDRAULIC DIAMETER
$D_H = \frac{1}{6} \frac{HW}{(H + W)}$
CALCULATE VELOCITY
$V = \frac{Q\,(144L\,\frac{W}{12})}{60\,HW}$
CALCULATE REYNOLDS NUMBER
$Re = \frac{VD_H}{(14.7)\,(1.3)} \times 10^5$
CALCULATE FRICTION FACTOR
$F = \frac{.079}{Re^{.25}}$
CALCULATE PRESSURE DROP
$\Delta P = \frac{4FLV^2}{2g\,D_H}$
CALCULATE MASS FLOWRATE
$\dot{m} = \frac{HWV}{(14.7)\,(144)}\,3600$
CALCULATE FAN POWER REQUIRED
$P = 778\,\dot{m}\,\Delta P$
OUTPUT HEIGHT, WIDTH, Q, L, D_H, V, Re, F, ΔP, P
H = CHANNEL HEIGHT
W = CHANNEL WIDTH
L = CHANNEL LENGTH